LECTURE NOTES ON TRANSVERSE-MOMENTUM-DEPENDENT PARTON DISTRIBUTION FUNCTION AND SOFT FUNCTIONS IN THE LARGE-MOMENTUM EFFECTIVE THEORY

Yizhuang Liu

Institute of Theoretical Physics, Jagiellonian University, 30-348 Kraków, Poland
yizhuang.liu@uj.edu.pl

Received 19 March 2022, accepted 23 March 2022,
published online 12 May 2022

We study the theoretical foundations of the recently developed large-momentum effective theory (LaMET) approach to the transverse-momentum-dependent parton distribution function (TMDPDF). We first show that the quasi-TMDPDF can be consistently defined and it relates to the physical TMDPDFs through a factorization formula in the large-momentum limit. We show that the factorization involves the intrinsic soft function which is related to the off-lightcone soft functions for the Drell–Yan process and can be realized as a form factor. We also study properties of the off-lightcone soft functions, such as IR safety, analyticity, rapidity divergence, *etc.* Universality classes of the off-lightcone soft functions are discussed. Finally, we show that the intrinsic soft function can be extracted by combining a light-meson form factor with large-momentum transfer and quasi-TMD wave functions for the light meson.

DOI:10.5506/APhysPolB.53.4-A2

1. Introduction

The transverse-momentum-dependent (TMD) parton distribution functions (TMDPDFs) are important in understanding the experimental processes where the transverse momenta of final state particles are measured, which will be one of major purposes of the upcoming Electron-Ion Collider (EIC) in US. In Drell–Yan (DY) processes (lepton pair and W, Z productions) and $e^+e^- \to \gamma^* \to 2\,\mathrm{jets} + X$, it is known that the differential cross section $\mathrm{d}\sigma/\mathrm{d}Q_\perp^2$ normally peaks at relatively small transverse momentum ($k_\perp \ll Q$), where the large logarithms $\log Q/k_\perp$ and nonperturbative effects ($k_\perp \sim \Lambda_{\mathrm{QCD}}$) spoil the collinear factorization. Therefore, the TMD factorization was developed to analyze such processes [1–5]. For semi-inclusive deep inelastic scattering (SIDIS) processes in small $Q_\perp$ region, the TMD factorization can also be applied [6, 7]. For these processes, it was shown that the cross section can be factorized in the form of $\sigma = \hat{\sigma} \otimes f \otimes f \otimes S$, where $\hat{\sigma}$, f, S are hard, collinear, and soft contributions.

The unsubtracted TMDPDF f is defined with lightlike gauge links pointing to infinities which results in a new type of divergence, the rapidity divergences (also called lightcone singularities), due to gluon radiation collinear to the gauge links. Therefore, a rapidity regulator is needed and its renormalization results in a rapidity scale whose evolution is governed by the so-called Collins–Soper kernel [1]. Unlike the standard collinear factorization, a TMD soft function S is also required to capture soft-gluon radiations from the fast moving color charges. Here, the TMD soft function $S(b_\perp, \mu, Y)$ is defined as a vacuum expectation value (VEV) of a Wilson loop composed of lightlike gauge links and usually depends on three variables: the rapidity regulator Y, the transverse separation $b_\perp$ (conjugate to transverse momentum), and the renormalization scale μ associated to the cusps of gauge links. Similar to the unsubtracted TMDPDF, the lightlike gauge links in S lead to the rapidity divergences as well. Later, the TMD factorization was reinvestigated in the framework of soft-collinear effective theory [8–10]. A standard definition of physical TMDPDFs which is a rapidity divergence-free combination of unsubtracted TMDPDF and soft function, was proposed in Refs [8, 11–13]. Within the standard formalism, the perturbative calculations of TMDPDFs and the soft functions have proceeded to 2-loops [14–17] and recently to 3-loops [18]. Also, the property of rapidity divergences has been extensively studied, including [19] which builds the rapidity factorization with the use of conformal transformations.

Besides the importance of understanding the high-energy experiments, the TMDPDFs are also important by themselves for their crucial role in understanding hadron structures. Under a Lorentz boost, the longitudinal size of hadron contracts, but the transverse directions remain unchanged. Thus, one can simultaneously probe the fast-moving collinear physics from the longitudinal x-dependencies and the rest-frame-like nonperturbative physics from the transverse $\vec{k}_\perp$-dependencies. Moreover, unlike the $k_\perp$-integrated collinear PDFs, the TMDPDF is sensitive to soft radiations. Therefore, the physics in the presence of transverse degrees of freedom is rather rich. This is particularly the case in studies of spin-dependent phenomena where one can define more TMDPDFs through the Lorentz decompositions. One example is the Sivers function for an unpolarized parton in a transversely polarized proton, $f_{1\mathrm{T}}^{\perp}(x, k_\perp)$, which is time-reversal odd and is predicted to change the sign between the DY and SIDIS processes [11]. Similar properties also exist in the Boer–Mulders function $h_1^{\perp}(x, k_\perp)$ [20] concerning a transversely polarized parton in an unpolarized proton. These two functions are related to the single transverse spin asymmetry.

Regardless of the fact that the TMD factorization has been established, it is difficult to extract the TMDPDFs accurately due to the limited amount of available experimental data. There are many efforts on global analysis [21–30], however, the fitting still suffers from relatively large uncertainties in the nonperturbative region, $k_\perp \sim \Lambda_{\rm QCD}$. It is expected to be much harder to obtain a global fit for spin-dependent TMDPDFs. Although the future EIC will make up the gap and produce more data for TMD observable measurements, it is still important to develop first-principle methods for the determination of nonperturbative TMDPDFs, which can serve as a comparison or provide useful inputs to constrain the models in global fits.

The recent development of the large-momentum effective theory (LaMET) proposed in Refs. [31, 32] has opened up a possibility of directly calculating TMDPDFs on lattice. The essence of LaMET is as follows: the lightcone time-dependencies at the operator level can be transmuted into the fast-moving external hadrons state, from which the lightcone physics can be extracted through the large-momentum factorization of equal-time correlation functions. LaMET has been successfully applied to collinear PDFs, distribution amplitudes (DAs), and the generalized parton distribution functions (GPDs), see Ref. [33] for a review. Early studies [34–37] have made an effort constructing a quasi-TMDPDF that is calculable on the lattice, but its relation to the physical TMDPDF is expected to be nonperturbative due to complications in the soft function. Nevertheless, the Collins–Soper kernel can be extracted by taking the ratio at two different momenta to cancel the soft contributions [36, 38, 39]. In order to match the physical-TMDPDFs, we must study its factorization property at large hadron momentum and prove that it is indeed related to the targeting TMDPDFs. The recent works in Refs. [33, 40–42] provide a Euclidean formulation of soft functions and other TMD-related quantities so that a perturbative matching formula can be established between the quasi- and physical TMDPDFs, and thus allow for a complete determination of the latter from the lattice QCD.

In this note, we provide a careful investigation of the theoretical properties of the quasi-TMDPDFs and the soft functions in the lightcone limit. In Sec. 2, we make a brief introduction to the lightcone TMDPDFs and related TMD soft functions. In Sec. 3, we first study IR divergences of the quasi-TMDPDF, which factorizes into physical TMDPDF and intrinsic soft function by analyzing the leading region in $1/(b_\perp \mathcal{P}^z)$ expansion in the lightcone limit. Various one-loop results and some two-loop predictions are also presented. In Sec. 4, we investigate the TMD soft function in the off-lightcone scheme, which has not been extensively studied as the on-lightcone one. The off-lightcone scheme helps to understand how the lightcone physics emerges from the off-lightcone observable in lightcone limit. We find that the soft function for the DY process can be formulated in the heavy quark effective theory (HQET) as a form factor, which allows the Euclidean realization. A classification of off-lightcone soft functions is provided. In Sec. 5, we discuss the intrinsic soft function which is a crucial quantity to match the quasi-TMDPDF to the physical TMDPDF. An alternative method to extract the intrinsic soft function is through the light-meson form factor and the TMD wave function (TMDWF). The cross section of DY process in small-$k_\perp$ region can be obtained from the first-principle using the quasi-TMDPDF and the intrinsic soft function. Discussions and conclusions are given in Sec. 6.

2. Basic properties of TMDPDF

Let us onsider the quark unpolarized TMDPDF (it is straightforward to include a spin-dependent component or generalize to gluon distribution) as an example. Without taking into account the theoretical subtleties, such as rapidity divergence, the unsubtracted TMDPDF is defined as

$$\begin{aligned} f\left(x,\vec{b}_\perp\right) &= \frac{1}{2\mathcal{P}^+}\int\frac{\mathrm{d}\lambda}{2\pi}\mathrm{e}^{-i\lambda x} \\ &\times\langle\mathcal{P}|\bar{\psi}\left(\lambda n+\vec{b}_\perp\right)\gamma^+\mathcal{W}_n\left(\lambda n+\vec{b}_\perp\right)\psi(0)|\mathcal{P}\rangle\,, \end{aligned} \tag{1}$$

where x is the longitudinal momentum fraction, λ is the invariant length $\xi\cdot\mathcal{P}=\xi^-\mathcal{P}^+$, $\xi^\pm=(\xi^t\pm\xi^z)/\sqrt{2}$ are the lightcone coordinates, and $\mathcal{W}_n(\lambda n+\vec{b}_\perp)$ is the staple-shaped gauge link of the form of

$$\mathcal{W}_n(\xi) = W_n^\dagger(\xi)W_\perp W_n(0)\,, \tag{2}$$

$$W_n(\xi) = \mathcal{P}\exp\left[-ig\int_0^{-\infty}\mathrm{d}\lambda\, n\cdot A(\xi+\lambda n)\right]\,, \tag{3}$$

along the lightcone direction $n^\mu=\frac{1}{\sqrt{2}\mathcal{P}^+}(1,\vec{0}_\perp,-1)$ in the $(t,\vec{\perp},z)$ coordinate, as shown in Fig. 1. The $W_\perp$ is a transverse gauge link at infinity to maintain gauge invariance. The staple $\mathcal{W}_n$ is defined with the past-pointing lightlike gauge link from 0 to $-\infty$ in accordance with the DY kinematics. Similarly, for SIDIS, we can define the future-pointing version of the gauge link staple $\mathcal{W}_n^+$ simply by changing $-\infty$ to ∞ in the definition, as shown in Fig. 1. For unpolarized TMDPDFs, there is no distinction between the two choices, but for the spin-dependent TMDPDFs, there are physical consequences based on the time-reversal symmetry.

There exists a new type of singularity, called the rapidity divergence, associated with the infinitely long lightlike gauge links. These divergences are caused by radiation of gluons collinear with the lightlike gauge link and cannot be regularized by the standard UV regulators. The physical interpretation of TMD observables is then obscured by the complicated pattern

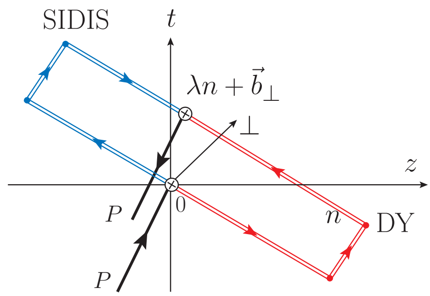

Fig. 1. The spacetime picture of TMDPDF for DY and SIDIS processes. The $\otimes$ sign denotes the quark-link vertices.

of rapidity regulator dependencies. However, the rapidity divergence to the lightcone physics is as fundamental as the UV divergence to the quantum field theory. The former is caused by approximation of the hadron in infinite momentum frame (infinite rapidity limit), and the latter is due to quantum fluctuation at short distance (continuum limit). An example is the following integral in dimensional regularization (DR) [37]:

$$I = \int \mathrm{d}k^+ \mathrm{d}k^- \frac{f\left(k^+k^-\right)}{\left(k^+k^-\right)^{1+\epsilon}} = \frac{1}{2} \int \frac{\mathrm{d}y}{y} \int \mathrm{d}m^2 \frac{f\left(m^2\right)}{m^{2+2\epsilon}}\,, \tag{4}$$

where $y = k^+/k^-$ is the rapidity-related variable and $m^2 = k^+k^-$. The divergences in y arise from large and small y where the integral cannot be regulated by DR.

To regulate the rapidity divergences, a number of methods have been introduced in the literature (for a review see [37]). They can be categorized into two classes: on-lightcone and off-lightcone regulators. In the former case, the gauge links are kept along the lightcone direction n^μ after regularization. For example, the δ regulator [15, 43] modifies the gauge link as

$$W_n(\xi) \to W_n(\xi)|_{\delta^-} = \mathcal{P} \exp\left[-ig \int_0^{-\infty} \mathrm{d}\lambda\, A^+(\xi + \lambda n)\, \mathrm{e}^{-\frac{\delta^-}{2p^+}|\lambda|}\right]\,, \tag{5}$$

and similarly for the conjugate direction. The δ regulator breaks the gauge invariance, but preserves the boost invariance $\delta^\pm \to \mathrm{e}^{\pm Y}\delta^\pm$, where Y is the rapidity of the Lorentz boost. Other on-lightcone regulators include the exponential regulator [10], η regulator [44], analytical regulator [45], *etc.* In the rest of this section, we will use the δ regulator as a representative whenever we need an on-lightcone regulator.

The off-lightcone regulator was introduced in [1, 6, 7, 11]. This type of regulator chooses the Wilson lines tiled in the off-lightcone direction to avoid the rapidity divergence. One can, for instance, deform the gauge links into the spacelike region

$$n \to n_Y = n - \mathrm{e}^{-2Y} \frac{p}{(\mathcal{P}^+)^2}\,, \tag{6}$$

where $p = \frac{\mathcal{P}^+}{\sqrt{2}}(1,0,0,1)$ such that $n \cdot p = 1$. Here, Y plays the role of a rapidity regulator, as $n_Y \to n$ when $Y \to \infty$. In certain cases, one can also deform n_Y into a timelike region [46].

To avoid lightcone divergences, from now on we include the rapidity regulator in the definition of the unsubtracted TMDPDFs

$$f(\lambda, b_\perp, \mu, \delta^-) = \langle \mathcal{P}|\bar{\psi}\left(\lambda n + \vec{b}_\perp\right)\gamma^+ \mathcal{W}_n\left(\lambda n + \vec{b}_\perp\right)|_{\delta^-}\psi(0)|\mathcal{P}\rangle\,. \tag{7}$$

Due to rotational invariance, the unpolarized TMDPDF defined above is a function of $b_\perp = |\vec{b}_\perp|$. The subscript δ^- denotes that the staple-shaped gauge link $\mathcal{W}$ is regulated by the δ regulator in the lightcone minus direction. The TMDPDF f diverges logarithmically as $\delta^- \to 0$, and the finite part also depends on the rapidity regulator. The above TMDPDF must remove all its rapidity divergences and regularization scheme dependencies to define the physical TMDPDF, in a way similar to the removal of UV divergences in physical quantities.

The rapidity divergence for TMDPDFs can be removed by the soft function, which also plays an important role in the TMD factorization. Intuitively, the soft function represents a cross section for fast-moving charged particles emitting soft gluons into final states. It has the rapidity divergence associated with the lightcone direction. The TMD soft function consistent with the Drell–Yan process is defined [15, 47] as

$$\begin{aligned} S\left(b_\perp, \mu, \delta^+, \delta^-\right) &= \frac{\mathrm{Tr}\langle 0|\bar{\mathcal{T}} W_p\left(\vec{b}_\perp\right)|_{\delta^+} W_n^\dagger\left(\vec{b}_\perp\right)|_{\delta^-}\mathcal{T} W_n(0)|_{\delta^-} W_p^\dagger(0)|_{\delta^+}|0\rangle}{N_\mathrm{c}} \\ &= \frac{\mathrm{Tr}\langle 0|\mathcal{W}_n\left(\vec{b}_\perp\right)|_{\delta^+}\mathcal{W}_p^\dagger\left(\vec{b}_\perp\right)|_{\delta^-}|0\rangle}{N_\mathrm{c}}\,, \end{aligned} \tag{8}$$

where $\mathcal{T}/\bar{\mathcal{T}}$ stands for time/anti-time ordering. The first equality defines the soft function in terms of cut-diagrams as an amplitude square. Since the soft function for the DY process is independent of the time-ordering because every two points on the Wilson loop are either spacelike or lightlike separated, one can also define it with a single time-ordering or no time-ordering, leading to the second equality. The staple-shaped gauge link $\mathcal{W}_n$

is defined in Eq. (2), while $\mathcal{W}_p$ is defined similarly with the replacement $n \to p$. The soft function is shown in Fig. 2 as a Wilson loop in Minkowski space.

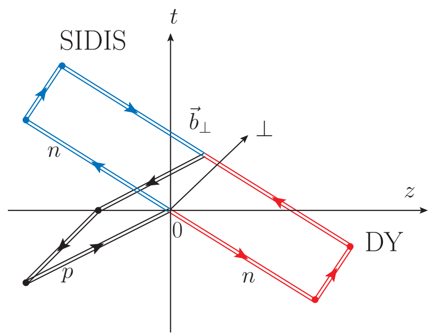

Fig. 2. The spacetime picture of the soft function $S(b_\perp, \mu, \delta^+, \delta^-)$ as a Wilson loop arising in the factorization of DY and SIDIS processes.

If the rapidity divergences are multiplicative in nature, one can use S as the rapidity renormalization factor for the TMDPDF. In on-lightcone schemes such as the δ regularization, it has been argued in [19] based on the conformal transformation that the rapidity divergences are indeed multiplicative. For each of the staple-shaped lightlike gauge link, the rapidity divergence is proportional to

$$\mathrm{e}^{-\frac{1}{2}K(b_\perp,\mu)\ln\frac{\mu^2}{(\delta^\pm)^2}}, \tag{9}$$

where $K(b_\perp, \mu)$ is known as the nonperturbative Collins–Soper evolution kernel. Thus at small $\delta^\pm$, we can write

$$S\left(b_\perp, \mu, \delta^+, \delta^-\right) = \mathrm{e}^{K(b_\perp,\mu)\ln\frac{\mu^2}{2\delta^+\delta^-}+\mathcal{D}_2(b_\perp,\mu)}, \tag{10}$$

where $\mathcal{D}_2(b_\perp, \mu)$ is a $b_\perp$-dependent but rapidity-independent function. The soft function in δ regularization satisfies the renormalization group equation (RGE)

$$\mu^2\frac{\mathrm{d}}{\mathrm{d}\mu^2}\ln S\left(b_\perp, \mu, \delta^+, \delta^-\right) = -\mathit{\Gamma}_{\mathrm{cusp}}(\alpha_\mathrm{s})\ln\frac{\mu^2}{2\delta^+\delta^-} + \gamma_\mathrm{s}(\alpha_\mathrm{s}), \tag{11}$$

where $\mathit{\Gamma}_{\mathrm{cusp}}(\alpha_\mathrm{s})$ is the lightlike cusp anomalous dimension and the $\gamma_\mathrm{s}(\alpha_\mathrm{s})$ is the soft anomalous dimension. They are all known to 3-loops [18, 48]. Recently, the cusp-anomalous dimensions have been calculated to 4-loops [49].

The Collins–Soper kernel and the rapidity-independent part $\mathcal{D}_2$ satisfy the RGEs

$$\mu^2 \frac{\mathrm{d}}{\mathrm{d}\mu^2} K(b_\perp, \mu) = -\mathit{\Gamma}_{\mathrm{cusp}}(\alpha_{\mathrm{s}}) \,, \tag{12}$$

$$\mu^2 \frac{\mathrm{d}}{\mathrm{d}\mu^2} \mathcal{D}_2(b_\perp, \mu) = \gamma_{\mathrm{s}}(\alpha_{\mathrm{s}}) - K(b_\perp, \mu) \,. \tag{13}$$

At one-loop, the soft function $S(b_\perp, \mu, \delta^+, \delta^-)$ is given by [37]

$$S\left(b_\perp, \mu, \delta^+, \delta^-\right) = 1 + \frac{\alpha_{\mathrm{s}} C_{\mathrm{F}}}{2\pi} \left(L_b^2 - 2L_b \ln \frac{\mu^2}{2\delta^+\delta^-} + \frac{\pi^2}{6} \right) , \tag{14}$$

where

$$L_b = \ln \frac{\mu^2 b_\perp^2}{4\mathrm{e}^{-2\gamma_{\mathrm{E}}}} \,. \tag{15}$$

Therefore, at the leading order,

$$K(b_\perp, \mu) = -\frac{\alpha_{\mathrm{s}} C_{\mathrm{F}}}{\pi} L_b \,, \tag{16}$$

$$\mathcal{D}_2(b_\perp, \mu) = \frac{\alpha_{\mathrm{s}} C_{\mathrm{F}}}{2\pi} \left(L_b^2 + \frac{\pi^2}{6} \right) , \tag{17}$$

$$\mathit{\Gamma}_{\mathrm{cusp}} = \frac{\alpha_{\mathrm{s}} C_{\mathrm{F}}}{\pi} \,, \tag{18}$$

$$\gamma_{\mathrm{s}} = \mathcal{O}\left(\alpha_{\mathrm{s}}^2\right) \,. \tag{19}$$

The kernels K and $\mathcal{D}_2$ (hence S) are known to 3-loop order in the exponential regularization scheme [18]. With the above soft function, we can take its square root to perform rapidity renormalization for the unsubtracted TMD correlator. The square root can be explained as follows: S contains two staples, while f contains only one, thus the rapidity divergences, as well as scheme dependencies in S, are squared as those in f. This leads to the following definition of the renormalized physical TMDPDF [8, 12]:

$$f^{\mathrm{TMD}}\left(x, b_\perp, \mu, \zeta\right) = \lim_{\delta^- \to 0} \frac{f\left(x, b_\perp, \mu, \delta^-\right)}{\sqrt{S\left(b_\perp, \mu, \delta^- \mathrm{e}^{2y_n}, \delta^-\right)}} \,, \tag{20}$$

where the rapidity scale reads

$$\zeta = 2\left(x\mathcal{P}^+\right)^2 \mathrm{e}^{2y_n} \,, \tag{21}$$

and $2y_n$ originates in the off-lightcone scheme [11, 47] but an arbitrary parameter to track rapidity scale in the on-lightcone scheme. The rapidity dependence in the numerator f has the form of $\exp[-\frac{1}{2}K(b_\perp,\mu)\ln\frac{(\delta^-)^2}{(x\mathcal{P}^+)^2}]$, while in the denominator, it behaves like $\exp[\frac{1}{2}K(b_\perp,\mu)\ln\frac{\mu^2}{2(\delta^-)^2 e^{2y_n}}]$ [15, 19]. The δ^- dependence cancels out and leaves $\exp[-\frac{1}{2}K(b_\perp,\mu)\ln\frac{\mu^2}{\zeta}]$ depending on the rapidity scale ζ, which is controlled by the Collins–Soper evolution equation

$$2\zeta\frac{\mathrm{d}}{\mathrm{d}\zeta}\ln f^{\mathrm{TMD}}(x,b_\perp,\mu,\zeta) = K(b_\perp,\mu)\,. \tag{22}$$

The ζ dependence comes from the initial-state quark radiation and is intrinsically nonperturbative for large $b_\perp$. $f^{\mathrm{TMD}}(x,b_\perp,\mu,\zeta)$ is the target object to be matched to in LaMET.

We should emphasize that although f^{TMD} is free from rapidity divergences, it does contain collinear contributions from soft radiations due to the charged particles in the external state. This can be seen by considering Feynman diagrams for the unsubtracted TMDPDF f and applying the soft approximation to gluons. At one-loop level, this has been demonstrated in [37], and the scheme-independent one-loop TMDPDF for an external quark state reads

$$\begin{aligned} f^{\mathrm{TMD}}(x,b_\perp,\mu,\zeta) = \delta(1-x) + \frac{\alpha_{\mathrm{s}}C_{\mathrm{F}}}{2\pi}\Bigg\{ & F(x,\epsilon_{\mathrm{IR}},b_\perp,\mu)\theta(x)\theta(1-x) \\ & +\delta(1-x)\left[-\frac{1}{2}L_b^2 + \left(\frac{3}{2} - \ln\frac{\zeta}{\mu^2}\right)L_b + \frac{1}{2} - \frac{\pi^2}{12}\right]\Bigg\}\,, \end{aligned} \tag{23}$$

where

$$F(x,\epsilon_{\mathrm{IR}},b_\perp,\mu) = \left[-\left(\frac{1}{\epsilon_{\mathrm{IR}}} + L_b\right)\frac{1+x^2}{1-x} + 1 - x\right]_+\,. \tag{24}$$

The two-loop order results for quarks and gluons can be found in [48].

The physical TMDPDF also satisfies the RGE

$$\mu^2\frac{\mathrm{d}}{\mathrm{d}\mu^2}\ln f^{\mathrm{TMD}}(x,b_\perp,\mu,\zeta) = \frac{1}{2}\mathit{\Gamma}_{\mathrm{cusp}}(\alpha_{\mathrm{s}})\ln\frac{\mu^2}{\zeta} - \gamma_J(\alpha_{\mathrm{s}}) \equiv \gamma_f(\alpha_{\mathrm{s}})\,, \tag{25}$$

where γ_J is the rapidity-independent part of anomalous dimension. At one-loop, the cusp and hard anomalous dimensions are

$$\mathit{\Gamma}_{\mathrm{cusp}}(\alpha_{\mathrm{s}}) = \frac{\alpha_{\mathrm{s}}C_{\mathrm{F}}}{\pi}\,; \qquad \gamma_J(\alpha_{\mathrm{s}}) = -\frac{3\alpha_{\mathrm{s}}C_{\mathrm{F}}}{4\pi}\,. \tag{26}$$

Beyond one-loop, they have been calculated up to 3-loops [18, 48].

Combining the RGE and the rapidity evolution equation for the TMD-PDF, one obtains the consistency condition

$$\mu^2 \frac{\mathrm{d}}{\mathrm{d}\mu^2} K(b_\perp, \mu) = -\Gamma_{\mathrm{cusp}}(\alpha_{\mathrm{s}}(\mu)) \tag{27}$$

from which one finds a resummed form for the Collins–Soper kernel

$$K(b_\perp, \mu) = -2 \int\limits_{1/b_\perp}^{\mu} \frac{\mathrm{d}\mu'}{\mu'} \Gamma_{\mathrm{cusp}}\left(\alpha_{\mathrm{s}}\left(\mu'\right)\right) + K\left(\alpha_{\mathrm{s}} \frac{1}{b_\perp}\right) . \tag{28}$$

Here $K(\alpha_{\mathrm{s}}(1/b_\perp))$ contains all the nonperturbative contributions when $1/b_\perp \sim \Lambda_{\mathrm{QCD}}$. The TMDPDFs at different scales are then related by

$$\begin{aligned} f^{\mathrm{TMD}}(x, b_\perp, \mu, \zeta) \;=\; & \exp\left[\frac{1}{2} K(b_\perp, \mu) \ln \frac{\zeta}{\zeta_0}\right] \\ & \times \exp\left[\int\limits_{\mu_0}^{\mu} \frac{\mathrm{d}\mu'}{\mu'} \gamma_f\left(\mu', \zeta_0\right)\right] f^{\mathrm{TMD}}(x, b_\perp, \mu_0, \zeta_0) . \end{aligned} \tag{29}$$

With the scheme-independent physical TMDPDF defined above, the DY cross section at small $\vec{Q}_\perp$ can be factorized as

$$\begin{aligned} \frac{\mathrm{d}\sigma}{\mathrm{d}Q_\perp^2} \;=\; & \int \mathrm{d}x_A \mathrm{d}x_B \mathrm{d}^2\vec{b}_\perp \mathrm{e}^{i\vec{b}_\perp \cdot \vec{Q}_\perp} \hat{\sigma}\left(x_A x_B s, \mu\right) \\ & \times f_A^{\mathrm{TMD}}\left(x_A, b_\perp, \mu, \zeta_A\right) f_B^{\mathrm{TMD}}\left(x_B, b_\perp, \mu, \zeta_B\right) + \ldots , \end{aligned} \tag{30}$$

where s is the center-of-mass energy and the rapidity scales satisfy $\zeta_A \zeta_B = Q^4 = (x_A x_B s)^2$, which can be obtained using Eq. (21). The $\ldots$ are power corrections or "higher-twist" contributions, and its general behavior should be $(\Lambda^2/Q^2)^\alpha \ln^\beta(\Lambda^2/Q^2)$ with $\alpha \geq 1$ and Λ being a soft-scale [50]. The QCD hard cross section $\hat{\sigma}$ at the one-loop level reads

$$\hat{\sigma}(x_A, x_B) = \left| 1 + \frac{\alpha_{\mathrm{s}} C_{\mathrm{F}}}{4\pi} \left(-L_Q^2 + 3L_Q - 8 + \frac{\pi^2}{6} \right) \right|^2 , \tag{31}$$

where $L_Q = \ln \frac{-Q^2 - i0}{\mu^2}$ and higher-order expressions can be found in [13, 51, 52]. Similarly for the SIDIS process, we have

$$\begin{aligned} \frac{\mathrm{d}\sigma}{\mathrm{d}Q_\perp^2} \;=\; & \int \mathrm{d}x \, \mathrm{d}z \, \mathrm{d}^2\vec{b}_\perp \mathrm{e}^{i\vec{b}_\perp \cdot \vec{Q}_\perp} \hat{H}(x, z, \mu, Q) \\ & \times f^{\mathrm{TMD}}(x, b_\perp, \mu, \zeta_A) D^{\mathrm{TMD}}(z, b_\perp, \mu, \zeta_B) + \ldots , \end{aligned} \tag{32}$$

where $\hat{H}$ is the hard kernel and D^{TMD} is the TMD fragmentation function.

3. TMDPDF in LaMET

After the introduction of LaMET, there are attempts to include TMDPDFs into the framework [34–37]. Unlike the case of quasi-PDFs, the quasi-TMDPDF and the targeting physical TMDPDFs all contain contributions from soft radiations. Therefore, a proper treatment of the soft function subtraction and matching is essential. Furthermore, the quasi-TMDPDFs as well as soft functions, defined with spacelike gauge links, suffer from additional complications due to the self-interactions of the staple-shaped gauge link. Recently, Refs. [33, 40, 41] provide a Euclidean realization of quasi-TMDPDFs and soft functions which include the proper treatment of those subtleties, capture the IR physics to all-orders, and allow for a perturbative matching to the physical TMDPDFs.

In this section, we discuss how to define and factorize quasi-TMDPDFs. The next sections are organized as follows: In Sec. 3.1, we review the definition of quasi-TMDPDF and discuss its new type of divergence, the pinch-pole singularity. In Sec. 3.2, we investigate the physical nature of pinch-pole singularity of quasi-TMDPDF, which can be removed by a rectangular Wilson loop using the exponentiation property. In Sec. 3.3, the ultra-soft mode of quasi-TMDPDF caused by two infinite long parallel gauge links with the opposite color flow is discussed. In Sec. 3.4, we provide a heuristic argument for factorization of quasi-TMDPDFs by observing that quasi-TMDPDFs are equivalent to TMDPDFs in the off-lightcone scheme. In Sec. 3.5, we perform the power-counting analysis of quark quasi-TMDPDFs and obtain the leading region of IR divergences in the large momentum limit. In Sec. 3.6, we provide the result of quasi-TMDPDF factorization in the on-lightcone scheme based on the leading region analysis. In Sec. 3.7, we present one-loop results and use RGE to make predictions for the two-loop hard kernel. A calculation strategy beyond the two-loop order is also suggested.

3.1. Definitions and basic properties

We define the quasi-TMDPDF with staple-shaped gauge link along the z direction [34, 35, 37, 41] as

$$\tilde{f}(x, b_\perp, \mu, \zeta_z) = \lim_{L\to\infty} \frac{1}{N} \int \frac{\mathrm{d}\lambda}{2\pi}\, \mathrm{e}^{i\lambda x} \frac{\langle \mathcal{P}|\tilde{O}_z(\lambda, b_\perp, L)|\mathcal{P}\rangle}{\sqrt{Z_{\mathrm{E}}(2L, b_\perp, \mu)}}\,, \tag{33}$$

where μ and $\zeta_z = (2x\mathcal{P}^z)^2$ are the renormalization and rapidity scales of the quasi-TMDPDF,

$$\tilde{O}_z(\lambda, b_\perp, L) = \bar{\psi}\left(\frac{\lambda\hat{z}}{2} + \frac{\vec{b}_\perp}{2}\right) \Gamma \mathcal{W}_z\left(\frac{\lambda\hat{z}}{2} + \vec{b}_\perp; L\right) \psi\left(-\frac{\lambda\hat{z}}{2} - \frac{\vec{b}_\perp}{2}\right)\,, \tag{34}$$

$\hat{z}=(0,\vec{0}_\perp,1)$, the normalization factor $N=|\mathrm{Tr}(\not{\mathcal{P}}\Gamma)|/2$, the invariant length $\lambda=z\mathcal{P}^z$, and

$$\mathcal{W}_z(\xi;L) = W_z^\dagger(\xi;L)W_\perp W_z(-\xi^z\hat{z};L)\,, \tag{35}$$

$$W_z(\xi;L) = \mathcal{P}\exp\left[-ig\int_0^{L-\xi^z}\mathrm{d}\lambda\hat{z}\cdot A(\xi+\hat{z}\lambda)\right]. \tag{36}$$

Here, $\xi^z=-\xi\cdot\hat{z}$. The transverse gauge link $W_\perp$ is inserted at $z=L$ to maintain the explicit gauge invariance, and $\sqrt{Z_\mathrm{E}(2L,b_\perp,\mu)}$ is the square root of the VEV of a rectangular spacelike Wilson loop along the z direction with length $2L$ and width $b_\perp$

$$Z_\mathrm{E}(2L,b_\perp,\mu)=\frac{1}{N_\mathrm{c}}\mathrm{Tr}\langle 0|W_\perp\mathcal{W}_z\left(\vec{b}_\perp;2L\right)|0\rangle\,, \tag{37}$$

where the subscript 'E' denotes that it is equivalent to the Euclidean Wilson loop. The definition in Eq. (33) is for DY process, whereas, for the SIDIS process, one should choose $-z$ direction for the staple-shaped gauge links. For a depiction of $\tilde{f}$ and Z_E, see Fig. 3.

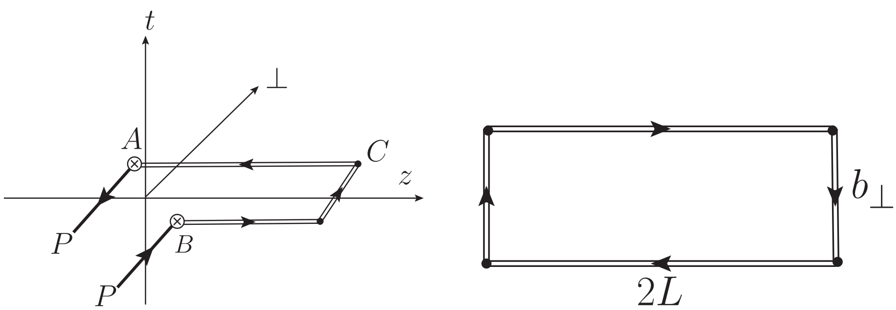

Fig. 3. The quasi-TMDPDF (left) and the Euclidean Wilson loop $Z_\mathrm{E}(2L,b_\perp,\mu)$ (right): $A=\lambda\hat{z}/2+\vec{b}_\perp/2$, $B=-\lambda\hat{z}/2-\vec{b}_\perp/2$, and $C=L\hat{z}+\vec{b}_\perp/2$. The $\otimes$ sign denotes the quark-link vertex.

The factor Z_E serves many purposes. First, it subtracts out the "pinch-pole singularity." At large L, the naïve quasi-TMD correlator in the numerator of Eq. (33) contains divergences that go as $\mathrm{e}^{-LE(b_\perp,\mu)}$, where $E(b_\perp,\mu)=2\delta m+V(b_\perp,\mu)$ is the ground-state energy of a pair of static heavy quarks. The factor δm is the linear divergent mass corrections part and $V(b_\perp,\mu)$ is the heavy-quark potential. In the perturbation theory, the "pinch-pole singularity" raised from interaction between two parallel non-lightlike gauge links with infinite length is equivalent to the heavy-quark potential term in $E(b_\perp,\mu)$ [53]. Second, Z_E removes the self-interactions of the gauge links and the cusp UV divergences from the gauge-link junctions. Therefore, we introduce the square root of $Z_{\mathrm{E}}(2L, b_\perp, \mu)$ to cancel the above divergences. The existence of the $L \to \infty$ limit will be proved formally based on a generalization of the exponentiation property of Wilson loops [54] in the next section.

We emphasize that since the quasi-TMDPDFs are defined by operators with purely spacelike separation, the time ordering is irrelevant. Therefore, we can interpret it in a single time-ordering as an amplitude, or in double time-ordering as the squared amplitude. The former and the latter can be evaluated in uncut and cut diagrams, respectively.

The quasi-TMDPDFs defined in Eq. (33) still contain logarithmic UV divergences associated with quark-Wilson-line vertices, and satisfy the following RGE:

$$\mu^2 \frac{\mathrm{d}}{\mathrm{d}\mu^2} \ln \tilde{f}(x, b_\perp, \mu, \zeta_z) = \gamma_{\mathrm{F}}(\alpha_{\mathrm{s}}(\mu))\,, \tag{38}$$

where γ_{F} is the anomalous dimension for the heavy-to-light quark current, which has been calculated to three loops [55–59]. In the $\overline{\mathrm{MS}}$ scheme, the one-loop quasi-TMDPDF in an external quark state with momentum $(p^z, 0, 0, p^z)$ reads [35, 37]

$$\begin{aligned} \tilde{f}(x, b_\perp, \mu, \zeta_z) \;=\; & \delta(1-x) + \frac{\alpha_{\mathrm{s}} C_{\mathrm{F}}}{2\pi} \Bigg\{ F(x, \epsilon_{\mathrm{IR}}, b_\perp, \mu)\theta(x)\theta(1-x) \\ & + \delta(1-x) \left[-\frac{1}{2} L_b^2 + L_b \left(\frac{5}{2} - L_z \right) - \frac{3}{2} - \frac{1}{2} L_z^2 + L_z \right] \Bigg\}\,, \end{aligned} \tag{39}$$

where F and L_b are defined in Eqs. (24) and (15), and

$$L_z = \ln \frac{\zeta_z}{\mu^2}\,. \tag{40}$$

As one can see, the L dependence has been canceled in the large-L limit. Since there is no lightlike gauge link in $\tilde{f}$, no additional rapidity regulator is needed. Instead, there is an explicit dependence on the hadron momentum, which is similar to the momentum RGE for the collinear quasi-PDF.

3.2. Pinch-pole singularity and exponentiation

In order to classify the diagrammatic structures of the pinch-pole singularity for the spacelike staple-shaped gauge link, we first consider a one-loop example shown in Fig. 4, then generalize to all orders. This diagram, called dipolar amplitude, can be understood as the elastic scattering of two color sources propagating in imaginary time, see Appendix A for more details

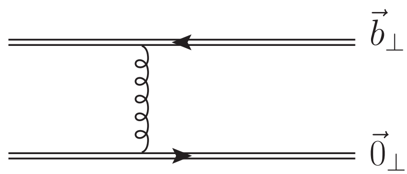

Fig. 4. The Feynman diagram of dipolar amplitude.

about analytic continuation between spacelike and timelike gauge link staples. The Feynman integral for the diagram is

$$\int \frac{\mathrm{d}k^0\,\mathrm{d}k^z}{(2\pi)^2}\frac{1}{k^z+i0}\frac{1}{k^z-i0}\frac{1}{(k^0)^2-(k^z)^2-k_\perp^2+i0}\,. \tag{41}$$

The $k^z=0$ poles for the two eikonal propagators are pinched due to opposite $i0$ prescriptions. Notice that the eikonal part can be rewritten as

$$\begin{aligned}\frac{1}{k^z+i0}\frac{1}{k^z-i0} &= \int_0^\infty \mathrm{d}z_1\,\mathrm{e}^{i(k^z-i0)z_1}\int_0^\infty \mathrm{d}z_2\mathrm{e}^{-i(k^z+i0)z_2}\\ &= \int_0^\infty \mathrm{d}z_2\int_0^{z_2}\mathrm{d}z_1\,\mathrm{e}^{i(k^z+i0)(z_1-z_2)}+\int_0^\infty \mathrm{d}z_1\int_0^{z_1}\mathrm{d}z_2\,\mathrm{e}^{i(k^z-i0)(z_1-z_2)}\\ &= \left(\frac{1}{k^z+i0}-\frac{1}{k^z-i0}\right)\frac{1}{-2i0}\,.\end{aligned} \tag{42}$$

We rearrange the ordering of z_1 and z_2 to obtain the last line. The first term corresponds to $z_1>z_2$ ordering while the second term corresponds to $z_2>z_1$. Since the gluon propagator is symmetric under $k^z\to -k^z$, we can make a change of variable to make the two terms identical. Therefore, we obtain a one-gluon exchange diagram

$$\frac{1}{-i0}\int\frac{\mathrm{d}k_0\,\mathrm{d}k^z}{(2\pi)^2}\frac{1}{k^z+i0}\frac{1}{(k^0)^2-(k^z)^2-k_\perp^2+i0}\,. \tag{43}$$

This result is almost identical to one particle irreducible (1PI) self-energy diagrams of a single gauge link except for an extra factor $1/i0$*, which makes the pinch-pole manifest.* The spirit of the above manipulation is that since a spacelike staple is independent of time ordering, we can include ordering of the z coordinates for the two gauge link staples at once, instead of doing it separately. Therefore, we introduce a composite gauge link, drawing in a single-line notation, to represent two parallel gauge links, see Fig. 5.

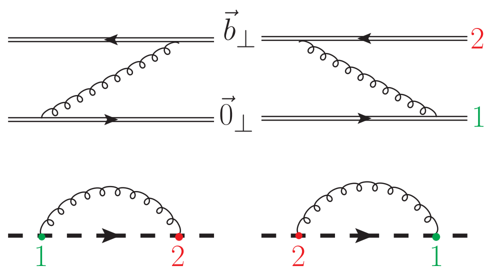

Fig. 5. The original Feynman diagram can be ordered in z coordinate (upper two), which can be represented using a single line (lower two).

In general, all the Feynman diagrams and their integrals for the staple-shaped gauge link can be represented using the single-line notation. However, the gluon-link vertices are distinguished into two types (1 for $\vec{0}$ and 2 for $\vec{b}_\perp$). For each diagram we need to sum over all different assignments of the vertices. For every type 2 vertex, there is an extra minus sign corresponding to the opposite color charge and an $\mathrm{e}^{-i\vec{k}_\perp\cdot\vec{b}_\perp}$ factor taking into account the transverse separation. To obtain the correct color factor, we first multiply all the color factors for type-1 vertices according to the path-ordering of the single line, then multiply with color factors for the type-2 vertices according to anti-path-ordering. See Fig. 6 for an example.

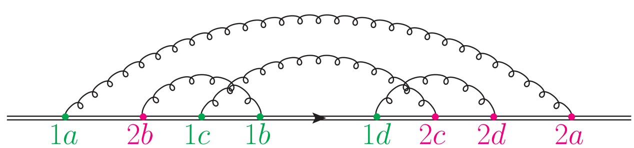

Fig. 6. To obtain the correct color factor $(T^bT^cT^dT^a)(T^dT^bT^cT^a)$: First multiply the color factors for type-1 vertices according to the path-ordering $(a \to c \to b \to d)$, and then for type-2 vertices according to the anti-path-ordering $(a \to d \to c \to b)$.

The purpose of introducing the single-line notation is to make the physical meaning clear: a pair of parallel gauge links with the opposite color flow can be treated as a composite particle propagating along the link direction. The timelike gauge link can be viewed as a heavy quark propagator in HQET, while the spacelike gauge link can be identified as an analytic continuation of the timelike link into imaginary time, see Appendix A for more details. In this single-line notation, the pinch-pole singularity is due to the link propagators between the self-interaction insertions becoming on-shell. This is similar to a single on-shell particle with the self-energy insertions, which need to be resumed to generate a field renormalization factor Z as well as a divergent imaginary time evolution factor $\lim_{t\to\infty} \mathrm{e}^{-Et}$, where E is the energy of the on-shell particle, calculated as the pole of the resumed one-particle propagator. To calculate a scattering amplitude, the external legs should be amputated by subtracting the time evolution phase factor and multiplying with the factor $Z^{-1/2}$ to maintain unitarity. This is the imaginary time version of the Lehmann–Symanzik–Zimmermann (LSZ) reduction formula. Similar to the single-particle case, the subtraction using $\sqrt{Z_{\mathrm{E}}}$ in Eq. (33) removes the divergent time evolution factor and removes a $Z^{1/2}$ factor. This is a generalization of the (LSZ) reduction formula for the staple-shaped gauge link.

In the standard double line notation of gauge link, it is the dipolar 2PI amplitudes insertions on the staple that generates the pinching, see Fig. 7. After the amputation of the dipolar amplitudes, the quark-link 2PI vertex is free from the pinching. This can also be shown by analyzing the pinching condition for the original eikonal propagators in the double line representation using other methods such as the Landau equation.

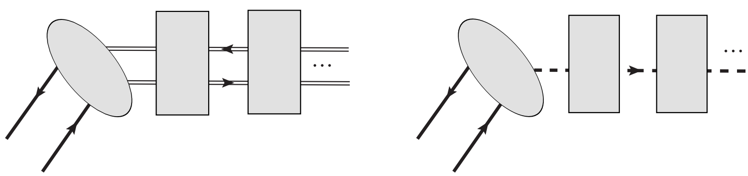

Fig. 7. The 2PI decomposition of quasi-TMDPDF. The elliptic blob is the quark-link 2PI vertex, and the rectangular box is the dipolar 2PI amplitude (also called self-interaction). The left figure uses the standard double line notation for gauge link, while the right one uses the single-line notation to represent a gauge link pair.

With the exponentiation property of gauge link, we show that the pinch-pole singularities can be removed by the Euclidean subtraction factor Z_{E}. It has been known that a vacuum expectation value of a Wilson loop can be exponentiated with a modified color factor [54, 60]

$$\mathrm{Tr}\langle 0|W(\mathcal{C})|0\rangle = \mathrm{e}^{\sum_{\mathrm{webs}} \Phi_{\mathrm{web}}(\mathcal{C})} = \mathrm{e}^{\Phi(\mathcal{C})}\,, \tag{44}$$

where $\Phi(\mathcal{C}) = \sum_{\mathrm{webs}} \Phi_{\mathrm{web}}(\mathcal{C})$ is the contribution from all web diagrams for an arbitrary contour $\mathcal{C}$. The web diagrams are 2PI diagrams for the Wilson loop with the modified "maximal non-Abelian" color factor. For example, at the two loop level, one normally encounters the color factor $T^bT^aT^bT^a = C_{\mathrm{F}}(C_{\mathrm{F}} - \frac{C_{\mathrm{A}}}{2})$ in which we only keep the maximal non-Abelian part $-C_{\mathrm{F}}C_{\mathrm{A}}/2$ in web diagrams, while the C_{F}^2 term will combine with the non-2PI diagram to form the exponential of one-loop contribution. In Appendix B, we briefly summarize the replica method to derive the exponentiation of Wilson loop.

Furthermore, we prove a stronger statement in Appendix B, namely the gauge link of arbitrary shape in a correlation function of a bilinear operator can be exponentiated. For example, consider the correlation function of the form of

$$F\left(\mathcal{C},x,x'\right)=\mathrm{Tr}\left\langle O(x)W\left(\mathcal{C},x'\to x\right)O'\left(x'\right)\right\rangle\,, \tag{45}$$

where O and O' are operators; the color indices are summed by taking the trace; $W(\mathcal{C},x'\to x)$ is a Wilson line of arbitrary shape, starting from x' and ending at x. Using diagrammatic methods, one can prove a partial exponentiation, which indicates that although the quantity inside the correlation functions is not a Wilson loop, the webs for the gauge link $W(\mathcal{C})$ still factorize

$$F\left(\mathcal{C},x,x'\right)=\mathrm{e}^{\Phi(\mathcal{C})}\mathrm{Tr}\left\langle O(x)W\left(\mathcal{C},x'\to x\right)O'\left(x'\right)\right\rangle_{\mathrm{2PI}}\,. \tag{46}$$

Here, $\mathrm{e}^{\Phi(\mathcal{C})}$ is the VEV of $W(\mathcal{C})$ with an overall trace, and $\mathrm{Tr}\langle\ldots\rangle_{\mathrm{2PI}}$ consists of the 2PI part of interactions of Os and gauge link with modified color factors. Given the partial exponentiation, we can apply it to the quasi-TMDPDF

$$\langle\mathcal{P}|\tilde{O}_z(\lambda,b_\perp,L)|\mathcal{P}\rangle=\mathrm{e}^{\Phi(\mathcal{W}_z)}\langle\mathcal{P}|\tilde{O}_z(\lambda,b_\perp,L)|\mathcal{P}\rangle_{\mathrm{2PI}}\,, \tag{47}$$

where $\tilde{O}$ is defined in Eq. (34), and $\Phi(\mathcal{W}_z)$ stands for the webs for the staple-shaped gauge links. As shown in Fig. 7, the quark-link 2PI vertex is free from pinching, all the pinch-pole singularities are included in $\mathrm{e}^{\Phi(\mathcal{W}_z)}=\langle 0|\mathcal{W}_z|0\rangle$. The VEV of a pair of spacelike gauge links can be interpreted as a pair of heavy quarks propagating in imaginary time, and is indeed of the form of $\mathrm{e}^{-LE(b_\perp)}$ in the large L limit. Since $Z_{\mathrm{E}}(2L,b_\perp,\mu)$ can also be interpreted as a pair of such heavy-quarks propagating in twice the imaginary time, its large-L behavior is of the form of $\mathrm{e}^{-2LE(b_\perp)}$. Thus, the pinch-pole singularities are indeed removed by $\sqrt{Z_{\mathrm{E}}}$.

This analysis is also helpful for higher-order calculations of quasi-PDFs and other distributions.

3.3. Ultra-soft mode and IR safety

After subtraction of the pinch-pole singularities, the quasi-TMDPDFs $\tilde{f}(x,b_\perp,\mu,\zeta_z)$ evaluated to a higher order in perturbation theory are still not IR safe. This is due to the ultra-soft modes for the gauge link staple, which is equivalent to a pair of heavy quarks in HQET.

It is known that the ground-state energy of this bound state (known as the heavy-quark potential) suffers from spurious IR divergences starting at the α_{s}^4 order [61, 62]. To explain such divergences, we first review similar problems in quantum electrodynamics (QED). Then we move on to the IR safety problem of the heavy-quark pair bound state. Finally, we discuss the ultra-soft mode of quasi-TMDPDF.

In a hydrogen atom, the Bohr radius is of the order of $1/(\alpha_e m_e)$, where α_e is the fine structure constant and m_e is the electron mass, but the binding energy is of the order of $\alpha_e^2 m_e$. The difference in the two scales can result in deep consequences. To calculate the correction to the binding energy, one needs to consider the diagram where a soft photon is emitted from the electron at time t_1 and reabsorbed later at t_2, between which there can be arbitrary numbers of Coulomb exchanges between the electron and the proton. Naïvely evaluating those diagrams to high order in α_e will generate IR divergences, see Fig. 8. After resumming the Coulomb exchanges, the dressed electron self-energy is regulated by δE, the difference between the ground and the first excited state, which gives $\ln(\delta E/m_e) \sim \ln \alpha_e$. This leads to the famous Lamb shift [63]. In the language of non-relativistic QED, there are soft gluons with momenta $k \sim m_e \alpha_e$ as well as the ultra-soft gluon with momenta $k \sim m_e \alpha_e^2$. It is the exchange of these ultra-soft gluons as soft as the binding energy that generates the additional logarithms $\ln \alpha_e$.

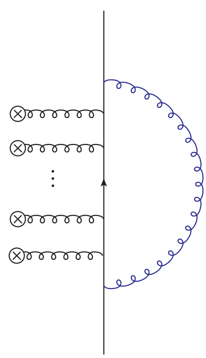

Fig. 8. A typical Lamb shift diagram receiving ultra-soft contribution. The spurious IR divergences generated by this diagram are removed after resummation of external field insertion (indicated by the $\otimes$ symbol).

For the bound-state formed by a pair of color–anti-color charges (equivalent to a pair of heavy quarks in HQET) with a transverse separation b, similar to the QED case, we again encounter the ultra-soft contributions generating additional $\ln \alpha_{\rm s}$ after resummation of heavy-quark mutual-interactions, as shown in Refs. [61, 62]. This is due to similar diagrams where the 2PI self-interactions are inserted between the soft-gluon emission and absorption, see Fig. 9. The color charges in the soft-gluon exchanges can be either in the singlet or the octet channel. Therefore, we expect that there are two energy scales available: the heavy-quark potential $V(b)$ in the singlet channel and $V_8(b)$ in the octet channel. After exponentiation, however, only their difference $V_8 - V$ contributes to the web diagrams, since the time evolution

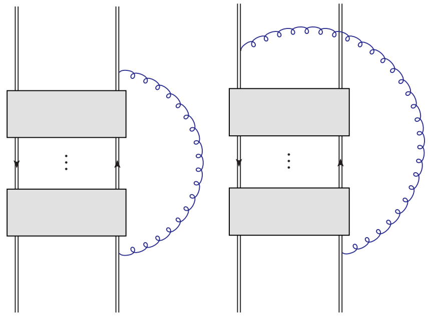

Fig. 9. Diagrams receiving ultra-soft contribution in binding energy in HQET. The bound state is formed by color–anti-color sources with a transverse separation. Similar to the Lamb shift in QED, the spurious IR divergences are removed after resummation of 2PI self-interactions.

factor in the singlet channel has already been captured by the overall factor $\mathrm{e}^{-iTV(b)}$. Thus, it is the energy difference between the singlet and octet channels that regulates the IR divergence [61]. In the perturbation theory, the heavy-quark potential is of the order of α_s/b, as well as the ultra-soft modes after the resummation. Again, the ultra-soft modes are $\mathcal{O}(\alpha_\mathrm{s})$ smaller compared to the size of the system b.

For the quasi-TMDPDFs, the staple-shaped gauge links can be viewed as a pair of color–anti-color charges, therefore, it naturally suffers from IR divergences associated with ultra-soft modes, see Fig. 10. Beyond three-loops, they cause power divergences in the high-order calculation, and the ultra-soft divergence scales as $1/L$. The IR safety is restored after the resummation of dipolar 2PI amplitude, which corresponds to the self-energy resummation in the single-line notation. After the resummation, individual diagrams with the dressed single-line propagator diverge at most logarith-

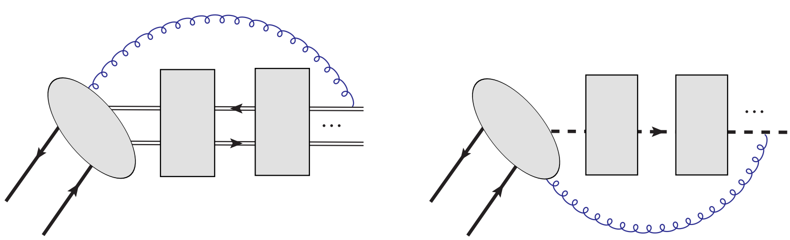

Fig. 10. Diagrams receiving ultra-soft contribution in quasi-TMDPDFs. The left figure is the standard Feynman diagram, while the right one is using the single-line notation to represent a pair of gauge links. The spurious IR divergences are removed after resummation of 2PI self-interactions.

mically, and a leading order analysis is possible. We should emphasize that in the perturbation theory, the ultra-soft modes after resummation are of the order of $\alpha_\mathrm{s}/b_\perp$. For $1/b_\perp \sim \Lambda_\mathrm{QCD}$, $\alpha_\mathrm{s} \sim 1$, thus in the completely non-perturbative situation, we expect that there is no clear distinction between the soft modes at the energy scale $1/b_\perp$ and the ultra-soft modes.

3.4. Heuristic argument for the factorization

In this subsection, we study the factorization from quasi-TMDPDFs to physical TMDPDFs and provide a heuristic argument for the matching formula. The idea lies in the rapidity regularization scheme independence of the physical TMDPDF f^TMD. To define f^TMD, one can choose an off-lightcone scheme such that the gauge links in both unsubtracted TMDPDF f and soft function S are off the lightcone [11]. In the off-lightcone scheme, there are pinch-pole singularities for space-like staple-shaped gauge links which require $\sqrt{Z_\mathrm{E}}$ subtractions similar to quasi-TMDPDFs in Eq. (33). Due to the Lorentz invariance, the stapled-shaped gauge link $\mathcal{W}_n$ as well as the subtraction factors for f can be boosted to z direction. One then obtains the equality between the unsubtracted TMDPDFs and the quasi-TMDPDFs with large momentum external state enhanced by the boost. The off-lightcone rapidity divergences of the unsubtracted TMDPDFs have been transmuted into the $\ln\mathcal{P}^z$ dependence of the quasi-TMDPDFs. The $\mathcal{P}^z$ evolution of $\tilde{f}$ is therefore equivalent to the rapidity evolution of TMDPDFs. Indeed, the momentum (rapidity) evolution equation for $\tilde{f}$ is proved in Ref. [1]

$$\mathcal{P}^z \frac{\mathrm{d}}{\mathrm{d}\mathcal{P}^z} \ln \tilde{f}(x, b_\perp, \mu, \zeta_z) = K(b_\perp, \mu) + \mathcal{G}\left(\frac{\zeta_z}{\mu^2}\right), \tag{48}$$

where $\mathcal{G}(\zeta_z/\mu^2)$ is perturbative, $K(b_\perp, \mu)$ is the Collins–Soper kernel, and $K + \mathcal{G}$ is independent of μ [1]. From this equation, it is clear that a correct matching to $f^\mathrm{TMD}(x, b_\perp, \mu, \zeta)$ with arbitrary ζ must include $(\ln\mathcal{P}^z)K(b_\perp, \mu)$ terms to compensate for the $\mathcal{P}^z$ dependence. After subtracting the $\mathcal{P}^z$ dependent part, there is still an off-lightcone scheme dependence which is independent of $\mathcal{P}^z$ and must be removed using the off-lightcone soft function.

The soft function for the DY process in the off-lightcone scheme in Eq. (8) is

$$S_\mathrm{DY}\left(b_\perp, \mu, Y, Y'\right) = \frac{\mathrm{Tr}\langle 0|\mathcal{W}_{n_{Y'}}\left(\vec{b}_\perp\right)\mathcal{W}^\dagger_{p_Y}\left(\vec{b}_\perp\right)|0\rangle}{N_\mathrm{c}\sqrt{Z'_\mathrm{E}}\sqrt{Z_\mathrm{E}}}, \tag{49}$$

where Y and Y' are the rapidities of the off-lightcone spacelike vectors $p \to p_Y = p - \mathrm{e}^{-2Y}(p^+)^2 n$ and $n \to n_{Y'} = n - \mathrm{e}^{-2Y'}\frac{p}{(p^+)^2}$; $\mathcal{W}_{n_{Y'}}(\vec{b}_\perp)$ and $\mathcal{W}^\dagger_{p_Y}(\vec{b}_\perp)$

are staple-shaped gauge links in $n_{Y'}$, p_Y directions. $\sqrt{Z_{\mathrm{E}}}$ is introduced to subtract the pinch-pole singularities for the off-lightcone staple-shaped gauge links. At large Y and Y', we have

$$S_{\mathrm{DY}}\left(b_\perp,\mu,Y,Y'\right)=\exp\left[\left(Y+Y'\right)K(b_\perp,\mu)+\mathcal{D}(b_\perp,\mu)+\mathcal{O}\left(\mathrm{e}^{-(Y+Y')}\right)\right]. \tag{50}$$

Due to the boost invariance, $S_{\mathrm{DY}}(b_\perp,\mu,Y,Y')=S_{\mathrm{DY}}(b_\perp,\mu,Y+Y',0)$. We discover that the off-lightcone soft function can be formulated in the Euclidean space as a form factor, see Sec. 4 for a detailed discussion.

Since the rapidity-dependent part proportional to K has been taken into account by the $(\ln\mathcal{P}^z)K$ terms introduced before, the square root of the rapidity-independent part $\mathrm{e}^{\mathcal{D}(b_\perp,\mu)}$ is exactly what is needed to cancel the remaining rapidity-scheme dependence. We define it as the intrinsic soft function

$$S_{\mathrm{I}}(b_\perp,\mu)\equiv\mathrm{e}^{-\mathcal{D}(b_\perp,\mu)}\,. \tag{51}$$

We emphasize that S_{I} is defined only in the off-lightcone scheme. In Secs. 4.4 and 5, we will show that S_{I} is rapidity-scheme-independent, while the rapidity-independent part of the soft function is, in general, scheme-dependent.

With the above ingredient, we can write down the matching formula between the quasi-TMDPDF and the physical TMDPDF

$$\begin{aligned}\tilde{f}(x,b_\perp,\mu,\zeta_z)\sqrt{S_{\mathrm{I}}(b_\perp,\mu)} &= H\left(\frac{\zeta_z}{\mu^2}\right)\mathrm{e}^{\frac{1}{2}\ln\left(\frac{\zeta_z}{\zeta}\right)K(b_\perp,\mu)}f^{\mathrm{TMD}}(x,b_\perp,\mu,\zeta)\\ &\quad+\mathcal{O}\left(\frac{\Lambda_{\mathrm{QCD}}^2}{\zeta_z},\frac{M^2}{(\mathcal{P}^z)^2},\frac{1}{b_\perp^2\zeta_z}\right).\end{aligned} \tag{52}$$

The above relation except for the definition of $S_{\mathrm{I}}(b_\perp,\mu)$ was argued to hold in [37] and recently confirmed in [41, 64].

The perturbative matching kernel $H\left(\frac{\zeta_z}{\mu^2}\right)$ is responsible for the large logarithms of $\mathcal{P}^z$ generated by the $\mathcal{G}\left(\frac{\zeta_z}{\mu^2}\right)$ term of the momentum evolution equation. Unlike the quasi-PDFs, the momentum fractions of the quasi-TMDPDF and the physical TMDPDF are the same. This is due to the fact that at leading power in $\frac{1}{\zeta_z}$ expansion, the $k_\perp$ integral is naturally cut-off by the transverse separation around $k_\perp\sim\frac{1}{b_\perp}\ll\mathcal{P}^z$. Therefore, the momentum fraction can only be modified by collinear modes for which there are no distinction between $x=\frac{k^z}{\mathcal{P}^z}$ and $x=\frac{k^+}{\mathcal{P}^+}$. This is also consistent with the fact that the momentum evolution equation for quasi-TMDPDF is local in x instead of being a convolution.

From the momentum evolution equation, the factor $\exp[\ln(\zeta_z/\zeta)K(b_\perp,\mu)]$ is required to match the TMDPDFs at arbitrary ζ. An important implication of this property is that one can obtain the Collins–Soper kernel $K(b_\perp,\mu)$

by constructing the ratio of quasi-TMDPDFs at two different momenta or ζ_zs [36]

$$\frac{\tilde{f}(x, b_\perp, \mu, \zeta_{z,1})}{\tilde{f}(x, b_\perp, \mu, \zeta_{z,2})} = \frac{H\left(\frac{\zeta_{z,1}}{\mu^2}\right)}{H\left(\frac{\zeta_{z,2}}{\mu^2}\right)} \left(\frac{\zeta_{z,1}}{\zeta_{z,2}}\right)^{K(b_\perp,\mu)} . \tag{53}$$

Thus, given the $\tilde{f}$s at the two rapidity scales, the Collins–Soper kernel $K(b_\perp, \mu)$ can be obtained.

3.5. Leading region analysis

We now perform the leading region analysis for the quark quasi-TMDPDFs with a lightlike external state. The structure of IR divergences can be obtained by solving the Landau equation, see Appendix C. There are collinear divergences associated with the external state, and soft divergences caused by soft-gluon radiations from the fast moving color-charges and/or the gauge link staples. The pinch-pole singularities for the staple-shaped gauge links correspond to a different type of solution to the Landau equation. As we have seen, they have been removed by the subtraction factor Z_{E}. We first discuss the power-counting in $1/(b_\perp \mathcal{P}^z)$ of the hard, collinear, and soft contributions, then show that there is only one collinear direction corresponding to that of the external state, whereas the gauge link propagator cannot participate in the collinear divergences.

We first discuss the scaling behavior and then determine the power-counting formula between the different regions. In the collinear region, the momentum is of the order of $(1, \lambda^2, \lambda)$ in $(+, -, \perp)$ coordinate where $\lambda \sim 1/(b_\perp \mathcal{P}^z)$ is the power-counting parameter. The soft region at the individual order of α_{s} can be very complicated. The standard soft momentum scale as $(\lambda, \lambda, \lambda)$, but there can also be an ultra-soft momentum scale as $1/L$ where L is the length of the staple shaped gauge link. As we have seen in Sec. 3.3, after resummation of the gauge link self-energy in the single-line notation, the ultra-soft modes scale as $\alpha_{\mathrm{s}}(\lambda, \lambda, \lambda)$. Since $\alpha_{\mathrm{s}} \sim 1$, the soft and ultra-soft cannot be distinguished anymore. Besides the soft/ultra-soft and collinear propagators, there are hard propagators scaling as $(1, 1, 1)$ around the quark-link vertexes. If a collinear gluon inserts into a gauge link, then the momentum of the gauge link is of the order of $1/\mathcal{P}^z$, which is hard, see Fig. 11. A gauge link sourced by a soft gluon is still soft.

Given the scaling behavior of propagators, we present the power-counting formula. We adopt the single-line notation of the gauge link staple in Sec. 3.2. The vertexes around $0_\perp$ or $b_\perp$ are hard. The hard sub-diagram which contains the quark-link vertex is denoted as H. Other hard sub-diagrams, not connected to H, containing no gauge link insertion are denoted as H', otherwise they are labeled H'', see Fig. 12. Both H' and H''

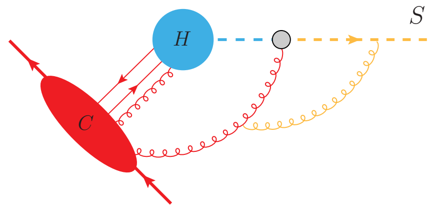

Fig. 11. The gauge link of TMDPDF with gluon insertion. The gauge link sourced by a collinear gluon is hard, and by a soft gluon is still soft.

are called the isolated hard kernels. The collinear sub-diagram is denoted as C, according to the Landau equation, the collinear region associated with the external hadron must be connected. The soft sub-diagram is denoted as S.

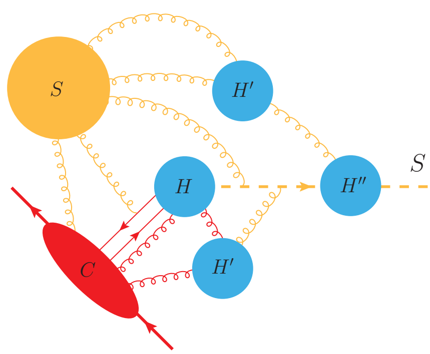

Fig. 12. Examples of the isolated hard kernels H' and H''.

To obtain the power-counting formula, we use the single-line notation of the staple defined in Sec. 3.2 to avoid complications caused by the ultra-soft modes from gauge links in the standard Feynman diagrams. Notice that the staple in the single-line notation has mass dimension 3/2. Based on the standard dimensional analysis and a boost argument, the power-counting formula is of the form of

$$\lambda^{F(H)}\lambda^{F(SC)}\lambda^{F(H')}\lambda^{F(H'')}\,, \tag{54}$$

where $F(H)$, $F(SC)$, $F(H')$, and $F(H'')$ are the power-counting exponents associated to H, soft to collinear, H', and H'' sub-diagrams. We use the $N(CH, d, s)$ to denote the connection numbers of the collinear to hard from a particle with the mass dimension d and spin s. For $d = 1$, there are gluons ($s = 1$) and ghosts ($s = 0$); For $d = 3/2$, there are quarks ($s = 1/2$) and staple in single-line notation ($s = 0$). Other connection numbers, such as

$N(CH', d, s)$ and $N(SC, d, s)$, are defined similarly. The $\mathcal{P}^z$ dependence in factors Fs must be compensated by the soft scale $b_\perp$, since the overall mass dimension of quasi-TMDPDF is a constant. Therefore, we can obtain the power-counting in λ by only considering $\mathcal{P}^z$. The factors are derived as follows:

— Hard kernel sub-diagrams H.

$$F(H) = -D(H) - B(H) + 1\,, \tag{55}$$

where $D(H)$ is the mass dimension of the hard kernel counted as the amputated Feynman diagram, and $B(H)$ is the boost enhancement factor of the operator insertion to the hard kernel. Since the momenta inside the hard core is of the order of $\mathcal{P}^z$, the contribution of the hard core is proportional to $(\mathcal{P}^z)^{D(H)}$. The mass dimension $D(H)$ reads

$$D(H) = \tfrac{9}{2} - N_i d_i\,, \tag{56}$$

where $9/2$ is the mass dimension of the quark-link vertex in the single-line notation, and it comes from two external quarks operator $(2\times 3/2)$ and the gauge link in the single-line notation $(3/2)$. N_i and d_i are the numbers and mass dimensions of collinear and soft propagator insertions for a given type i. Since the staple does not contribute to collinear divergence (see Appendix C), we consider quarks, gluons, gauge link staple, and ghosts

$$\begin{aligned}\sum_i N_i d_i \;=\; & \sum_{s_i=0,1} \left[N(CH,1,s_i) + N(SH,1,s_i)\right] \\ & + \tfrac{3}{2} N\left(CH, \tfrac{3}{2}, \tfrac{1}{2}\right) + \sum_{s_i=0,\,\frac{1}{2}} \tfrac{3}{2} N\left(SH, \tfrac{3}{2}, s_i\right)\,. \end{aligned} \tag{57}$$

Besides the mass dimension, there is a boost enhancement factor $B(H)$ associated with the total spin of collinear particles inserted into the hard core. For the spin-0 particle (ghost), there is no enhancement factor. For each of the spin-1/2 fermions, we receive a $(\mathcal{P}^z)^{\frac{1}{2}}$ enhancement from the Dirac spinor. For the longitudinal polarized gluon, A^+ component gets $\mathcal{P}^z$ enhancement and A^- component receives $1/\mathcal{P}^z$ suppression, while for the transverse polarized gluon, no enhancement appears in $A^\perp$. We have

$$B(H) = N(CH, 1, \ell) + \tfrac{1}{2} N\left(CH, \tfrac{3}{2}, \tfrac{1}{2}\right)\,, \tag{58}$$

where ℓ denotes the longitudinal component of gluon. Finally, there is an overall normalization factor $1/\mathcal{P}^z$, which gives an extra +1 in $F(H)$. Thus, we obtain

$$\begin{aligned} F(H) &= \sum_{s_i=0,1}\left[N(CH,1,s_i)+N(SH,1,s_i)\right]+N\left(CH,\tfrac{3}{2},\tfrac{1}{2}\right) \\ &\quad+\sum_{s_i=0,\,\frac{1}{2}}\tfrac{3}{2}N\left(SH,\tfrac{3}{2},s_i\right)-N(CH,1,\ell)-\tfrac{7}{2}\,. \end{aligned} \tag{59}$$

— Soft-to-collinear sub-diagrams.
Since the gauge link staple does not participate in collinear divergence, we consider soft particles (gluons, quarks, and ghosts) inserted into the collinear sub-diagram. There is a $1/\mathcal{P}^z$ factor caused by the collinear propagator in the soft-to-collinear approximation $(k_C+k_S)^2 \approx 2k_C \cdot k_S \sim \mathcal{P}^z k_S^-$ where k_C and k_S are generic collinear and soft momenta and the boost enhancement factor is $(\mathcal{P}^z)^s$ for the spin s particle. Therefore, we have

$$F(SC)=\tfrac{1}{2}N\left(SC,\tfrac{3}{2},\tfrac{1}{2}\right)+N(SC,1,0)\,. \tag{60}$$

— Isolated hard kernel sub-diagrams H'.
Without gauge link insertion, they can be classified into three types of sub-diagrams for H', $F(H')=F(SH')+F(CH')+F(SCH')$, see Fig. 13 for an example.

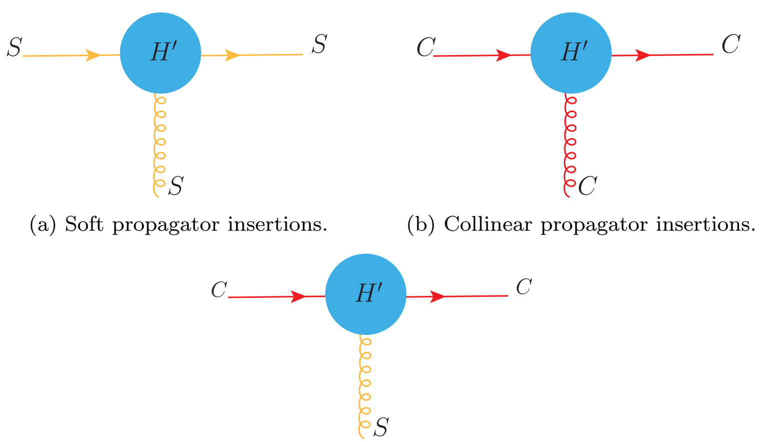

(a) Soft propagator insertions.

(b) Collinear propagator insertions.

(c) Soft and collinear propagator insertions.

Fig. 13. Isolated hard region H' without gauge link insertion. S and C denote soft and collinear propagator insertions. In (a), (b), and (c) cases, the hard region can be absorbed into the soft, collinear, and soft-to-collinear regions.

1. Only soft propagator insertions.
   The hard momentum inside the isolated hard kernel H' can only come from UV sub-divergences. UV sub-divergences generate additional logarithms unless they are power-divergent, which is forbidden in QCD due to the gauge invariance and chiral symmetry. Such logarithmic divergences can be removed by renormalization. Thus, $F(SH') = 0$ and H' can be absorbed into the soft region.

2. Only collinear propagator insertions.
   Since there is one collinear direction (we will prove it later), we can perform a boost, such that all the collinear propagators become soft. Based on the same argument, the UV sub-divergences can be removed by renormalization, and $F(CH') = 0$. Therefore, this sub-diagram can be absorbed into the collinear region.

3. Soft and collinear propagator insertions.
   Since there is only one collinear direction, the collinear propagator insertion cannot generate a hard scale. Thus, H' comes from UV sub-divergences which can be removed by renormalization. Since the Lorentz structure of quark–gluon and gluon–gluon vertices is unchanged by renormalization, the soft insertion into H' still receives the same Lorentz enhancement as the soft-to-collinear insertion. Thus, the power-counting of $F(SCH')$ is identical to $F(SC)$

$$F(SCH') = F(SC)\,. \tag{61}$$

   Therefore, one can absorb $F(SCH')$ into the soft-to-collinear region, $F(SC)$.

In conclusion, since the divergence of the isolated hard kernel can always be absorbed into anther region, H' cannot contribute to power counting, $F(H') = 0$.

— Isolated hard kernel sub-diagrams H''.
With the gauge link insertion, if there is also collinear propagator insertion, see Fig. 14 (a), there will be contradiction to the Landau equation and $N(CH'', d_i, s_i) = 0$. Diagrammatically, this can be obtained by analyzing the gauge link propagators. The momentum k^z integration for the gauge link propagator between H and H'' can always be deformed away due to the $i\epsilon$ prescriptions in the link propagator. Next, we are left with an isolated hard region with the soft propagator insertion, see Figs. 14 (b) and 14 (c). The hard scale must come from the

UV sub-divergence, and thus can be removed by renormalization. For more detailed analysis, take the case with no other propagator insertion as an example, see Figs. 14 (c). This isolated hard region can be removed by self-energy resummation in the single-line notation. Such self-energy contribution in standard Feynman diagrams actually corresponds to two cases, one is gauge link self-energy, and the other is interaction between two gauge links; we can remove the divergence by renormalization of gauge link in the former case, and resummation of the gauge link propagator in the latter case. In summary, this type of isolated hard kernel cannot contribute to power counting, $F(H'') = 0$. We emphasize that the isolated hard region without other propagator insertion can induce the ultra soft region, see Fig. 10, scaling as $1/L$, as discussed in Sec. 3.3.

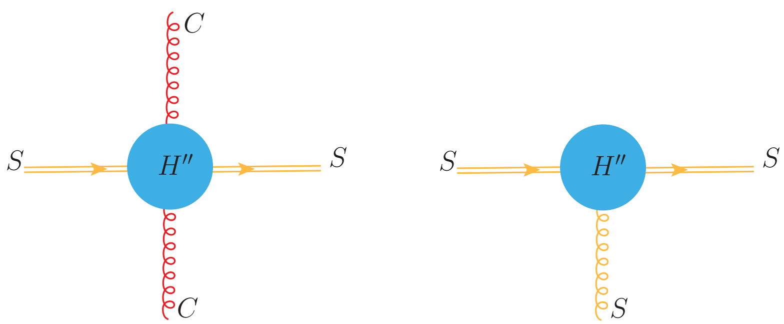

(a) Collinear propagator insertions.

(b) Soft propagator insertion.

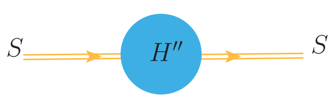

(c) No other propagator insertion.

Fig. 14. Isolated hard region H'' with gauge link insertions. In Fig. (a), the collinear propagator insertion is not allowed. In Figs. (b) and (c), the hard region can be absorbed into the soft regions. The H'' in Fig. (c) can induce ultra-soft divergence, which can be removed by resummation.

Based on the power-counting formula above, we need further discussions to obtain the leading region for the quark quasi-TMDPDFs. First, we have assumed that there is only one collinear direction, which needs to be justified. Second, we show that there is no "super leading" region. Finally, we show that the hard sub-diagram is homogeneously hard, namely all the components of the momentum scale as $\mathcal{P}^z$.

We first show that collinear divergence can only be in p direction associated with the external state (we also show this result based on the Landau equation in Appendix C). This property is straightforward using the uncut diagram. To cause collinear divergence, the on-shell particles carrying collinear momenta must propagate to infinity. However, there are only external states moving in p direction. Thus, there is no other possibility to have a different collinear direction. Alternatively, we can use a cut diagram to argue this property (the equivalence of an uncut and cut diagram for quasi-TMDPDFs is explained in Sec. 2). For individual cut diagram, since there is large momentum transfer at the vertex, there may be additional collinear divergences caused by on-shell particles passing through the cut. See Fig. 15 for example, at $t = 0$, two collinear particles with three-momenta $\vec{p}_1$ and $\vec{p}_2$ are emitted by the gauge link at $\vec{z}$ and the vertex, respectively. If $p_1^z = 0$, the gauge link also participates in the collinear singularity. At $t > 0$, the particles collide and participate in the isolated hard region H', and then create two collinear particles with three-momenta $\vec{p}'_1$ and $\vec{p}'_2$ passing through the cut. However, following the "sum-over-cuts" argument [11], all the collinear divergences except the one in p direction canceled between diagrams. Therefore, we are left with only one collinear region C, and the gauge link propagators decouple from collinear divergences.

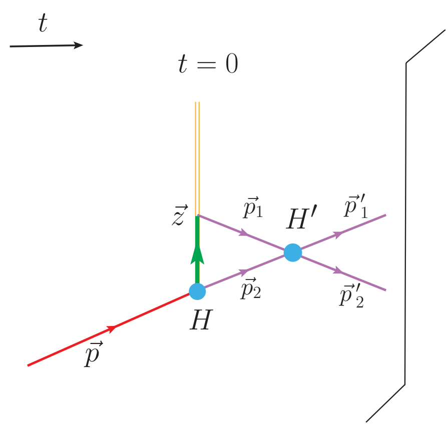

Fig. 15. An example of a possible sub-diagram with more than one collinear direction in the cut diagram. The particles collide at an isolated hard region H', and then create two collinear particles. The three-momenta $\vec{p}_1$, $\vec{p}_2$, $\vec{p}'_1$, and $\vec{p}'_2$ can be in different directions. If $p_1^z = 0$,, the gauge link segment $\vec{z}$ also participates in the collinear singularity. As required by the Landau equation, the displacement $\vec{z}$ relates to the particle momenta through $\frac{\vec{p}_1}{E_{\vec{p}_1}} t + \vec{z} = \frac{\vec{p}_2}{E_{\vec{p}_2}} t$, where $t > 0$ is the time where the two collinear particles collide. The collinear divergences other than the one in p direction are canceled between diagrams.

Second, we show that there is no "super leading" region which means the exponents of the power-counting formula become negative. For the hard region $F(H)$, since there are always two external quarks inserted into this region, $N\left(CH, \frac{3}{2}, \frac{1}{2}\right) + \frac{3}{2}N\left(SH, \frac{3}{2}, \frac{1}{2}\right) \geq 2$ (the equality satisfies if both quarks are collinear). There is also away one external soft staple in single-line notation inserted into H, $\frac{3}{2}N\left(SH, \frac{3}{2}, 0\right) = \frac{3}{2}$. Besides, $N(CH, 1, 1) - N(CH, 1, \ell) \geq 0$, and therefore, $F(H) \geq 0$. For soft-to-collinear subdiagrams, it is obvious that $F(SC) \geq 0$. Thus, there is no super leading region.

Finally, we should mention that although there is a special direction z, in which the Lorentz invariance is broken by the gauge link propagator, the hard region is still homogeneously hard, namely, all components of hard momenta in H are of the order of $\mathcal{P}^z$. The previous power-counting result relies on this homogeneity assumption. To show the above statement, the gauge link propagators with momenta p_i in the hard region H can always be written in the form of

$$\prod_{j=1}^{N} \frac{1}{\sum_{k=j}^{N} p_k^z + i0}\,, \tag{62}$$

where p_1^z to p_N^z are momenta of hard gluons inserted into the gauge links labeled according to the path ordering. Inside the 2PI vertex in Fig. 7, one can write p_i^zs to be linear combinations of loop momenta k_j, such that

$$p_i = \sum_{l} a_{ij} k_j\,, \tag{63}$$

where $a_{ik} \geq 0$ and at least one a_{ij} is non-zero for any i. In this case, the contour integration for all the k_j^z can be deformed away from $k_j^z = 0$ region into the upper half-plane, similar to the reason that H'' allows no collinear insertion. Therefore, in the hard region the gauge link propagators are not pinched in the small k^z region. pinching means that there is no IR contribution. Therefore, the hard kernel is homogeneously hard. The same representation also leads to the absence of the Glauber region ($k^+k^- \ll k_\perp$) at small k^+ and k^-. By writing $\sqrt{2}k^z = k^+ - k^-$, the Glauber region can be avoided by deforming k^+ into the upper half-plane. Thus, the deformations that one chooses to get rid of the small k^z modes inside the hard region are essentially identical to avoiding the Glauber region.

Thus, based on the above analysis for quark quasi-TMDPDFs, we summarize the power-counting of the leading region

$$
\begin{aligned}
N\left(CH, \tfrac{3}{2}, \tfrac{1}{2}\right) &= 2\,, & (64)\\
N\left(SH, \tfrac{3}{2}, 0\right) &= 1\,, & (65)\\
N(CH, 1, \ell) &= \text{arbitrary}\,, & (66)\\
N(SC, 1, 1) &= \text{arbitrary}\,, & (67)\\
N(\text{others}) &= 0\,. & (68)
\end{aligned}
$$

The leading region is then shown in Fig. 16 in the single-line notation and in Fig. 17 using the standard Feynman diagram notation.

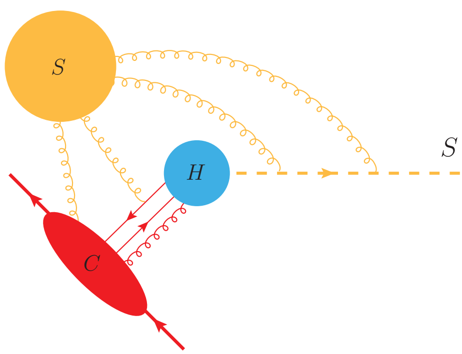

Fig. 16. The leading region of the quasi-TMDPDF in the single-line notation.

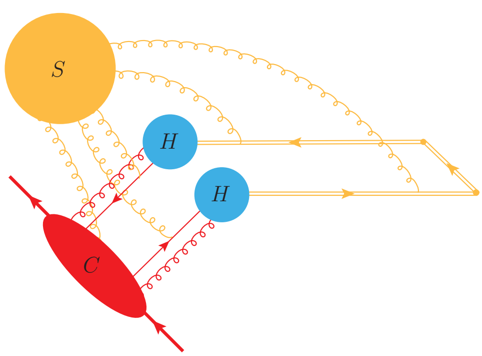

Fig. 17. The leading region of the quasi-TMDPDF in the standard Feynman diagram notation.

3.6. Factorization in on-lightcone regulator

Given the structure of the leading region in Figs. 16 and 17, we can use standard soft-to-collinear and collinear-to-hard approximations [11] to factorize the leading soft and collinear contributions of quasi-TMDPDFs. The soft-to-collinear approximation is possible since the Glauber region can be deformed away, as shown in Sec. 3.5. Here, we briefly summarize the soft-to-collinear approximations. For a soft gluon with momentum k_S inserted into the collinear diagram, the integrand can be written in the form of

$$S^{\mu}(k_S)C_{\mu}(k_S+k_C)\,. \tag{69}$$

Here, the S^{μ} denotes the contribution of the soft sub-diagram, and μ is the Lorentz index. $C_{\mu}(k_S+k_C)$ is the contribution of the collinear sub-diagram, where k_C is a generic collinear momentum. The leading contribution is given by

$$S^{-}(k_S)C^{+}(k_S+k_C)\sim S^{\mu}(k_S)\frac{p_{\mu}}{k_S\cdot p}(k_S\cdot p\,n^{\nu})C_{\nu}(k_S\cdot p\,n+k_C)\,. \tag{70}$$

In the formula, we keep only the largest components of the collinear sub-diagram $C^{+}\propto n^{\nu}C_{\nu}$ and the soft momentum $k_S^{-}\propto k_S\cdot p$. By writing $\bar{k}_S=k_S\cdot p\,n^{\nu}$, the $(k_S\cdot p\,n^{\nu})C_{\nu}(k_S\cdot p\,n+k_C)$ can be written as a longitudinal insertion

$$(k_S\cdot p\,n^{\nu})C_{\nu}(k_S\cdot p\,n+k_C)=\bar{k}_S^{\nu}C_{\nu}\left(\bar{k}_S+k_C\right)\,. \tag{71}$$

We then fix the soft sub-diagram S and sum over all possible insertions into the collinear sub-diagram. Ward-identities shall be used to simplify the longitudinal insertions and factorize the soft contributions into soft functions following the arguments in [11]. Following this approach, the soft radiations of quasi-TMDPDFs between the gauge link staple in z direction and the external state is factorized using the soft function

$$S(b_\perp,\mu,\delta^+,\hat{z})=\frac{\langle 0|\mathcal{W}_z\left(\vec{b}_\perp;L\right)\mathcal{W}_p^{\dagger}\left(\vec{b}_\perp\right)|_{\delta^+}|0\rangle}{\sqrt{Z_{\mathrm{E}}(2L,b_\perp,\mu)}}\,, \tag{72}$$

where δ^+ is a generic on-lightcone rapidity regulator, and $\hat{z}$ in the argument indicates that the gauge link staple is pointing to z direction. This soft function contains pinch-pole singularity of the staple in z direction, which requires subtraction $\sqrt{Z_{\mathrm{E}}}$, while the other lightcone staple is free from such divergence. Similar to the soft-to-collinear approximation summarized above [11], the collinear contribution of quasi-TMDPDF can be obtained using the collinear-to-hard approximation, which leads to the TMDPDFs with soft function subtraction

$$\frac{f\left(x,b_\perp,\mu,\delta^-\right)}{S\left(b_\perp,\mu,\delta^+,\delta^-\right)}\,, \tag{73}$$

where $S(b_\perp,\mu,\delta^+,\delta^-)$ is defined in Eq. (8). In conclusion, by performing the leading region analysis, we find the following factorization formula:

$$\tilde{f}(x,b_\perp,\mu,\zeta_z)=H\left(\frac{\zeta_z}{\mu^2}\right)\frac{f(x,b_\perp,\mu,\delta^-)}{S(b_\perp,\mu,\delta^+,\delta^-)}S\left(b_\perp,\mu,\delta^+,\hat{z}\right)\,, \tag{74}$$

where H is the hard kernel. By expressing the above equation in terms of the physical TMDPDFs, we found that

$$\tilde{f}(x,b_\perp,\mu,\zeta_z)\sqrt{S_{\rm I}(b_\perp,\mu)}=H\left(\frac{\zeta_z}{\mu^2}\right)\mathrm{e}^{K(b_\perp,\mu)\ln\frac{\zeta_z}{\zeta}}f^{\rm TMD}(x,b_\perp,\mu,\zeta)\,, \tag{75}$$

where $\exp\left[K(b_\perp,\mu)\ln(\zeta_z/\zeta)\right]$ takes into account the rapidity dependence between $\tilde{f}$ and $f^{\rm TMD}$, and

$$\sqrt{S_{\rm I}(b_\perp,\mu)}=\lim_{\delta^+\to 0}\frac{\sqrt{S(b_\perp,\mu,\delta^+,\delta^-=\delta^+)}}{S(b_\perp,\mu,\delta^+,\hat{z})} \tag{76}$$

is again called the intrinsic soft function. Although the definition of $S_{\rm I}$ in Eq. (76) looks quite different from Eq. (51), in Secs. 4.4 and 5, we will show that they are equivalent .

The method given here can be applied to other quasi-TMD observables. As an example, in Sec. 5, we will consider the TMDWFs for a light meson.

3.7. One-loop results and two-loop predictions

Based on the renormalization property of Wilson loop, the intrinsic soft function satisfies the RG equation

$$\mu^2\frac{\mathrm{d}}{\mathrm{d}\mu^2}\ln S_{\rm I}(b_\perp,\mu)=-\mathit{\Gamma}_{\rm S}(\alpha_{\rm s})\,, \tag{77}$$

where $\mathit{\Gamma}_{\rm S}$ is the rapidity independent part of the cusp-anomalous dimension at large rapidity separation $Y+Y'$ for the off-lightcone soft function

$$\mu^2\frac{\mathrm{d}}{\mathrm{d}\mu^2}\ln S_{\rm DY}\left(b_\perp,\mu,Y,Y'\right)=-(Y+Y')\mathit{\Gamma}_{\rm cusp}(\alpha_{\rm s})+\mathit{\Gamma}_{\rm S}(\alpha_{\rm s})\,. \tag{78}$$

Notice that $\gamma_{\rm s}$ in Eq. (11) is different from $\mathit{\Gamma}_{\rm S}$ since the rapidity-regulator-independent part of the soft function is scheme dependent. At leading order, $S^{(0)}_{\rm DY}(b_\perp,\mu,Y,Y')=1$. At one-loop level [37],

$$S^{(1)}_{\rm DY}(b_\perp,\mu,Y,Y')\;=\;\frac{\alpha_{\rm s}C_{\rm F}}{\pi}\left[1-\left(Y+Y'\right)\right]L_b\,, \tag{79}$$

$$\mathit{\Gamma}^{(1)}_{\rm S}(\alpha_{\rm s})\;=\;\frac{\alpha_{\rm s}C_{\rm F}}{\pi}\,, \tag{80}$$

where L_b is defined in Eq. (15). Based on the RGE, the intrinsic soft function at the two-loop level can be predicted to be

$$\ln S_{\mathrm{I}}^{(2)}(b_\perp,\mu) = c_2 - \mathit{\Gamma}_{\mathrm{S}}^{(2)} L_b + \alpha_{\mathrm{s}}^2 \frac{\beta_0 C_{\mathrm{F}}}{2\pi} L_b^2\,, \tag{81}$$

where

$$\mathit{\Gamma}_{\mathrm{S}}^{(2)} = \frac{\alpha_{\mathrm{s}}^2}{\pi^2}\left[C_{\mathrm{F}} C_{\mathrm{A}}\left(-\frac{49}{36}+\frac{\pi^2}{12}-\frac{\zeta_3}{2}\right)+C_{\mathrm{F}} N_{\mathrm{F}}\frac{5}{18}\right]$$

is the two-loop anomalous dimension for S_{I}^{-1} [65], $\beta_0 = -(\frac{11}{3}C_{\mathrm{A}} - \frac{4}{3}N_{\mathrm{f}} T_{\mathrm{F}})/(2\pi)$ is the coefficient of one-loop β-function, and c_2 is a constant to be determined by explicit calculation.

Therefore, by combining the RGEs of the quasi-TMDPDF $\tilde{f}$, the intrinsic soft function S_{I} and physical TMDPDF f^{TMD} [Eqs. (38), (77), and (25)], we obtain the RGE of the matching kernel $H\left(\frac{\zeta_z}{\mu^2}\right)$

$$\mu^2 \frac{\mathrm{d}}{\mathrm{d}\mu^2} \ln H\left(\frac{\zeta_z}{\mu^2}\right) = \frac{1}{2}\mathit{\Gamma}_{\mathrm{cusp}}(\alpha_{\mathrm{s}}) \ln\frac{\zeta_z}{\mu^2} + \frac{\gamma_C(\alpha_{\mathrm{s}})}{2}\,, \tag{82}$$

where $\gamma_C = 2\gamma_{\mathrm{F}} - \mathit{\Gamma}_{\mathrm{S}} + 2\gamma_J$. The matching kernel is closely related to the perturbative part of the rapidity evolution kernel $\mathcal{G}\left(\frac{\zeta_z}{\mu^2}\right)$ through

$$2\zeta_z \frac{\mathrm{d}}{\mathrm{d}\zeta_z} \ln H\left(\frac{\zeta_z}{\mu^2}\right) = \mathcal{G}\left(\frac{\zeta_z}{\mu^2}\right)\,. \tag{83}$$

In fact, the above equation demonstrates that the unsubtracted TMDPDF in the off-lightcone scheme is equivalent to quasi-TMDPDF up to a Lorentz boost, as the argument we used in Sec. 3.4. Combining Eqs. (82) and (83), we can see that the anomalous dimension of $\mathcal{G}$ is the cusp anomalous dimension $\mathit{\Gamma}_{\mathrm{cusp}}$

$$\mu^2 \frac{\mathrm{d}}{\mathrm{d}\mu^2}\mathcal{G}\left(\frac{\zeta_z}{\mu^2}\right) = \mathit{\Gamma}_{\mathrm{cusp}}(\alpha_{\mathrm{s}})\,. \tag{84}$$

Collecting all the above results, one obtains the one-loop matching kernel [35, 37]

$$H\left(\frac{\zeta_z}{\mu^2}\right) = 1 + \frac{\alpha_{\mathrm{s}} C_{\mathrm{F}}}{2\pi}\left(-2 + \frac{\pi^2}{12} - \frac{L_z^2}{2} + L_z\right)\,, \tag{85}$$

where L_z is defined in Eq. (40). The two-loop matching kernel is predicted to be

$$\begin{aligned}\ln H^{(2)}\left(\frac{\zeta_z}{\mu^2}\right) &= c_2' - \frac{1}{2}\left(\gamma_C^{(2)} - \alpha_{\mathrm{s}}^2\beta_0 c_1\right)\ln\frac{\zeta_z}{\mu^2} \\ &\quad -\frac{1}{4}\left(\mathit{\Gamma}_{\mathrm{cusp}}^{(2)} - \frac{\alpha_{\mathrm{s}}^2\beta_0 C_{\mathrm{F}}}{2\pi}\right)\ln^2\frac{\zeta_z}{\mu^2} - \frac{\alpha_{\mathrm{s}}^2\beta_0 C_{\mathrm{F}}}{24\pi}\ln^3\frac{\zeta_z}{\mu^2}\,, \end{aligned} \tag{86}$$

where $c_1 = \frac{C_F}{2\pi}\left(-2+\frac{\pi^2}{12}\right)$ and c_2' is again a constant to be determined in the perturbation theory at the two-loop level.

We should mention that beyond the three-loop level, the quasi-TMDPDFs start to develop power IR-divergences due to the ultra-soft modes discussed in Sec. 3.3. Fortunately, to obtain the matching kernel, one only needs virtual diagrams which are free from ultra-soft modes. The ultra-soft modes only contribute to real diagrams which have no overall UV divergences.

4. Off-lightcone soft functions

The soft function, which takes into account the soft radiation from fast-moving charged particles, naturally appears in TMD factorization. The naïve definition of the soft function using lightlike gauge links suffers from the rapidity divergence due to infinitely long gauge links in the lightlike direction. In factorization formulas, the soft function is always combined with another TMD observable which suffers from the same type of rapidity divergences. There are two major classes of rapidity regulators, on-lightcone and off-lightcone regulators, which are discussed in Sec. 2. The regulator dependencies then cancel between the soft functions and TMD observables to maintain scheme independence of the total cross section. This allows the definition of physical TMD observables where soft functions play the role of "rapidity renormalization" factors.

In the LaMET framework, spacelike staple-shaped gauge links are chosen to define the lattice calculable quasi-TMD observables. To match the physical TMDPDFs, all the artifacts and scheme dependencies associated with the off-lightcone staples must be removed by an appropriate soft function, which must be off-lightcone as well. However, the time dependence in S cannot be removed with a Lorentz boost, since there are two staple-shaped gauge links in conjugate lightlike directions. Recently [33, 40], we found that such an off-lightcone soft function can be simulated by a form factor of a fast-moving heavy-quark pair state. In this section we study the off-lightcone soft function relevant to the matching between the quasi-TMDPDF, quasi-Wave Function(WF) to the physical one. The major results of the section are:

— We first define two specific off-lightcone soft functions. The first one is defined with spacelike gauge links for the DY process in the double time-ordering. The second one is defined with timelike vectors in a single time-ordering. Being in single time-ordering, the second one can be represented as a form-factor for a pair of fast-moving color charges, thus can be formulated in the Euclidean space. We will state a lemma which asserts that although one is defined for cross section and one for the form factor, they are equal.

— We then study their properties. We show that although they suffer from IR divergences starting from the 3-loop level due to the presence of the "ultra-soft" modes known in the literature of HQET, the IR divergences are artifacts of perturbative calculation and can be resolved after an exact resummation of gauge link self-interactions. We carefully analyze the relevant modes in the lightcone limit and show that they factorize into the product of two TMDWFs for the color-charge pairs.

— We then study other possible off-lightcone soft functions, defined with different time-orderings and vectors. We will show that all the single-time-ordered off-lightcone soft functions relate with each-other through a single analytic function of the rapidity and are universal in the lightcone limit. The lemma in the first subsection is related to the analyticity and proved here.

— Once the timelike gauge links are involved, in the double time-ordering the universality is less transparent. Based on a factorization argument, in the lightcone limit, all the off-lightcone soft functions with timelike vectors can be expressed in terms of three independent ingredients: TMDPDF for a "single quark-state", fragmentation for a "single quark-state" and lightcone wave function of a heavy-quark pair. In principle, they can be quite different.

— Although the major part of the section is on the off-lightcone soft functions, we prove in Appendix H that the SIDIS and DY soft functions defined in delta regulator equal to each other by using an analyticity argument. This is similar to the universality of spacelike off-lightcone soft functions.

4.1. Definitions and basic properties

The TMD factorization in DY and SIDIS processes involves soft functions with two staple-shaped gauge links. To discuss the properties of such kind of soft functions in an off-lightcone scheme, we define the generic off-lightcone Wilson loop vacuum expectation value

$$W(\ell_1, \ell_2, b_\perp, \mu, q_1, q_2) = \frac{1}{N_c} \mathrm{Tr} \langle \Omega | \mathcal{T} \left[\mathcal{W}^\dagger_{q_2} \left(\vec{b}_\perp, -\ell_2 \right) \mathcal{W}_{q_1} \left(\vec{b}_\perp, \ell_1 \right) \right] | \Omega \rangle \,, \tag{87}$$

where ℓs are the length of the staple, μ is the renormalization scale, qs are unit vectors indicating the direction of the staple, $|\Omega\rangle$ is the vacuum state, $\mathcal{T}$ is the time ordering operator. The gauge link staple is defined by

$$\mathcal{W}_q(\xi, \ell) = W_q(0, \ell) W_\perp W^\dagger_q(\xi, \ell) \,, \tag{88}$$

where

$$W_q(\xi,\ell) = \mathcal{P}\exp\left[-ig\int_{-\ell}^{0} \mathrm{d}s\, q\cdot A(s\,q+\xi)\right]. \tag{89}$$

is a gauge link along the q direction, and the $W_\perp$ is a transverse gauge link to maintain manifest gauge-invariance.

In the definition of Eq. (87), we used the single time-ordering in the correlation function. There is another type of correlation functions defined by the cut diagram which contains the double time-ordering

$$\begin{aligned} W_{\rm cut}(\ell_1,\ell_2,b_\perp,\mu,q_1,q_2) &= \frac{1}{N_c}\mathrm{Tr}\,\langle\Omega|\bar{\mathcal{T}}W^\dagger_{q_1}\left(\ell_1,\vec{b}_\perp\right)W_{q_2}\left(-\ell_2,\vec{b}_\perp\right)W_\perp \\ &\quad \mathcal{T}W_\perp W^\dagger_{q_2}(-\ell_2,0)W_{q_1}(\ell_1,0)|\Omega\rangle\,. \end{aligned} \tag{90}$$

Similar to quasi-TMDPDF, the off-lightcone gauge link staple contains Wilson line self-interactions, which can be removed by the rectangular Wilson loops

$$Z(2\ell,b_\perp,\mu,q) = W(\ell,\ell,b_\perp,\mu,q,q)\,, \tag{91}$$

$$Z_{\rm cut}(2\ell,b_\perp,\mu,q) = W_{\rm cut}(\ell,\ell,b_\perp,\mu,q,q)\,. \tag{92}$$

The soft functions are defined by taking the large ℓ_1 and ℓ_2 limit using rectangular Wilson loop subtractions in Eqs. (87) and (90)

$$S(b_\perp,\mu,q_1,q_2) = \lim_{\substack{\ell_1\to\infty\\ \ell_2\to\infty}}\frac{W(\ell_1,\ell_2,b_\perp,\mu,q_1,q_2)}{\sqrt{Z(2\ell_1,b_\perp,\mu,q_1)Z(2\ell_2,b_\perp,\mu,q_2)}}\,, \tag{93}$$

$$S_{\rm cut}(b_\perp,\mu,q_1,q_2) = \lim_{\substack{\ell_1\to\infty\\ \ell_2\to\infty}}\frac{W_{\rm cut}(\ell_1,\ell,b_\perp,\mu,q_1,q_2)}{\sqrt{Z_{\rm cut}(2\ell_1,b_\perp,\mu,q_1)Z_{\rm cut}(2\ell_2,b_\perp,\mu,q_2)}}\,. \tag{94}$$

The existence of the limit will be shown in Sec. 4.2.

Throughout this section, we will use the timelike unit vectors $v = \gamma(1,\beta,\vec{0}_\perp)$ and $v' = \gamma'(1,-\beta',\vec{0}_\perp)$ in $(t,z,\vec{\perp})$ coordinate, and the spacelike unit vectors $u = \gamma(\beta,1,\vec{0}_\perp)$ and $u' = \gamma'(-\beta',1,\vec{0}_\perp)$. We assume $0<\beta<1$ and $\gamma = 1/\sqrt{1-\beta^2}$. For large β, v is approaching the lightcone plus direction, while v' is approaching the lightcone minus direction.

As an example, we consider the following soft functions related to DY process.

DY soft function: Both staples are tilted in spacelike directions: $q_1 = u$ and $q_2 = u'$.
This soft function was proposed by Collins [11]. For large Y and Y',

$$S_{\rm DY}\left(b_\perp,\mu,Y,Y'\right) = S\left(b_\perp,\mu,u,u'\right) = S_{\rm cut}\left(b_\perp,\mu,u,u'\right)\,, \tag{95}$$

where $Y = \tanh^{-1}\beta$ is the rapidity regulator. Notice that in this case, the time-orderings are irrelevant since any two points on the Wilson loop are spacelike.

Form-factor soft function: Both staples are tilted in timelike directions: $q_1 = v$ and $q_2 = v'$.
We define the following single-time-ordered soft function, which can be interpreted as a form factor

$$S\left(b_\perp, \mu, Y, Y'\right) = S\left(b_\perp, \mu, v, v'\right) . \tag{96}$$

The parallel gauge links with transverse separation $\vec{b}_\perp$ in timelike v direction can be viewed as a pair of color charges separated by $\vec{b}_\perp$ traveling at speed v in $+z$ direction. At $t = 0$, the junctions of gauge links can be seen as the color charge receives a large momentum transfer, and then continue to propagate to $-z$ direction. Therefore, it can be viewed as a form factor and formulated by heavy-quark pairs in HQET

$$S\left(b_\perp, \mu, Y, Y'\right) = {}_{v'}\left\langle \bar{Q}Q\left(\vec{b}_\perp\right)\right| J\left(b_\perp, v', v\right) \left|\bar{Q}Q\left(\vec{b}_\perp\right)\right\rangle_v , \tag{97}$$

where $J(\vec{b}_\perp, v', v) = \bar{Q}^\dagger_{v'}(\vec{b}_\perp)Q^\dagger_{v'}(0)\bar{Q}_v(\vec{b}_\perp)Q_v(0)$ is the transition current and $|\bar{Q}Q(\vec{b}_\perp)\rangle_v$ is the heavy quark pair bound state with velocity v.

Timelike DY soft function: Both staples are tilted in timelike directions: $q_1 = v$ and $q_2 = -v'$.
This soft function is proportional to the total cross section for the DY process participated by two incoming heavy-quarks $Q(v)$ and $\bar{Q}(v')$ travelling at velocity v and v'

$$S_{\text{cut}}\left(b_\perp, \mu, v, -v'\right) \sim \sum_n \int \mathrm{d}\mathit{\Pi}_n \left|\left\langle n \left| j\left(v', v\right)\right| \bar{Q}_{v'}Q_v\right\rangle\right|^2 , \tag{98}$$

where $j(v', v) = \bar{Q}_{v'}(0)Q_v(0)$ is a heavy-quark pair annihilation operator. Here, the soft function S_{cut} is in double time-ordering because the corresponding timelike TMDPDFs are naturally defined in cut diagrams.

The first and third types of soft functions correspond to choosing spacelike and timelike rapidity regulator of TMDPDFs in the factorization theorem. Although they look differently, one can prove that the first two soft functions are equal

$$S_{\text{DY}}\left(b_\perp, \mu, Y, Y'\right) = S\left(b_\perp, \mu, Y, Y'\right) . \tag{99}$$

The proof of the equality will be given in Sec. 4.5.

4.2. Pinch-pole singularity subtraction

For the single-time-ordered soft functions, the pinch-pole singularity arises due to gauge link self-interactions. As discussed in Sec. 3.2 and Appendix A, the spacelike and timelike staples differ by an analytic continuation. In the infinite length limit, both cases generate divergent evolution factors, e^{-VL} and e^{-iEt} for spacelike and timelike staples, where V is the heavy-quark potential and E is the bound-state energy. On the other hand, for timelike staple in the double-time-ordered soft function, there is no pinch-pole singularity, see Appendix D. Therefore, we focus the following discussion on the single-time-ordered soft functions.

Given the exponentiation property for the Wilson loop (see Appendix B), we now examine the subtraction of pinch-pole singularity in the single-time-ordered soft function. Consider the webs Φ for Wilson loop amplitude $W = \mathrm{e}^{\Phi}$

$$\begin{aligned}&\ln W(\ell_1,\ell_2,b_\perp,\mu,q_1,q_2) = \Phi_{\text{vertex}}(\ell_1,\ell_2,b_\perp,\mu,q_1,q_2)\\&+\Phi_\perp^W(\ell_1,\ell_2,b_\perp,\mu,q_1,q_2) + \Phi_{\text{self}}(\ell_1,b_\perp,\mu,q_1) + \Phi_{\text{self}}(\ell_2,b_\perp,\mu,q_2)\,, \quad (100)\end{aligned}$$

which contains two gauge link staples with lengths ℓ_1 and ℓ_2 in arbitrary off-lightcone q_1 and q_2 directions. Here, Φ_{vertex} consists of 2PI vertex webs, which contain interactions between staples in q_1 and q_2 directions. Φ_{self} consists of self-interacting webs, which contain self-energy of gauge links and interactions between parallel gauge links. $\Phi_\perp$ consists of all the webs that involve the transverse gauge links.

At large ℓ_1 and ℓ_2, Φ_{vertex} and $\Phi_\perp$ have no IR divergence, see Sec. 4.3 and Appendix D. Thus, we will omit the ℓ_1 and ℓ_2 dependencies for Φ_{vertex}. However, the self-interacting webs contain linear IR divergences proportional to ℓ_1 and ℓ_2 caused by the time evolution of the heavy-quark pair state. Such linear divergence includes the Wilson line self-energy and the pinch-pole singularity. The pinch-pole divergences can be removed by considering the rectangular Wilson loop, which poses a similar web expansion

$$\ln Z(2\ell,b_\perp,\mu,q) = \Phi_0(b_\perp,\mu) + \Phi_\perp^Z(2\ell,b_\perp,\mu,q) + 2\Phi_{\text{self}}(\ell,b_\perp,\mu,q)\,, \quad (101)$$

where $\Phi_0(b_\perp,\mu) = \Phi_{\text{vertex}}(b_\perp,\mu,q,q)$ because Φ_0 is independent of q due to the Lorentz invariance. This can also be obtained by the substitutions $\ell_1,\ \ell_2 \to \ell$ and $q_1,\ q_2 \to q$ in $W(\ell_1,\ell_2,b_\perp,\mu,q_1,q_2)$. Thus, we obtain the soft function defined in Eq. (93)

$$\begin{aligned}S(b_\perp,\mu,q_1,q_2) &= \lim_{\substack{\ell_1\to\infty\\ \ell_2\to\infty}} \frac{W(\ell_1,\ell_2,b_\perp,\mu,q_1,q_2)}{\sqrt{Z(2\ell_1,b_\perp,\mu,q_1)Z(2\ell_2,b_\perp,\mu,q_2)}}\\&= \mathrm{e}^{\Phi_{\text{vertex}}(b_\perp,\mu,q_1,q_2)-\Phi_0(b_\perp,\mu)}\,, \quad (102)\end{aligned}$$

where in the last line $\Phi_\perp^W(\ell_1,\ell_2,b_\perp,\mu,q_1,q_2) - \frac{1}{2}\Phi_\perp^Z(2\ell_1,b_\perp,\mu,q_1) - \frac{1}{2}\Phi_\perp^Z(2\ell_2,b_\perp,\mu,q_2) \to 0$ in the ℓs $\to \infty$ limit, see Fig. 18.

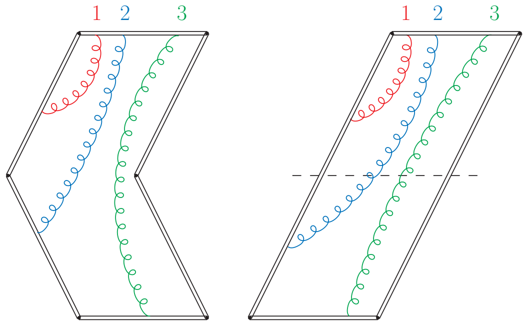

Fig. 18. Different types of web diagrams containing interaction to transverse gauge link. Left and right figures are $\Phi_\perp^W$ and $\Phi_\perp^Z$. In the large-ℓ limit, type 2 and type 3 web diagrams approach zero, and the rest type 1 web diagrams cancel in the equation $\lim_{\ell s\to\infty}\Phi_\perp^W(\ell_1,\ell_2,b_\perp,\mu,q_1,q_2) - \frac{1}{2}\Phi_\perp^Z(2\ell_1,b_\perp,\mu,q_1) - \frac{1}{2}\Phi_\perp^Z(2\ell_2,b_\perp,\mu,q_2) = 0$.

Next, we can define the physical TMDPDF in single time-ordering in the off-lightcone scheme. First, we consider an unsubtracted TMDPDF in the off-lightcone scheme whose gauge link staple is pointing to a nearly lightlike direction, $n_Y = (-\mathrm{e}^{-2Y}, 1, \vec{0}_\perp)$ in $(+,-,\vec{\perp})$. The correlation function in the off-lightcone scheme contains pinch-pole singularity as well as gauge link self-energy, which are similar to quasi-TMDPDFs. Therefore, further subtraction is needed and the correlation function is defined similar to Eq. (33), and its web-diagram decomposition is similar to Eq. (47)

$$\mathrm{e}^{\Phi_{\mathrm{self}}(L,b_\perp,\mu,n_Y)+\Phi_\perp^{\mathcal{W}}(L,b_\perp,\mu,n_Y)}\langle\mathcal{P}|\tilde{O}_{n_Y}(\lambda,b_\perp,L)|\mathcal{P}\rangle_{\mathrm{2PI}}\,. \tag{103}$$

Therefore, before the Fourier transformation, we have

$$\lim_{L\to\infty}\frac{\langle\mathcal{P}|\tilde{O}_q(\lambda,b_\perp,L)|\mathcal{P}\rangle}{\sqrt{Z(2L,b_\perp,\mu,n_Y)}} = V_{\mathrm{2PI}}(\lambda,b_\perp,\mu,n_Y)\mathrm{e}^{-\frac{1}{2}\Phi_0(b_\perp,\mu)}\,, \tag{104}$$

where $\Phi_\perp^{\mathcal{W}}(L,b_\perp,\mu,n_Y) - \frac{1}{2}\Phi_\perp^Z(2L,b_\perp,\mu,n_Y) \to 0$ in $L\to\infty$ limit, and

$$V_{\mathrm{2PI}}(\lambda,b_\perp,\mu,n_Y) = \lim_{L\to\infty}\langle\mathcal{P}|\tilde{O}_{n_Y}(\lambda,b_\perp,L)|\mathcal{P}\rangle_{\mathrm{2PI}}\,, \tag{105}$$

see Fig. 19 for details. Before taking the lightcone limit, we need to perform the soft function subtraction

$$S(b_\perp,\mu,n_Y,p_Y) = \mathrm{e}^{\Phi_{\mathrm{vertex}}(b_\perp,\mu,n_Y,p_Y)-\Phi_0(b_\perp,\mu)}\,, \tag{106}$$

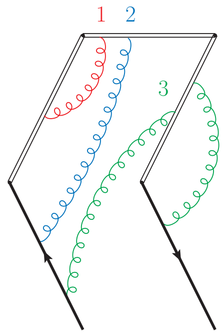

Fig. 19. Different types of web diagrams of the unsubtracted TMDPDF in the off-lightcone scheme. Type 1 web-diagram is $\Phi_\perp^{\mathcal{W}}(L, b_\perp, \mu, n_Y)$; Type 2 and type 3 web diagrams are $\langle\mathcal{P}|\tilde{O}_{n_Y}(\lambda, b_\perp, L)|\mathcal{P}\rangle_{2\mathrm{PI}}$. In the large L limit, type 2 web diagram approaches zero, and $V_{2\mathrm{PI}}(\lambda, b_\perp, \mu, n_Y) = \lim_{L\to\infty}\langle\mathcal{P}|\tilde{O}_{n_Y}(\lambda, b_\perp, L)|\mathcal{P}\rangle_{2\mathrm{PI}}$. We omit the $\Phi_{\mathrm{self}}(L, b_\perp, \mu, n_Y)$ web diagram in the figure.

where $p_Y = (1, -\mathrm{e}^{-2(Y+y_n)}, \vec{0}_\perp)$ is a nearly lightlike direction conjugate to n_Y. According to Eq. (20), we have

$$\tilde{f}^{\,\mathrm{TMD}}(x, b_\perp, \mu, \zeta, \zeta_Y) = \frac{1}{2\mathcal{P}^+}\lim_{Y\to\infty}\int\frac{\mathrm{d}\lambda}{2\pi}\,\mathrm{e}^{i\lambda x} \times V_{2\mathrm{PI}}(\lambda, b_\perp, \mu, n_Y)\,\mathrm{e}^{-\frac{1}{2}\Phi_{\mathrm{vertex}}(b_\perp,\mu,n_Y,p_Y)}\,, \quad (107)$$

where $\zeta = 2(x\mathcal{P}^+)^2\,\mathrm{e}^{2y_n}$ and $\zeta_Y = 2(x\mathcal{P}^+)^2\,\mathrm{e}^{2Y}$. There is still one step away from the physical TMDPDF because there is a hard scale ζ_Y which generates hard contribution and requires perturbative matching [11], similar to the argument in Sec. 3.4. After subtracting out the hard contribution, we obtain the physical TMDPDF

$$f^{\mathrm{TMD}}(x, b_\perp, \mu, \zeta) = H^{-1}\left(\frac{\zeta_Y}{\mu^2}\right)\tilde{f}^{\,\mathrm{TMD}}(x, b_\perp, \mu, \zeta, \zeta_Y)\,, \quad (108)$$

where the hard kernel H is related to the perturbative part of the rapidity evolution kernel of quasi-TMDPDF, which is discussed in Secs. 3.4 and 3.7.

For the double-time-ordered soft function S_{cut}, if the gauge link staple is spacelike, the time ordering is irrelevant and $Z_{\mathrm{cut}} = Z$. In this case, the subtraction factor works in the same way as that of the single-time-ordered soft function. If the gauge link staple is timelike, there is no pinch-pole singularity (See Appendix D). However, the subtraction factor Z_{cut} still serves to remove linear divergence of the Wilson line self-energy.

4.3. Ultra-soft modes

As we have shown in Refs. [33, 40], S can be viewed as scattering amplitudes of fast-moving bound states formed by a pair of color charges at fixed transverse separation. In comparison, the double-time-ordered soft functions are cross sections for single heavy quarks. Since the internal structure of a heavy-quark pair is more complicated than that of a single heavy quark, S is expected to carry more physical information relevant or not relevant to high-energy scattering. Notice also that spacelike separations are insensitive to time-orderings, thus we expect that the soft function defined with spacelike gauge links contains information of the bound states as well, even defined with two time-orderings.

As shown in the previous section, in the rest frame of the heavy-quark pair or a spacelike staple, there are indeed subtleties caused by "ultra-soft" modes scale as $\frac{\alpha_{\rm s}}{b_\perp}$. By boosting into large rapidity, we naturally expect that there are soft-collinear modes corresponding to their boosted versions. As in the case of quasi-TMDPDF, for $\alpha_{\rm s} \sim 1$, there is no need to distinguish them. The binding energy after the boost, however, is of the order of $\alpha_{\rm s}\,{\rm e}^{-Y}/b_\perp$. This "ultra–ultra" soft scale is rapidity-dependent and can be very dangerous since any logarithms in it would naturally lead to Y dependencies which can break factorization. We now show that such modes cannot exist. There are two arguments. The first and the simplest one is that for large Y, this scale is much softer than the confinement scale, therefore, it will be suppressed by the mass gap of theory. Second, we argue that after resummation of the effective link self-energy consistently, such modes cancel after summation over diagrams.

As an example, let us consider the "lamb-shift" diagrams in Fig. 20. At the individual diagram level, if the number of ladders is larger than 1, there are power-IR divergences and even the color cancellation has been taken into account. The reason can be explained as follows. The soft-gluon momentum provides a time scale where the heavy-quarks can propagate. Then, there should be a factor of the form of ${\rm e}^{-\frac{V}{|k|}}$. By expand the exponential we then obtain the $\frac{1}{|k|}$ factors which make the integral divergent. Thus, we expect a resummation of the ladder would be sufficient to make the integral IR finite. We now sum over the ladders. To obtain the web diagram, we need to treat the color factor carefully. The full color factor of the diagram is $C_{\rm F}(C_{\rm F}-\frac{C_{\rm A}}{2})^N$ if there are N ladders, but to form the web diagram, one can show that only the "maximal non-Abelian" part $C_{\rm F}(-C_{\rm A}/2)^N$ will be kept. The integration after the resummation of webs then reads

$$\int {\rm d}^{4-4\epsilon}k \frac{1}{k\cdot v+i0}\frac{{\rm e}^{i\vec{b}_\perp\cdot k_\perp}-1}{k\cdot v'-\Sigma\left(k\cdot v',b_\perp\right)+i0}\frac{1}{k^2+i0}\,. \tag{109}$$

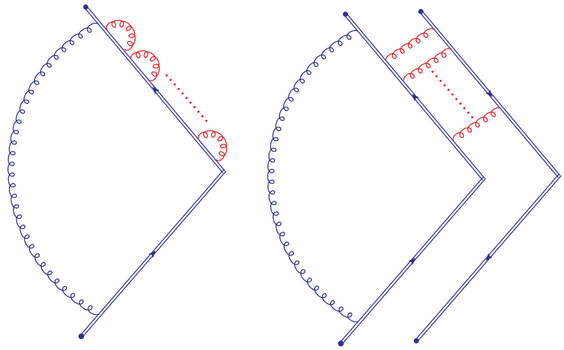

Fig. 20. A typical diagram generating power-IR divergences in single line (left) and double line (right) representations. The red gluons are collinear to the gauge links, while the blue one is soft.

Here, the $\Sigma(k \cdot v')$ is the self-energy of the heavy-quark pair or the effective gauge link. In the "ultra–ultra" soft-region, the self-energy can be approximated as

$$\Sigma\left(k \cdot v' = 0, b_\perp\right) \sim \mathrm{e}^{-Y} \frac{\alpha_\mathrm{s} C_\mathrm{A}}{2b_\perp} \,. \tag{110}$$

This is actually the ground-state energy difference between the heavy-quark pair in the octet channel and in the singlet channel, consistent with the observation in the quasi-TMDPDF section. If one expands the dressed propagator $\frac{1}{k \cdot v' - \Sigma(k \cdot v', b_\perp) + i0}$ to any given order in Σ, then one will encounter integrals of the form of

$$\int \mathrm{d}^{4-4\epsilon} k \frac{1}{k \cdot v + i0} \frac{\mathrm{e}^{i\vec{b}_\perp \cdot k_\perp} - 1}{\left(k \cdot v' + i0\right)^{n+1}} \Sigma^n \left(k \cdot v', b_\perp\right) \frac{1}{k^2 + i0} \,, \tag{111}$$

which are power-divergent if $n > 3$. However, after resummation into the dressed propagator, the power-IR divergences all cancel. We should also notice that if there were only the -1 or $\mathrm{e}^{\vec{b}_\perp \cdot k_\perp}$ terms in Eq. (109), although the integral is convergent, the "ultra–ultra" soft region would generate Y dependent logarithms. However, with the color cancellation between $\mathrm{e}^{\vec{b}_\perp \cdot k_\perp}$ and -1, the ultra-soft region is now suppressed by the boost factor. The softest momentum that one can probe in the vertex diagram is still around the natural cutoff $\frac{1}{b_\perp}$. However, if we were in the rest frame of the gauge link staple, the so-called soft-collinear modes do exists, although they do not generate IR divergent logarithms, namely, if we treat this as an independent scale δE, then we have well-posed limit as $\delta E \to 0$ of the form $\delta E \ln \delta E$. But in our case, they differ from the collinear modes simply by a factor of α_s. For $\alpha_\mathrm{s} \sim 1$, the contribution is leading.

There is another type of diagrams that are capable of generating logarithmic divergences. Namely, a diagram in which a soft gluon is emitted from a higher-order vertex diagram of the effective gauge link, see Fig. 21 for a depiction. In the example above, the soft gluon can be emitted from the

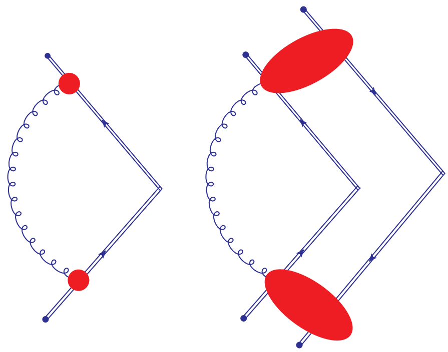

Fig. 21. A typical diagram generating logarithmic IR divergences in single line (left) and double line (right) representations. The red blobs are collinear to the gauge links.

ladders. In the single-line representation, the resulting diagram then corresponds to the first-order vertex diagram. When both ends of a soft gluon are inside such vertex diagrams, there appears to be no color cancellation available, thus to show the absence of Y-dependent ultra-soft scales, one must demonstrate the cancellation of such logarithms after summing over all the diagrams. This can be argued as follows. Since the IR divergence is logarithmic now, we can only keep the power-leading part of the IR divergence. We now factorize the “ultra-ultra” soft, “ultra” soft and soft modes into a single soft function from the collinear and soft collinear modes. This is possible since for all the three modes, the connections to the collinear and soft collinear sub-diagram can be approximated by the standard soft-to-collinear eikonal approximation. In order for the Ward-identity argument to be valid, the resummation must be performed consistently to preserve the corresponding Ward identities. This can be achieved by first calculating the self-energy diagram to a given order, then resum to the dressed propagator. Then we consider only the vertexes formed by insertion of a gluon into these already resumed self-energy diagrams. If we need more vertexes, then we need more self-energy diagrams. Then the Ward identity can still be satisfied. This is in fundamental contrast to many “off-shell” regulators where gauge-invariance has been explicitly broken and no Ward identity is applicable. The resulting soft function, however, is nothing but the standard TMD soft function, which is clearly free from such Y-dependent “ultra–ultra” soft modes as well as separate “ultra”-soft modes. The wavelength for the soft gluon, therefore, is still bounded by $b_\perp$. It is the applicability of Ward identity that guarantees the independence of the soft contribution to the internal structures of a hadron.

In conclusion, the off-lightcone soft function in single time-ordering is IR finite only after the resummation of gauge link self-interactions, due to the so-called "ultra"-soft modes in the rest frame of a heavy-quark–anti-quark pair. These modes carry the energy-scale at the order of the binding energy $\frac{\alpha_s}{b_\perp}$. After boosting, the ultra-soft modes become the "soft-collinear" modes. The Y-dependent "ultra–ultra" soft modes at the order of $e^{-Y}\frac{\alpha_s}{b_\perp}$ is suppressed by the color-neutrality condition after summation over diagrams. Therefore, for the off-lightcone soft function, we obtain the modes listed below in the unit of $b_\perp$

$$\text{collinear:}\quad k_C \sim \left(e^Y, e^{-Y}, 1, 1\right)/b_\perp\,. \tag{112}$$

$$\text{soft-collinear:}\quad k_{SC} \sim \alpha_s\left(e^Y, e^{-Y}, 1, 1\right)/b_\perp\,. \tag{113}$$

$$\text{soft:}\quad k_S \sim (1,1,1,1)/b_\perp\,. \tag{114}$$

The absence of the Y-dependent "ultra"-soft modes is crucial for the TMD-factorization. In the following section, we will factorize the "soft" modes from the "collinear+soft collinear" modes using lightlike TMD observables for heavy-quark state. These factorization will build the relation between on-lightcone and off-lightcone regulators.

4.4. Factorization in the lightcone limit

A crucial property of the soft functions is the factorization of rapidity divergences in the lightcone limit. This is one of the cornerstones of the TMD factorization formalism and deserves a throughout study. In early 1980s, Collins and Soper have developed a diagrammatic technic for the derivation of rapidity evolution equations for TMD observables. When applied to the off-lightcone soft functions, it was claimed in Ref. [47] that collinear modes responsible for the rapidity divergences are power-suppressed by the Feynman rules for the evolution kernel, therefore in the lightcone limit, the rapidity evolution kernel is a constant. This leads to the rapidity factorization. However, a detailed explanation regarding how the collinear modes were suppressed to the extent that were sufficient to kill all the rapidity divergences beyond one-loop level is not presented. The nature of the rapidity divergence has also been studied in Ref. [19] using the conformal transformation method. It was claimed that the rapidity divergence can be mapped to UV divergences for Wilson-line cusps, thus can be factorized. In this subsection, we show that based on the region analysis of the off-lightcone soft function, a factorization formula can be found that matches the off-lightcone soft functions into the lightcone WFs for the external color-charge state. This implies the rapidity factorization for the off-lightcone soft functions. In Appendix E, a more direct approach will be provided.

The region analysis can be performed similar to the quasi-TMDPDF. The power-counting parameter is $\lambda = \mathrm{e}^{-(Y+Y')/2}$. In the lightcone limit, one can consistently label all the eikonal propagators sourced by soft gluons to be collinear, since in this case one can keep only the $k^{\pm}$ components of the soft-gluon momentum in the eikonal propagator. For the power-counting of the hard kernel, there are no Lorentz contraction or enhancement associated with the gauge links, since they are now of spin 0. There is Lorentz boost factor enhancement associated with longitudinal polarized collinear gluons. The disconnected hard regions can be argued to be non-essential similar to that of quasi-TMDPDF. Thus in the leading region, there are two hard cores around $\vec{0}$ and $\vec{b}_\perp$, two collinear gauge links and arbitrary many collinear gluons inserted into the hard core. There can be arbitrary many soft gluon connections to the collinear sub-diagram.

The major distinction from the quasi-TMDPDF is that the hard kernel is actually trivial, due to the lacking of a natural hard scale. The absence of the hard kernel can also be shown in the following way. Since all the "real" diagrams do not contribute to the hard kernel, one can obtain the hard kernel by calculating with a form factor of two external gauge links. Similar to the standard calculation of such form factors, to calculate the hard kernel, one can put the external gauge links on shell with large momentum/enenrgy, and then subtract out the corresponding IR divergences. However, the on-shell external momentum will be killed in all the eikonal propagators due to the linearity of the gauge link propagators. Therefore, the form factor and, consequently, the hard kernel are independent of the external momenta. Thus, the hard kernel can only be trivial.

With the hard kernel being trivial, the factorization for the form factor soft function then reads

$$S\left(b_\perp, \mu, Y, Y'\right) = \varPsi^\dagger\left(b_\perp, \mu, Y'\right)\varPsi(b_\perp, \mu, Y)\,, \tag{115}$$

where the lightcone Wave function for the color-charged state reads

$$\varPsi(b_\perp, \mu, Y) = \lim_{\delta\to\infty}\frac{\left\langle 0\middle|\bar{Q}_v\left(\vec{b}_\perp\right)\mathcal{W}_n^+\left(\vec{b}_\perp\right)\Big|_\delta Q_v(0)\middle|\bar{Q}Q\left(\vec{b}_\perp\right)\right\rangle_v}{\sqrt{S(b_\perp, \mu, \delta, \delta)}}\,, \tag{116}$$

in which the lightlike gauge links in W_n^+ chosen to be future pointing differ from the past pointing case only by an overall complex conjugation due to the time-reversal symmetry. We now examine this factorization formula.

First, we notice that the "un-subtracted" TMDWF for the heavy-quark pair depends on Y and δ only through the combination $\mathrm{e}^{-Y}\delta$ due to the boost invariance. Therefore, we can always boost the $\bar{Q}Q$ state to be purely static, namely to $v=(1,0,0,0)$. The corresponding un-subtracted WF can then be interpreted as a soft function with an off-lightcone timelike staple and a lightlike staple

$$S(b_\perp,\mu,\delta,\hat{t}) = \frac{\langle 0|\mathcal{T}\mathcal{W}_t\left(\vec{b_\perp};t\right)W_p^\dagger\left(\vec{b_\perp}\right)|_\delta|0\rangle}{\sqrt{Z(2t,b_\perp,\mu)}}\,, \tag{117}$$

where $\mathcal{W}_t$ is a gauge link staple in t direction pointing to the future. The self-interaction is removed by $\sqrt{Z}$. It is defined with a single time-ordering as that of the form factor. Comparing the soft function $S(b_\perp,\mu,\delta,\hat{z})$ defined in quasi-TMDPDF section, which is independent of time-ordering, we find that the only difference is that the $\mathcal{W}_z$ have been replaced by $\mathcal{W}_t$. However, based on the analyticity property of the single time-ordered soft function to be discussed later, we can show that they relate to each other through an analytic continuation

$$\left\langle 0\middle|\bar{Q}_v\left(\vec{b}_\perp\right)\mathcal{W}_n^+\left(\vec{b}_\perp\right)\Big|_\delta Q_v(0)\middle|\bar{Q}Q\left(\vec{b}_\perp\right)\right\rangle_v^\dagger = S\left(b_\perp,\mu,\delta,\hat{t}\right) = S(b_\perp,\mu,-i\delta,\hat{z}) \tag{118}$$

for $\delta>0$. In the lightcone limit, the soft function only depends on $\ln\delta$ and they are equal up to a phase factor associated with $\ln\delta^+\to\ln -i\delta^+$, which will cancel between Ψ and $\Psi^\dagger$. Thus, we will omit the imaginary part and write

$$\left|\left\langle 0\middle|\bar{Q}_v(\vec{b}_\perp)\mathcal{W}_n^+\left(\vec{b}_\perp\right)\Big|_\delta Q_v(0)\middle|\bar{Q}Q\left(\vec{b}_\perp\right)\right\rangle_v\right| = \mathrm{e}^{-\frac{1}{2}K(b_\perp,\mu)\ln\frac{\mu^2}{\delta^2\mathrm{e}^{-2Y}}+\mathcal{D}_1(b_\perp,\mu)}\,, \tag{119}$$

where $\mathcal{D}_1$ is the same as that for $S(b_\perp,\mu,\delta,\hat{z})$. Using the similar expansion of the on-lightcone regulator, we found that

$$|\Psi(b_\perp,\mu,Y)| = \mathrm{e}^{K(b_\perp,\mu)Y+\mathcal{D}_1(b_\perp,\mu)-\frac{1}{2}\mathcal{D}_0(b_\perp,\mu)}\,. \tag{120}$$

Thus, the off-lightcone soft function S has the following expansion:

$$S\left(b_\perp,\mu,Y,Y'\right) = \mathrm{e}^{K(b_\perp,\mu)(Y+Y')+2\mathcal{D}_1(b_\perp,\mu)-\mathcal{D}_0(b_\perp,\mu)}\,. \tag{121}$$

Using the relation $S=S_{\mathrm{DY}}$, we found that

$$\mathcal{D}(b_\perp,\mu) = 2\mathcal{D}_1(b_\perp,\mu)-\mathcal{D}_0(b_\perp,\mu)\,. \tag{122}$$

This demonstrates the scheme independence of the intrinsic soft function claimed in the previous section. It also reveals the physical meaning of the intrinsic soft function: it can be interpreted as the lightcone wave function for a $\bar{Q}Q$ state.

4.5. Analyticity in hyperbolic angle

Although the soft function depends on two vectors v_1 and v_2, in the single-time-ordered case one only needs a single function to represent all the choices. This is due to the fact that the single-time-ordered soft function is an analytic function of the relative hyperbolic angle defined as

$$\theta(v_1, v_2) = \mathrm{Arcosh}\frac{v_1 \cdot v_2 - i0}{\sqrt{v_1^2 + i0}\sqrt{v_2^2 + i0}} \,. \tag{123}$$

A general proof of this property will be given later. Intuitively, it can be explained in the following way. The single-time-ordered soft function can be viewed as a form factor where the external incoming momenta p_1, p_2 are replaced by v_1 and $-v_2$. Thus, we expect it poses similar analyticity property as that of a form factor. The form factor is an analytic function of $p_1^2 + i0$, $p_2^2 + i0$ and the momentum transfer $p_1 \cdot p_2 + i0$. Thus, the soft function should be an analytic function of three variables $v_1 \cdot v_2 - i0$, $v_1^2 + i0$, and $v_2^2 + i0$. However, the soft function is invariant under Lorentz boost in longitudinal plan and as well as independent rescalings of v_1 and v_2. Thus, it can only depend on the ratio $\frac{-v_1 \cdot v_2 + i0}{\sqrt{v_1^2 + i0}\sqrt{v_2^2 + i0}}$, which enters into the definition of the hyperbolic angle. The square root and the $i0$ are introduced to properly take into account the additional imaginary parts as one moves from spacelike vector/momentum transfers to the timelike ones.

We now start to prove the analyticity. We first start with the DY shape soft function. We fix $v_1^z = v_2^z = 1$ and $v_1^0 = -v_2^0 = v^0$. We chose to work in physical gauge where the Hilbert space consists of positive norm states only. We assume that there is a regularization in which the energy is positive and satisfies the relation $E - \beta \mathcal{P}^z \geq 0$ for arbitrary $|\beta| < 1$. We further assume that the Lorentz invariance in t, z plane for gauge-invariant quantities is preserved by the regularization. Using the definition of the soft function, we expand the gauge links in terms of gluon fields, and order all the gluon fields according to the time. The consecutive differences in the time components then read

$$v^0 \left(t - t'\right) \,, \tag{124}$$

where $0 > t > t' > -t_0$ parameterizing the gauge links. After insertion of intermediate states, the energy exponentials for the time-differences then read

$$\mathrm{e}^{-iEv^0(t-t')} \,. \tag{125}$$

Due to the positivity of the energy, $E > 0$, we can analytically continue in $v_0 \to v_0^x + iv_0^y$ with $v_0^y < 0$. We should mention that besides the exponential decay, which is the most decisive property, the analyticity has also some moderate regularity requirements on the "spectrum functions". For more details see [66]. For any finite t_0 by integrating over the t, t's we obtain an analytic function in $z = v_0^x + iv_0^y$. We now take the large-t_0 limit. Since the Hilbert space consists of a purely physical state, the energy is assumed to be uniformly gaped with respect to the regularization (although no one can prove it!). The $t_0 \to \infty$ is then at exponential speed. By performing the corresponding subtractions using $\sqrt{Z}$s which removes the leading exponential decay factor, the results converge uniformly in the region $v_0^y < \epsilon < 0$ for any ϵ. Thus, we obtain an analytic function $f(z)$ in the lower half-plane to any order in the expansion. Then, although we cannot claim that the expansion converges, it is natural to expect that the full result shares the same analyticity. See Fig. 22 for a depiction of the analytic domain for $f(z)$.

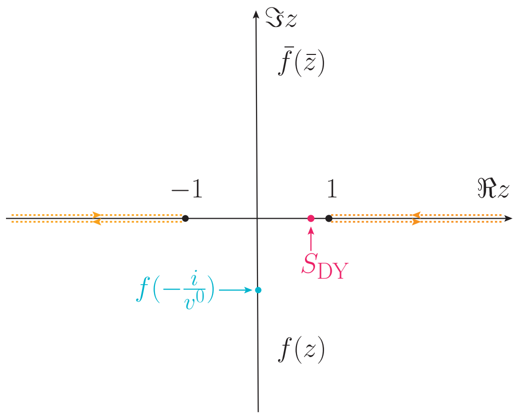

Fig. 22. A depiction of analytic domain of $f(z)$. The $f(z)$ was extended to upper half-plane through $\bar{f}(\bar{z})$ due the reality of $f(v^0)$ with $-1 < v^0 < 1$. There are branch cuts stating at $v^0 = \pm 1$ to $\pm\infty$. The $v^0 = \mp 1$ corresponds to the lightcone singularity.

Similarly, for the form-factor shape soft function, we fix $v_1^z = -v_2^z = 1$ and analytically continue in v_1^0. We again obtain an analytic function in the lower half-plane, this time called $g(z)$. We now consider $F(z) = \bar{f}(\frac{1}{\bar{z}})$. This is again an analytic function in the lower half-plane. We consider $z = -iv_0$. Then we have $F(-iv_0) = \bar{f}(-\frac{i}{v^0})$. However, with the imaginary time component, this is simply a Euclidean soft function in the (τ, z) plane. The ratio between the τ, z components then reads $\frac{\tau}{z} = \frac{1}{v_0}$. Let us consider $g(-iv_0)$. This is again a Euclidean soft function in the (τ, z). It is of the same shape up to a Euclidean rotation $\tau \to z$, $\tau \to z$. Thus, due to the Lorentz therefore rotational invariance, the two Euclidean Wilson loop must be real and equal and one has the relation $F(-iv_0) = g(-iv_0)$ for any $v_0 > 0$. Due to the uniqueness of analytic continuation the two analytic functions must be equal. Therefore, we have

$$\bar{f}\left(\frac{1}{\bar{z}}\right) = g(z)\,. \tag{126}$$

We can actually extend $f(z)$ and $g(z)$ into upper half-plane due to the fact that they are real for $-1 < v^0 < 1$ and $v^0 > 1, v^0 < -1$, respectively. Then the relation between the two functions reads

$$g(z) = f\left(\frac{1}{z}\right)\,. \tag{127}$$

See Fig. 23 for a depiction of the analytic domain of $g(z)$.

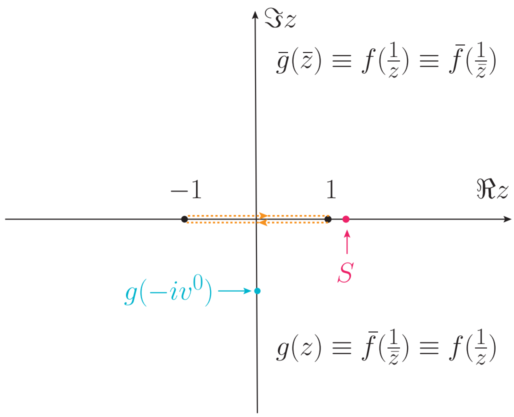

Fig. 23. A depiction of analytic domain of $G(z)$. The $G(z)$ was extended to upper half-plane through $\bar{g}(\bar{z})$ due to the reality of $f(v^0)$ with $v^0 > 1, v^0 < -1$. There are branch cuts between $-1 < v^0 < 1$. The $v^0 = \mp 1$ corresponds to the lightcone singularity.

Given this relation, we can now show the analyticity in hyperbolic angle. It suffices to consider $\Re(z) > 0$. We define the hyperbolic angle for the DY case

$$\mathrm{Cosh}(Y) = \frac{1+z^2}{1-z^2}\,, \tag{128}$$

$$Y = \ln\frac{1+z}{1-z}\,, \tag{129}$$

where the branch of ln is $-\pi \to \pi$, and for the form-factor case :

$$\mathrm{Cosh}(Y) = \frac{z^2+1}{z^2-1} \tag{130}$$

$$Y = \ln\frac{z+1}{z-1}\,. \tag{131}$$

Then in the DY case, one can show that the hyperbolic angle with $-\pi < \Im Y < 0$ is in one-to-one correspondence to z and in the form factor case one can choose $0 < \Im Y < \pi$. Denote the inverse as $z_{\rm DY}(Y)$ and $z_{\rm form}(Y)$, and we define

$$f(Y) = f(z_{\rm DY}(Y)) \,, \tag{132}$$
$$g(Y) = g(z_{\rm form}(Y)) \,. \tag{133}$$

Since we have $\bar{f}(\frac{1}{\bar{z}}) = g(z)$, we have

$$\bar{f}(Y) = \bar{f}\left(z_{\rm DY}(Y)\right) = \bar{f}\left(\frac{1}{\bar{z}_{\rm form}\left(\bar{Y}\right)}\right) = g\left(\bar{Y}\right) \,. \tag{134}$$

This relation extends the $f(z)$ into the upper plane. Comparing with the previous definition of the $\theta(Y)$ in terms of the hyperbolic cosine, we found complete consistency. The analyticity in the case where v_1, v_2 are both spacelike or timelike is therefore established. To extend to the case where one of v_1, v_2 is spacelike but another one is timelike, one can boost the spacelike staple to be time-independent and analytically continue in the other vector. By considering a purely imaginary time component, one again obtains a Euclidean Wilson loop which relates to the $f(-iv_0)$ or $g(-iv_0)$ through Euclidean rotations. Thus, all the soft functions can be connected with each other through a single analytic function. This finally builds the analyticity in the hyperbolic angle, see Fig. 24 for a depiction of the analyticity property of the soft function.

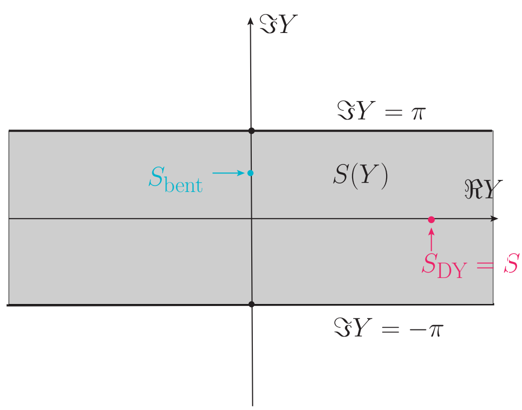

Fig. 24. A depiction of $S(Y)$, analytic in the shaded strip $-\pi \leq \Im Y \leq \pi$. The dots at $Y = \pm i\pi$ indicate the poles located there. The $S_{\rm bent}$ denotes the Euclidean Wilson loop at $\frac{\pi}{2}$ angle.

As a direct consequence of the analyticity relation, we now show that the DY soft function indeed equals the form-factor soft function. The DY soft function is given by $f(\beta-i\epsilon)$ with $z=\beta-i\epsilon$ and $\beta<1$. Based on the functional equation, it equals to $\bar{g}(\frac{1}{\beta+i\epsilon})=\bar{g}(\frac{1}{\beta}-i\epsilon/\beta^2)$. However, $g(\frac{1}{\beta})$ is nothing but the form-factor soft function: the two vectors read $(\frac{1}{\beta},\pm 1)$ which differ from v,v' only by overall re-scalings, therefore are completely equivalent. By taking the $\epsilon\to 0$ limit and noticing that the two soft functions are real, we obtain the equality.

One can also see this from the definition of the hyperbolic angle. For the DY soft function, $u=(\beta,1,0,0)$ and $z=\beta$, therefore, the hyperbolic angle reads $\mathrm{Arcosh}(Y)=\frac{1+\beta^2}{1-\beta^2}$. For the form factor soft function, $v=(\frac{1}{\beta},1)$ and $z=\frac{1}{\beta}$, the hyperbolic angle reads $\mathrm{Arcosh}(Y')=\frac{1+1/\beta^2}{1/\beta^2-1}=\frac{1+\beta^2}{1-\beta^2}$. Therefore, the hyperbolic angles in the two cases are indeed equal. A list of hyperbolic angles for various choices of v_1 and v_2 are given in Table 1.

Table 1. Hyperbolic angles for different off-lightcone vectors.

v_1	v_2	Orientation of v_1	Orientation of v_2	Hyperbolic angle
spacelike	spacelike	past	past	Y
timelike	timelike	past	past	$Y-i\pi$
timelike	timelike	past	future	Y
spacelike	spacelike	past	future	$Y+i\pi$
timelike	spacelike	past	future	$Y+\frac{i\pi}{2}$
timelike	spacelike	past	past	$Y-\frac{i\pi}{2}$

Due to the analyticity in hyperbolic angle, one can use the same symbol $S(b_\perp,\mu,Y+Y')$ to represent all the single-time-ordered soft functions. By taking the lightcone limit, the single-time-ordered soft functions can then be written in the universal form

$$S\left(b_\perp,\mu,Y+Y'\right)=\mathrm{e}^{(Y+Y')K(b_\perp,\mu)+\mathcal{D}(b_\perp,\mu)}\,. \tag{135}$$

To obtain this formula, we have assumed that the lightcone limit is uniform in the imaginary part of the rapidity. In the perturbation theory, the power-suppressed contributions decay exponentially in Y for $\Im Y=0,\pm\frac{\pi}{2},\pm\pi$, which are the only value for which the soft functions can be realized in a real Minkowski space. For another imaginary part this is also supposed to be true. Then, by considering the smallest decay speed, the lightcone limit is indeed uniform in $\Im Y$, in this case, one can show that $\lim_{Y_0\to\infty}\ln S(Y_0+Y')-(Y_0+Y')K(b_\perp,\mu)$ defines an analytic function and equals $Y'K+\mathcal{D}$.

We shall also mention that the methods presented here can be slightly adjusted to show that the "half on-lightcone, half off-lightcone" soft functions using δ regulator in the single time-ordering all relate with each other through analytic continuation as well. For example, we can show

$$S\left(b_\perp, \mu, \delta, \hat{z}\right) = S\left(b_\perp, \mu, -i\delta, \hat{t}\right) . \tag{136}$$

As discussed in the previous subsection, this relation combined with the TMD factorization of a $\bar{Q}Q$ form factor shows that the two definitions for the intrinsic soft function are equal. In the mixed time-ordered case, however, the analyticity is more complicated. The situation is similar to a cross section evaluated using cut-diagrams, where the left-hand side and the right-hand side of the cut poses opposite $i0$ prescriptions in the Feynman propagators, thus we expect that the analyticity of the left- and right-hand sides "collide with each other" when one tries to move from the timelike to the spacelike case, namely, one might encounter logarithms like $\ln(v_1\cdot v_2 - i0)\ln(v_1\cdot v_2 + i0)$. However, if one treats the rapidities in the two sides of the cut to be an independent variable, then one can still reach a certain form of analyticity, although much more complicated and weaker than that of the single-time-ordered case.

4.6. Soft functions in double-time-ordering

After introducing the single-time-ordered soft functions, we briefly comment on the double-time-ordered ones, especially those involving timelike vectors. They can be classified as:

SIDIS soft function. The SIDIS soft function is defined with the same v, v' as that of the form factor one, using double time-orderings

$$S_{\text{SIDIS}}\left(b_\perp, \mu, Y, Y'\right) = S_{\text{mix}}\left(b_\perp, \mu, v, v'\right) . \tag{137}$$

This soft function carries a clear physical meaning. It can be interpreted as a total cross section for a SIDIS process with incoming and outgoing heavy quarks

$$S_{\text{SIDIS}}\left(b_\perp, \mu, Y, Y'\right) = \sum_n \int \mathrm{d}\Pi_n |\langle Q\left(v'\right) n| J\left(v, v'\right)|Q(v)\rangle|^2 , \tag{138}$$

where $|Q(v)\rangle$ and $|Q(v')\rangle$ are heavy-quark state and $J(v, v')$ is a heavy-quark transition current. In the lightcone limit, based on the factorization theorem for the SIDIS process, it factorizes into TMDPDFs and TMD fragmentation functions for the heavy-quark state.

Timelike DY soft function. This soft function is defined as $S_{\rm mix}(b_\perp, \mu, v, -v')$. It is similar to $S_{\rm DY}$, but with timelike gauge links. It describes the total cross section of a DY process with a timelike heavy-quark state.

Spacelike SIDIS soft function This soft function is defined as $S_{\rm mix}(b_\perp, \mu, u, -u')$. In Appendix F, we will argue that in the lightcone limit, it is equivalent to $S_{\rm DY}$.

"Quasi-TMD" soft function. This soft function is defined as $S_{\rm mix}(b_\perp, \mu, v, \hat{z})$, where $\hat{z} = (0,1,0,0)$. It can be viewed as a quasi-TMDPDF for a heavy-quark state.

"Quasi-fragmentation" soft function. This soft function is defined as $S_{\rm mix}(b_\perp, \mu, \hat{z}, v)$. It describes the fragmentation of a spacelike gauge link into a heavy quark and other "hadrons".

The above enumerates all different classes of off-lightcone soft functions in the double time-ordering. Similar classification can be made for single-time-ordered soft functions as well, but as we have shown in detail, all the single-time-ordered soft functions are universal in the lightcone limit.

4.7. Universality in lightcone limit

In the lightcone limit, the off-lightcone soft function in double time-ordering is less universal in the case when there are timelike vectors. This is because timelike gauge links represent physical heavy-quarks propagating in real time, therefore, we can clearly distinguish between the two distinct situations, namely they are in the initial or final state along, or they are in the final-state jet. The former case corresponds to the TMDPDF while the latter case corresponds to the fragmentation function. There is no natural physical reason for their equality, therefore, we expect them to be different in general.

Using lightcone regulators, we found the following factorization formulas:

$$S_{\rm mix}\left(b_\perp, \mu, v, v'\right) = f^{\rm TMD}(b_\perp, \mu, Y) D^{\rm TMD}\left(b_\perp, \mu, Y'\right) , \tag{139}$$

$$S_{\rm mix}\left(b_\perp, \mu, v, -v'\right) = f^{\rm TMD}(b_\perp, \mu, Y) f^{\rm TMD\dagger}\left(b_\perp, \mu, Y'\right) , \tag{140}$$

$$S\left(b_\perp, \mu, v, v'\right) = \Psi^\dagger\left(b_\perp, \mu, Y'\right) \Psi(b_\perp, \mu, Y) . \tag{141}$$

The TMDPDF in the δ regularization scheme is defined as

$$f^{\rm TMD}(b_\perp, \mu, Y) = \lim_{\delta\to 0} \frac{\langle Q(v)|\bar{Q}_v\left(\vec{b}_\perp\right) \mathcal{W}_n\left(\vec{b}_\perp\right) |_\delta Q_v(0)|Q(v)\rangle}{\sqrt{S(b_\perp, \mu, \delta, \delta)}} , \tag{142}$$

and similarly for the wave function and the fragmentation function. All other can be expressed in terms of these functions, including those "quasi-observables". Therefore, in the lightcone limit, we expect that there are three independent off-lightcone soft functions in total, each associated with a natural physical interpretation. As we have seen, the form factor and the quasi-PDF/TMDPDF all allow Euclidean formulations or can be matched to Euclidean quantity, but the fragmentation functions are believed to be not. A list of the classification of off-lightcone soft functions is given in Table 2.

Table 2. Universality classes of off-lightcone soft functions in the lightcone limit.

Type	Time-order	v_1 (orientation)	v_2 (orientation)	Ultra-soft	Factorization	Euclidean formulation
form factor	single	arbitrary (arbitrary)	arbitrary (arbitrary)	yes	$\Psi^\dagger\Psi$	yes
spacelike DY	double	spacelike (past)	spacelike (past)	yes	$\Psi^\dagger\Psi$	yes
timelike DY	double	timelike (past)	timelike (past)	no	$f^{\rm TMD\dagger} f^{\rm TMD}$	yes
$\gamma^* \to \bar{Q}Q$+hadrons	double	timelike (future)	timelike (future)	no	$D^{\rm TMD\dagger} D^{\rm TMD}$	no
timelike SIDIS	double	timelike (past)	timelike (future)	no	$D^{\rm TMD} f^{\rm TMD}$	no
spacelike SIDIS	double	spacelike (past)	spacelike (future)	yes	$\Psi^\dagger\Psi$	yes
quasi-TMD	double	timelike (past)	spacelike (arbitrary)	yes	$\Psi^\dagger f^{\rm TMD}$	yes
quasi-fragmentation	double	spacelike (arbitrary)	timelike (future)	yes	$D^{\rm TMD}\Psi$	no

5. Intrinsic soft function and TMDWFs

In this section, we show that the intrinsic soft function can be extracted from combining the LFWFs and the TMD factorization for a light-meson form factor at large momentum transfer. This section is largely taken from Ref. [33] and we refer to [42] for more details on the LFWF amplitudes.

Let us consider the following form factor of a pseudoscalar light-meson state with constituents $\bar{\psi}\eta$,

$$F\left(b_\perp, \mathcal{P}, \mathcal{P}', \mu\right) = \left\langle \mathcal{P}' \middle| \bar{\eta}\left(\vec{b}_\perp\right) \Gamma' \eta\left(\vec{b}_\perp\right) \bar{\psi}(0) \Gamma \psi(0) \middle| \mathcal{P} \right\rangle \,, \tag{143}$$

where ψ and η are light-quark fields of different flavors; $\mathcal{P}^\mu = (\mathcal{P}^t, \mathcal{P}^z, \vec{0}_\perp)$ and $\mathcal{P}'^\mu = (\mathcal{P}^t, -\mathcal{P}^z, \vec{0}_\perp)$ are two large momenta which approach two opposite lightlike directions in the limit of $\mathcal{P}^z \to \infty$; Γ and Γ' are Dirac gamma matrices, which can be chosen as $\Gamma = \Gamma' = 1$ or $\Gamma = \gamma_\perp$ and $\Gamma' = \gamma_\perp$, so that the quark fields have leading components on the respective lightcones.

At large $\vec{b}_\perp$, the form factor factorizes through TMD factorization into LFWFs. To motivate the factorization, we need to consider the leading region of IR divergences in a similar way for SIDIS and Drell–Yan [6, 47], and the result is shown in Fig. 25.

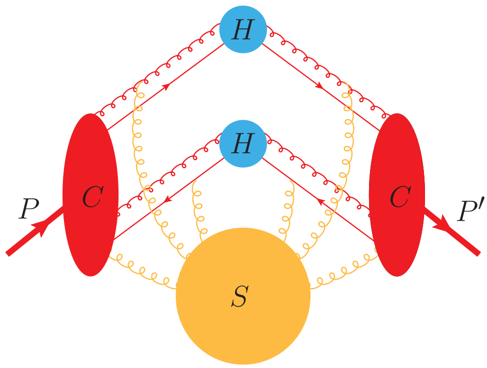

Fig. 25. The reduced diagram for the large-momentum form factor F of a meson. Two H denote the two hard cores separated in space by $\vec{b}_\perp$, C are collinear sub-diagrams, and S denotes the soft sub-diagram.

There are two collinear sub-diagrams responsible for collinear modes in p and n directions, and a soft sub-diagram responsible for soft contributions. Besides, there are two IR-free hard cores localized around 0 and $\vec{b}_\perp$. In the covariant gauge, there are arbitrary numbers of longitudinally-polarized collinear and soft gluons that can connect to the hard and collinear sub-diagrams. Based on the region decomposition, we now follow the standard procedure to make factorization [47].

We first factorize the soft divergences. This can be done with the soft function $S(b_\perp, \mu, \delta^+, \delta^-)$. It resums the soft-gluon radiations from fast-moving colored charges. Intuitively, soft gluons have no impact on the velocity of the fast-moving color charged partons, and the propagators of partons eikonalize to straight gauge links along their moving trajectory.

We then factorize the collinear divergences. For the incoming direction, the collinear divergences are captured by the un-subtracted WF amplitude for the incoming parton $\psi(x, b_\perp, \mu, \delta^{-'})$ defined with a future-pointing gauge link staple W_n^+ as

$$\psi\left(x, b_\perp, \mu, \delta^{-'}\right) = \int \frac{\mathrm{d}\lambda\, \mathrm{e}^{i\lambda x}}{4\pi} \left\langle 0 \middle| \bar{\psi}\left(\lambda n + \vec{b}_\perp\right) \mathcal{W}_n^+\left(\lambda n + \vec{b}_\perp\right)\Big|_{\delta^{-'}} \gamma^5 \gamma^+ \psi(0) \middle| \mathcal{P} \right\rangle . \tag{144}$$

However, the naive WF amplitude contains soft divergences as well, to avoid over-counting, we must subtract out the soft contribution from the bared collinear WF amplitude with the soft function $S(b_\perp, \mu, \delta^+, \delta^{-'})$. This leads to the collinear function for the incoming direction: $\frac{\psi(x,b_\perp,\mu,\delta^{-'})}{S(b_\perp,\mu,\delta^+,\delta^{-'})}$. Similarly, for the out-going direction, one obtains the collinear function $\frac{\psi^\dagger(x',b_\perp,\mu,\delta^{+'})}{S(b_\perp,\mu,\delta^{+'},\delta^-)}$.

Here, we briefly comment on the choices for the gauge link directions in the soft functions and the WF amplitudes. Naively looking, the gauge links along the p direction have to be past-pointing. However, similar to the arguments in Ref. [46] for the SIDIS process, based on the spacetime picture of collinear divergences, one can choose future-pointing gauge links along p direction as well. With all the gauge links being future pointing, the soft function is independent of time-ordering and equals to the standard DY soft function S, and the WFs for the incoming and outgoing hadrons are in complex conjugation to each other.

Besides the collinear and soft functions, we still need the hard core $H_1(Q^2, \bar{Q}^2, \mu^2)$, where $Q^2 = xx'\mathcal{P}\cdot\mathcal{P}'$, $\bar{Q}^2 = \bar{x}\bar{x}'\mathcal{P}\cdot\mathcal{P}'$, and an integral over the momentum fractions x, x' is assumed. Taking together, we have the TMD factorization of the form factor into hard, collinear, and soft functions

$$\begin{aligned} F\left(b_\perp, \mathcal{P}, \mathcal{P}', \mu\right) = &\int \mathrm{d}x\mathrm{d}x' H_1\left(Q^2, \bar{Q}^2, \mu^2\right) \\ &\times \frac{\psi^\dagger\left(x', b_\perp, \mu, \delta^{+'}\right)}{S\left(b_\perp, \mu, \delta^{+'}, \delta^-\right)} \frac{\psi\left(x, b_\perp, \mu, \delta^{-'}\right)}{S\left(b_\perp, \mu, \delta^+, \delta^{-'}\right)} S\left(b_\perp, \mu, \delta^+, \delta^-\right), \end{aligned} \tag{145}$$

noticing the manifest cancellation of all the rapidity regulators in all the WF amplitudes and the soft functions.

Let us consider a one-loop example. The incoming hadron state consists of a free quark with momentum $x_0\mathcal{P}^+$ and a free anti-quark with momentum $\bar{x}_0\mathcal{P}^+$. Similarly, the outgoing state consists of a pair of free quark and anti-quark with momentum $x_0'\mathcal{P}'^-$, $\bar{x}_0'\mathcal{P}'^-$, respectively. The spin projection operator for the incoming state is proportional to $\gamma^5\gamma^-$ and for the out-going state is proportional to $\gamma^5\gamma^+$. The tree-level form factor is normalized to 1. At the one-loop level, the pseudo-scalar form factor with vector currents $\Gamma = \gamma^\mu$, $\Gamma' = \gamma_\mu$ reads

$$F\left(b_\perp, \mathcal{P}, \mathcal{P}', \mu\right) = 1 + \frac{\alpha_s C_F}{2\pi} F^{(1)}\left(b_\perp, Q^2, \bar{Q}^2, \mu^2\right), \tag{146}$$

where $Q^2 = 2x_0x_0'\mathcal{P}^+\mathcal{P}'^-$, $\bar{Q}^2 = 2\bar{x}_0\bar{x}_0'\mathcal{P}^+\mathcal{P}'^-$, and

$$F^{(1)}\left(b_\perp, Q^2, \bar{Q}^2, \mu^2\right) = -7 + \left(-\frac{1}{2}\ln^2 b_\perp^2 Q^2 + \frac{3}{2}\ln b_\perp^2 Q^2 + (Q \to \bar{Q})\right). \tag{147}$$

This result can be obtained from the one-loop DY structure function [67] using the substitution $\ln^2(-Q^2b_\perp^2) \to \frac{1}{2}\ln^2 Q^2b_\perp^2 + \ln^2 \bar{Q}^2b_\perp^2$ and $\ln(-Q^2b_\perp^2) \to \frac{1}{2}\ln Q^2b_\perp^2 + \ln \bar{Q}^2b_\perp^2$. Similar to the TMD factorization for the SIDIS and DY processes, one should also notice that the hard kernel $H_1(Q^2, \bar{Q}^2, \mu^2)$ can be obtained from that of the spacelike Sudakov form factor

$$H_1\left(Q^2, \bar{Q}^2, \mu^2\right) = H^{\rm Sud}\left(-Q^2\right) H^{\rm Sud}\left(-\bar{Q}^2\right) , \tag{148}$$

where $H^{\rm Sud}(-Q^2)$ is given in Ref. [13]. At the one-loop level, we then obtain

$$H_1\left(Q^2, \bar{Q}^2, \mu^2\right) = 1 + \frac{\alpha_{\rm s}}{4\pi}\left(-16 + \frac{\pi^2}{3} + 3L_Q + 3L_{\bar{Q}} - L_Q^2 - L_{\bar{Q}}^2\right) ,$$

where $L_Q = \ln\frac{Q^2}{\mu^2}$ and $L_{\bar{Q}} = \frac{\bar{Q}^2}{\mu^2}$.

Now we construct the Euclidean version of the collinear contributions, left only with the intrinsic soft function and hard cores. We define the quasi-WF, similar to the quasi-TMDPDF as

$$\begin{aligned}\tilde{\psi}\left(x, b_\perp, \mu, \zeta, \bar{\zeta}\,\right) &= \int \frac{\mathrm{d}\lambda}{4\pi}\,\mathrm{e}^{-ix\lambda} \\ &\times \frac{\langle 0|\bar{\psi}\left(z\hat{z}/2 + \vec{b}_\perp\right)\widetilde{\varGamma}\,\mathcal{W}_z\left(z\hat{z}/2 + \vec{b}_\perp; -L\right)\psi\left(-z\hat{z}/2\right)|\mathcal{P}\rangle}{\sqrt{Z_{\rm E}(2L, b_\perp)}} ,\end{aligned} \tag{149}$$

where $\mathcal{W}_z(z\hat{z}/2 + \vec{b}_\perp; -L)$ is a spacelike gauge link staple pointing to $-z$ direction. Similar to the quasi-TMDPDF, we can factorize it using quantities defined in the on-lightcone rapidity scheme,

$$\tilde{\psi}\left(x, b_\perp, \mu, \zeta_z, \bar{\zeta}_z\right) = H_2\left(\frac{\zeta_z}{\mu^2}, \frac{\bar{\zeta}_z}{\mu^2}\right)\frac{\psi(x, b_\perp, \mu, \delta^-)}{S(b_\perp, \mu, \delta^+, \delta^-)} S\left(b_\perp, \mu, \delta^+\right) . \tag{150}$$

This factorization is the result of applying a similar leading-region analysis to the quasi-WF. One should notice that we have chosen the $+\infty$ version of the quasi-WF where the gauge links along the z direction are pointing to $-L$ instead of $+L$. It simply relates to the $+L$ through a complex conjugation. The $\frac{\psi(x,b_\perp,\mu,\delta^-)}{S(b_\perp,\mu,\delta^+,\delta^-)}$ resums all the collinear divergences, while the "half lightcone half off-lightcone" soft function $S(b_\perp, \mu, \delta^+)$ is the on-lightcone version of $S(b_\perp, \mu, Y, 0)$ where one of the off-lightcone directions is along $\hat{z}$. It re-sums the soft divergences of the quasi-WF. The soft functions $S(b_\perp, \mu, \delta^+, \delta^-)$ and $S(b_\perp, \mu, \delta^+)$ subtract away the regulator dependencies introduced in the bared LFWFs. The overall combination on the right-hand side of Eq. (150) is rapidity-regularization-scheme-independent. One needs

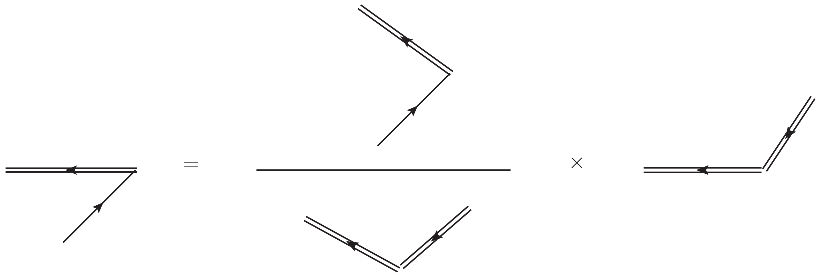

Fig. 26. A schematic depiction of the factorization formula of Eq. (150).

to pay attention to the gauge link directions again. Similar to the case of the form factor, we can choose all the gauge links along the incoming collinear direction to be future-pointing. See Fig. 26 for a depiction of Eq. (150).

Combining together Eq. (145) and Eq. (150) and using the relation $\zeta\zeta' = \zeta_z\zeta'_z$, one notices that all the wave functions and the Collins–Soper kernel contributions can be removed, left with the intrinsic soft function

$$S_{\mathrm{I}}(b_\perp,\mu) = \frac{F\left(b_\perp,\mathcal{P},\mathcal{P}',\mu\right)}{\int \mathrm{d}x\,\mathrm{d}x' H\left(x,x'\right)\tilde{\psi}^\dagger\left(x',b_\perp\right)\tilde{\psi}(x,b_\perp)}\,, \tag{151}$$

where the full expressions for the wave functions read $\tilde{\psi}^\dagger(x',b_\perp) = \tilde{\psi}^\dagger(x',b_\perp,\mu,\zeta'_z,\bar{\zeta}'_z)$, $\tilde{\psi}(x,b_\perp) = \tilde{\psi}(x,b_\perp,\mu,\zeta_z,\bar{\zeta}_z)$, and the matching kernel is given by

$$H\left(x,x'\right) = H\left(\zeta_z,\zeta'_z,\bar{\zeta}_z,\bar{\zeta}'_z,\mu^2\right) = \frac{H_1\left(Q^2,\bar{Q}^2,\mu^2\right)}{H_2\left(\zeta_z/\mu^2,\bar{\zeta}_z/\mu^2\right)H_2\left(\zeta'_z/\mu^2,\bar{\zeta}'_z/\mu^2\right)}\,, \tag{152}$$

where $Q^2 = \sqrt{\zeta_z\zeta'_z}$ and $\bar{Q}^2 = \sqrt{\bar{\zeta}_z\bar{\zeta}'_z}$.

Based on the one-loop results for the form factor, the quasi-WF, and the intrinsic soft function, the one-loop matching kernel for the vector current can be extracted as

$$\begin{aligned} H\left(\zeta_z,\zeta'_z,\bar{\zeta}_z,\bar{\zeta}'_z,\mu^2\right) \;&=\; 1+\frac{\alpha_{\mathrm{s}}C_{\mathrm{F}}}{4\pi}\left(-8+\ln^2\frac{\sqrt{\zeta_z}}{\sqrt{\zeta'_z}}+\ln\frac{\sqrt{\zeta_z\zeta'_z}}{\mu^2}+\left(\zeta\to\bar{\zeta}\right)\right) \\ &\quad +\frac{\alpha_{\mathrm{s}}C_{\mathrm{F}}}{2}i\ln\frac{\sqrt{\zeta_z\bar{\zeta}_z}}{\sqrt{\zeta'_z\bar{\zeta}'_z}}\,. \end{aligned} \tag{153}$$

Here, we briefly comment on the end-point problem. As $x \sim 1$, the hard kernel diverge logarithmically near the end points as $1+\alpha_{\mathrm{s}}\ln^2 x$, but the quasi-WF decay at large or small x linearly, thus the end-point regions behave as $x\ln^2 x$, which is free from those problems for the k_{T} factorization for electromagnetic form factor [68]. Moreover, we can fix the z-component momentum transfer at each of the vertexes to be $\mathcal{P}^z$, which indicates that $x + x' = 1$. In this case, the end-point behavior is improved to $x^2 \ln^2 x$.

Finally, we should point out that Eq. (151) can be rewritten in the form of

$$F\left(b_\perp, \mathcal{P}, \mathcal{P}', \mu\right) = S_{\rm I}(b_\perp, \mu) \int \mathrm{d}x\mathrm{d}x' H\left(x, x'\right) \tilde{\psi}^\dagger\left(x', b_\perp\right) \tilde{\psi}(x, b_\perp)\,, \quad (154)$$

which can be regarded as the gauge-invariant completion of the axial-gauge factorization [1].

Finally, we make a comment that combining the intrinsic soft function and the quasi-TMDPDF, one can effectively factorized the DY cross section in a manifestly regularization-independent fashion

$$\begin{aligned} \sigma &= \int \mathrm{d}x_A\, \mathrm{d}x_B\, \mathrm{d}^2 b_\perp \mathrm{e}^{i\vec{Q}_\perp \cdot \vec{b}_\perp} \hat{\sigma}\left(x_A, x_B, Q^2, \mu\right) \\ &\quad \times \tilde{f}\left(x_A, b_\perp, \mu, \zeta_A\right) \tilde{f}\left(x_B, b_\perp, \mu, \zeta_B\right) S_{\rm I}(b_\perp, \mu)\,. \end{aligned} \quad (155)$$

This can be regarded as the gauge-invariant completion of the axial-gauge factorization proposed in [1].

6. Discussion and conclusion

We should notice, however, that there are some issues not addressed in the paper. First, we did not address the issue regarding renormalization and matching for practical lattice calculations. They will be provided in a separate publication. Second, we did not study the polarized and gluon TMDPDFs. Third, we did not carefully discussed the analyticity property in the double time-ordering case, and we are not clear at this moment whether the heavy-quark TMDPDF and fragmentation functions are equal to all orders in the perturbation theory. We should also mention that all the proofs in the paper, except the ones for the analyticity, follow the typical rigorous standards in the TMD factorization literature. To promote all these "physical proofs" to fully mathematically consistent proofs at the level of those works for UV renormalization remains to be an important but difficult task since one is forced to define and study the rather singular Feynman integrals directly in Minkowski space and develop a rigorous multi-scale analysis which allows simultaneous decomposition of the longitudinal and transverse phase space. A study of these issues is beyond the scope of the paper.

The TMDPDFs are also crucial for understanding the small-x physics. Small-x or long wavelength gluons intercept the Lorentz-contracted pancake composed of active partons at transverse area $\Delta S \approx 1/\vec{k}_\perp^{\,2}$. The color neutrality of the hadron highly suppresses the fluctuations with ΔS comparable to the hadron size, while for small ΔS, the gluon can still probe the local color imbalance that is less suppressed. Therefore, it is natural that small-x gluons tend to concentrate at large $k_\perp$ [69]. At the quantum level, the fast-moving color sources tend to emit soft gluons, which in turn split into more and more soft gluons at smaller and smaller x. This leads to the BFKL or the BK evolution equation which controls the evolution of the soft-gluon population with respect to x and naturally involves the transverse momentum [70–73]. One of the major conjectures of small-x physics is that at sufficiently large rapidity or small-x, the intrinsic $k_\perp$ dependency of the hadron shifts towards the perturbative saturation scale Q_s. To achieve a good understanding of this deep interplay between the longitudinal and transverse degrees of freedom, we need a good understanding of the TMD parton densities [74].

If we generalize the TMDPDFs to include the impact parameter dependence, we can further define the Wigner function, the parton orbital angular momentum distributions, *etc.* [75, 76]. Therefore, the TMDPDFs allow for a more complete and refined 3-D description (or tomography) of the hadron structure [77, 78] rather than the simple 1-D picture offered by the collinear PDFs. The 3-D tomography of hadrons is also one of the major goals of EIC physics for the next several decades.

In conclusion, we have made a careful study of the factorization property for the lattice calculable quasi-TMDPDFs by showing that they match the physical TMDPDF through a factorization formula in the lightcone limit. We carefully studied the properties of the off-lightcone soft functions and have shown that the reduced soft functions defined in various ways are indeed equivalent. We also studied their analyticity and universality properties. We have also shown that the intrinsic soft function can be obtained from the light-meson form factor and quasi-TMDWFs. Therefore, all the gaps in [40, 41] have been filled, and the proposed methods for the lattice calculation of TMD parton densities are justified at the theoretical level.

This is an extended version of the lecture presented at the 61$^{\mathrm{st}}$ Cracow School of Theoretical Physics on the Electron–Ion Collider Physics, September 20–24, 2022, on-line, based on results obtained in collaboration with Prof. Xiangdong Ji. More detailed and refined analysis will be published somewhere else. We thank Stefan Meinel, Peng Sun, Wei Wang, Yi-Bo Yang, Feng Yuan, and Yong Zhao for valuable discussions. This work is supported partially by the U.S. DOE grant DE-FG02-93ER-40762, and by the Priority Research Area SciMat under the program Excellence Initiative — Research University at the Jagiellonian University in Kraków.

Appendix A

Analyticity of gauge links and HQET

It is well-known that the gauge link can be identified as a heavy quark propagator in HQET. First, we start from a segment of gauge link. Let us consider the correlation function

$$G_v(\xi) = \langle 0|\bar{\psi}(\xi)W_v(\xi,0)\psi(0)|0\rangle\,, \tag{A.1}$$

where $v = (v^0, \vec{v}\,)$ is the unit vector pointing from 0 to ξ, and the gauge link is defined by

$$W_v(\xi,0) = \mathcal{P}\exp\left[-ig\int\limits_0^{|\xi|} \mathrm{d}\lambda v\cdot A(\lambda v)\right]\,. \tag{A.2}$$

The gauge link can be written in terms of auxiliary field [79, 80]

$$\bar{\psi}(\xi)W_v(\xi,0)\psi(0) \to \bar{J}(\xi)J(0)\,, \tag{A.3}$$

where $J(x) = \bar{Q}_v(x)\psi(x)$ is the heavy-to-light quark current. Q_v is the auxiliary field with the Lagrangian

$$\mathcal{L}_{\mathrm{aux}} = \bar{Q}_v(iv\cdot D)Q_v\,. \tag{A.4}$$

The propagator for Q_v can be written as

$$\left\langle Q_v(x)\bar{Q}(0)\right\rangle = \langle x|\frac{1}{v\cdot D}|0\rangle = W_v(x,0)\delta^3\left(v^0\vec{x} - x^0\vec{v}\,\right)\theta(\pm v\cdot x) \tag{A.5}$$

which is a segment of gauge link along the v direction from 0 to x up to an overall normalization factor. If v is timelike ($v^2 > 0$ and plus sign in θ-function), then Q_v can be identified as the standard heavy-quark field in HQET. On the other hand, if v is spacelike ($v^2 < 0$ and minus sign in θ-function), the auxiliary field cannot be interpreted directly as physical modes propagating in the real time. However, based on analytic property and Lorentz invariance, they can be interpreted as a heavy-quark propagating in imaginary time.

One can show that with some assumptions, we can analytically continue $G(\xi)$ with timelike ξ into Euclidean space. Without loss of generality, we can consider $\xi = tn^t$ with $v = n^t = (1, 0, \vec{0}_\perp)$ in $(t, z, \vec{\perp})$ coordinate for all timelike ξ since we can boost the latter to the former one. We can denote $G_v(\xi) = G_{n^t}(tn^t)$ as $G(t)$. In the heavy-quark formalism, one can insert a complete set of heavy–light meson state $|n\rangle$ and write $G(t) = \langle 0|\bar{J}(t)J(0)|0\rangle$ as

$$G(t) = \sum_n \langle 0|\bar{J}(0)|n\rangle\langle n|J(0)|0\rangle\,\mathrm{e}^{-iE_nt} = \int \mathrm{d}E\rho(E)\,\mathrm{e}^{-iEt}\,, \tag{A.6}$$

where $\rho(E)$ is the spectral function, and we assume that $\rho(E)$ is not too singular to perform the Fourier transformation and the spectrum E is bounded from below. Furthermore, the UV regulator also needs to preserve the above properties. According to the Paley–Wiener theorem [81], one can analytically continue $t \to \zeta = x + iy$ into the lower half-plane $y < 0$. Thus, we define the y-axis in the lower half-plane, $\zeta = -i\tau$, to be the Euclidean time. The corresponding $G(-i\tau)$ is the Euclidean version of the correlation function. After the analytic continuation into the Euclidean time, the original gauge link along the real time direction then becomes a segment of Euclidean gauge link along the imaginary time direction. If the Euclidean theory preserves the invariance under $(\tau, z) \to (z, \tau)$ (rotation and time reversal), one obtains the equality between $G(-i\tau)$ and the spacelike correlation function $G_{n^z}(\tau n^z)$ where the gauge link is along the z direction with unit vector $n^z = (0, 1, \vec{0}_\perp)$. The above argument can be generalized to generic $v = \gamma(1, \beta, \vec{0}_\perp)$ in Refs. [82, 83].

We demonstrate the above argument in the dimensional regularization scheme ($d = 4 - 2\epsilon$). One can integrate out k^0 first and impose the DR on the transverse direction. This results in the time-ordered perturbation theory in the real time for $G(t)$. Denoting the Fourier variable conjugate to t as E, a generic term in the time-ordered perturbation theory in the real time then reads

$$G(t) \sim \int \frac{\mathrm{d}E \, \mathrm{d}\mu\left(\epsilon, \vec{k}\right)}{2\pi} \mathrm{e}^{-iEt} D\left(\epsilon, \vec{k}\right) \prod_{i=1}^{N} \frac{-i}{E - E_i\left(\vec{k}\right) + i0}\,, \tag{A.7}$$

where $\mathrm{d}\mu(\epsilon, \vec{k})$ is the phase space measure of the intermediate states with three momenta $\vec{k}$. $D(\epsilon, \vec{k})$ is the generic numerator of the integrand. $E_i > 0$ is the total energy of the i^{th} intermediate state. It is clear to see that we can perform the Wick rotation $t \to -i\tau$ and $E \to iE_\tau$ on Eq. (A.7). The result is exactly the imaginary time version $G(-i\tau)$

$$\int \frac{\mathrm{d}E_\tau \, \mathrm{d}\mu\left(\epsilon, \vec{k}\right)}{2\pi} \mathrm{e}^{-iE_\tau \tau} D\left(\epsilon, \vec{k}\right) \prod_{i=1}^{N} \frac{1}{iE_\tau - E_i\left(\vec{k}\right)} \sim G(-i\tau)\,. \tag{A.8}$$

Next, we show that the anomalous dimensions of timelike $[G(t)]$ and spacelike $[G_{n^z}(\tau n^z)]$ correlation functions are equal. The anomalous dimension of $G(t)$ can also be considered as an analytic function in $t \to \zeta = x + iy$. Since the anomalous dimension is constant at $\zeta = -i\tau$, it is constant everywhere in ζ. Thus, the anomalous dimensions of $G(t)$ and $G(-i\tau)$ are the same. We also notice that for the perturbation theory in the Euclidean space, before integrating out the time component k^τ in $G(-i\tau)$, the Feynman integrand in the Euclidean space is invariant under $(\tau, z) \to (z, \tau)$. This leads to $G(-i\tau) = G_{n^z}(\tau n^z)$. Consequently the anomalous dimensions of timelike $[G(t)]$ and spacelike $[G_{n^z}(\tau n^z)]$ correlation functions are equal. This is argued and directly verified to the two-loop level in Ref. [84] based on explicit parameterization of the Feynman integrals. On the contrary, our argument is a consequence of a general analyticity property of QFT.

For another example, one can also consider the vacuum expectation value of a gauge-link along the time-like direction $v = (1, 0, 0, 0)$ in a gauge preserving the Lorentz symmetry

$$F(t) = \frac{1}{N_\mathrm{c}} \mathrm{Tr} \langle 0 | \mathcal{P} \mathrm{e}^{-ig \int_0^t \mathrm{d}s A^t(s)} | 0 \rangle \,. \tag{A.9}$$

Based on similar assumptions, $F(t)$ can be analytically continued into the lower half-plane, $t \to \zeta = x + iy$ with $y < 0$. For $z = -i\tau$, $F(-i\tau)$ is then defined to be the Euclidean gauge link along the imaginary time direction. The Lorentz invariance of the original theory then leads to Euclidean invariance which indicates that $F(-i\tau)$ and a segment of spacelike gauge link along the z direction with the total length τ are equivalent.

Appendix B

Non-Abelian eikonal exponentiation

First, we briefly review the replica method to prove the exponentiation theorem. Let us consider an $\mathrm{SU}(N)^n$ gauge theory with $\mathcal{A} = \bigoplus_{i=1}^n A_i$, where i denote n copies of Yang–Mills fields with no interaction between each other. By definition, the VEV of the Wilson loop is

$$W(\mathcal{C}, \mathcal{A}) = W(\mathcal{C}, A)^n = 1 + n \ln W(\mathcal{C}, A) + \mathcal{O}\left(n^2\right) \,. \tag{B.1}$$

On the other hand, the perturbative expansion for $W(\mathcal{C}, \mathcal{A})$ consists of identical diagrams and momentum integrals as those for $W(\mathcal{C}, A)$. The only difference is that every gauge field now carries an extra label i ranging from 1 to n, and the results of the color trace will depend on the arrangement of these extra labels along the contour. Summing over all possible arrangements for each diagram, the color trace becomes a polynomial in n. Comparing with the expansion in Eq. (B.1), we obtain $\ln W(\mathcal{C}, A)$ from the linear term of n. One can show that only web diagrams contain contributions linear in n using diagrammatic analysis. Therefore, $W(\mathcal{C}, A)$ can be exponentiated.

Next, we consider the partial exponentiation of a gauge link in correlation function of bilinear operators, see Eq. (46),

$$F\left(\mathcal{C}, x, x'\right) = \mathrm{Tr}\left\langle O(x) W\left(\mathcal{C}, x' \to x\right) O'\left(x'\right)\right\rangle \,. \tag{B.2}$$

The replica method cannot be used in this case due to the presence of other operators. To show the partial exponentiation, we use the diagrammatic method proposed in Refs. [54, 60]. The color factor $C(G)$ of each diagram G can be written as a sum of color factors $C(d)$, where d belongs to a set of decompositions $\mathrm{dec}(G)$

$$C(G) = \sum_{d \in \mathrm{dec}(G)} C(d) \,. \tag{B.3}$$

Each decomposition of the color factor of G consists of an operator-link 2PI vertex w_0 and several webs w_i, where $i = 1 \sim n(d)$ with $n(d)$ being a number of webs, see Fig. 27 for an example. The color factor for each decomposition is equal to the product of color factors

$$C(d) = \prod_{i=0}^{n(d)} C(w_i) \,, \tag{B.4}$$

where $C(w_0)$ is the modified color factor of operator-link 2PI vertex, and $C(w_{i\neq 0})s$ are the standard "maximally non-Abelian" color factors. In general, $C(w_0)$ is not "maximally non-Abelian" because the gluon attached to the operators cannot be disentangled.

To prove the partial exponentiation, we need the generalized "eikonal identity"

$$\sum_{G \in G_d} I(G) = \frac{1}{S_d} \prod_{i=0}^{n(d)} I(w_i) \,, \tag{B.5}$$

where G_d is a set of diagrams whose decomposition set contains d, $I(G)$ denotes the Feynman integral of diagram G, and "symmetry factor"

$$S_d = \prod_i n_i! \,, \tag{B.6}$$

where n_i counts the multiplicity of identical web diagrams for a given d. For a Wilson loop, the product runs from 1 to $n(d)$ and Eq. (B.5) reduces to the standard eikonal identity [60]. To include operator-link 2PI vertex w_0, we must fix the diagram within the vertex and the proof is similar to the standard one.

With the above ingredient, we start to prove partial exponentiation

$$\begin{aligned} F(\mathcal{C}, x, x') &= \sum_G C(G) I(G) = \sum_G \sum_{d \in \mathrm{dec}(G)} \prod_{i=0}^{n(d)} C(w_i) I(G) \\ &= \sum_d \sum_{G \in G_d} I(G) \prod_{i=0}^{n(d)} C(w_i) = \sum_d \frac{1}{S_d} \prod_{i=0}^{n(d)} C(w_i) I(w_i) \,. \end{aligned} \tag{B.7}$$

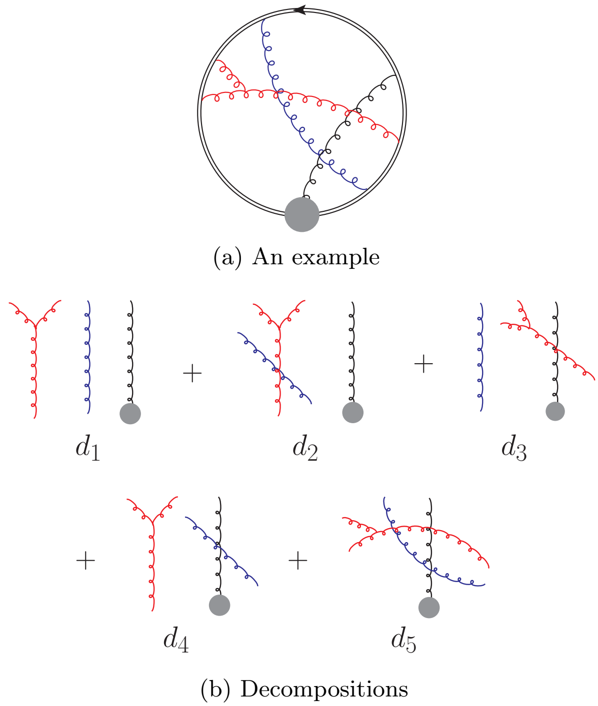

Fig. 27. Decomposition of color factors: In example (a), there are five different decompositions $[n(d) = 5]$, shown in (b). The grey blob is the operator-link 2PI vertex w_0, and the circled double line represents an arbitrary contour of the gauge link. The decomposition d_1 contains two webs and w_0; d_2, d_3, and d_4 each contains one web and w_0; d_5 belongs to w_0.

We used Eq. (B.5) to obtain the last line. Next, we change the sum of decompositions into the sum over webs by fixing w_0

$$F\left(\mathcal{C}, x, x'\right) = \sum_{w_0} C(w_0) I(w_0) \sum_{d'} \frac{1}{S_{d'}} \prod_{i=1}^{n(d')} C(w_i) I(w_i)\,, \tag{B.8}$$

where d' is the decomposition of the gauge link part without the operator-link 2PI vertex. Following the same argument in Ref. [60], we have the exponentiation

$$\sum_{d'} \frac{1}{S_{d'}} \prod_{i=1}^{n(d')} C(w_i) I(w_i) = \mathrm{e}^{\Phi(\mathcal{C})}\,, \tag{B.9}$$

which is similar to exponentiation of a vacuum bubble. By expressing the operator-link 2PI vertex as

$$\mathrm{Tr}\left\langle O(x)W\left(\mathcal{C},x'\to x\right)O'\left(x'\right)\right\rangle_{\mathrm{2PI}}=\sum_{w_0}C(w_0)I(w_0) \tag{B.10}$$

and combining Eqs. (B.8) and (B.9), the proof of Eq. (47) is concluded.

Appendix C

Landau equation

In this appendix, we briefly introduce the Landau equation that determines the IR divergences of a Feynman integral. The basic idea is that the Feynman integrand

$$\frac{N(k,x)}{\left[\sum_i x_i D_i(k)+i0\right]^N} \tag{C.1}$$

is analytic in the loop momenta k and Feynman parameters x_i. The singularity of the integrand is caused by $\sum_i x_i D_i(k)=0$. If the contour of the integration can be chosen in such a way that the singularities at $\sum_i x_i D_i(k)=0$ can be avoided completely, then the integral is called IR safe. If the integration contour cannot be deformed away from the singularities, then the singularities of the integral are "pinched." However, those pinched singularities may not lead to IR divergences due to the power suppression.

To determine the possible pinching solutions, we Taylor expand the denominator $\sum_i x_i D_i(k)$ around a singularity at x_i and k. It is sufficient to assume that x_is are not at the boundary of the integration domain, namely $x_i\neq 0,1$. Indeed, $x_i=0$ indicates that the propagator corresponding to x_i does not participate in the pinching and $x_i=1$ indicates that it is the only propagator that participates in the pinching. In both cases, one can remove all the propagators that do not participate in the pinching and perform the analysis in the remaining propagators. Notice that if there are linear terms in the expansion, then the integral is not pinched since in such cases, the integral near the singularity is of the form of

$$\frac{1}{(a_i z_i+i0)^N}\,, \tag{C.2}$$

where z_is are complex variables, which are linear combinations of x_i and k, and a_is are generic constants. Clearly such an integral is not pinched. However, if the linear terms all vanishe, then one encounters integrals of the form of

$$\frac{1}{\left(a_i z_i^2+i0\right)^N}\,, \tag{C.3}$$

which are generally pinched. Therefore, the coefficient of the linear term in the Taylor expansion of the denominator $\sum_i x_i D_i(k)$ in powers of x_i and k must vanish. We obtain the pinching corresponding to solutions to the equations

$$D_i(k) \;=\; 0\,, \tag{C.4}$$

$$\sum_i x_i \partial_k D_i(k) \;=\; 0\,. \tag{C.5}$$

The second one is called the Landau equation.

If all the D_is are massless relativistic propagators, $D_i = p_i^2 + i0$, the propagators can be classified as collinear or soft. Any $p_i^\mu \neq 0$ is called a collinear propagator, while $p_i^\mu = 0$ are called soft propagators. All the soft propagators decouple from the Landau equation since $\partial_k p_i^2 \propto p_i = 0$. The Landau equation applies to the collinear propagators and can be viewed as a constraint on the diagrammatic structure of all possible collinear divergences.

One can show that the condition has a clear physical meaning [11]: All the collinear propagators can be identified as classical trajectories of particles traveling with on-shell four-momenta p_i^μs in Minkowski space. In the constraint equation, $x_i \partial_k D_i(k) \propto x_i p_i^\mu$ can be interpreted as a total displacement of the collinear particle along a given propagator before joining with other particles at the same spacetime point. The Feynman parameter x_i can be viewed as the affine/proper time for the massless/massive particle. The Landau equation then describes the condition that the consecutive displacements must add up to zero along any closed momentum loop [85]. On the other hand, there are no constraints on the soft propagators.

As an example, let us consider the diagram in Fig. 28. The momenta for incoming and outgoing collinear particles are p and p', respectively. The momentum of the virtual gluon is k. Using the Feynman parametrization,

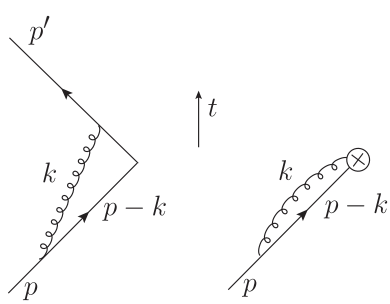

Fig. 28. Examples of an isolated hard kernel.

one has the following form of the denominator:

$$xk^2 + y(p-k)^2 + (1-x-y)\left(p'-k\right)^2 . \tag{C.6}$$

The Landau equation then reads

$$\begin{aligned} xk^2 + y(p-k)^2 + (1-x-y)\left(p'-k\right)^2 &= 0\,, &\text{(C.7)}\\ k^2 - \left(p'-k\right)^2 &= 0\,, &\text{(C.8)}\\ (p-k)^2 - \left(p'-k\right)^2 &= 0\,, &\text{(C.9)}\\ xk - y(p-k) - (1-x-y)\left(p'-k\right) &= 0\,. &\text{(C.10)} \end{aligned}$$

The first three equations require that all the propagators must be zero if $x, y, 1-x-y$ are all non-vanishing

$$k^2 = (p-k)^2 = \left(p'-k\right)^2 = 0\,. \tag{C.11}$$

However, since p and p' are non-parallel, in this case, the fourth equation cannot support non-trivial solutions. Thus either x, y or $1-x-y$ must vanish. If $x=0$, then the equation reads

$$\begin{aligned} (p-k)^2 = \left(p'-k\right)^2 &= 0\,, &\text{(C.12)}\\ y(p-k) + (1-y)\left(p'-k\right) &= 0\,. &\text{(C.13)} \end{aligned}$$

This can only be solved by $y=0, k=p_2$ or $y=1, k=p_1$. The two cases correspond to the quark with momenta $p-k$, $p'-k$ being soft. If $x \neq 0$, then y or $1-x-y$ must be zero. In the former case, we have

$$xk = (1-x)\left(p'-k\right) . \tag{C.14}$$

This corresponds to the collinear to p' region. In the latter case, we have

$$xk = (1-x)(p-k)\,. \tag{C.15}$$

This corresponds to collinear to p region. As shown in Fig. 28, xk and $(1-x)(p-k)$ can be interpreted as the displacements of the collinear gluon and quarks. The propagator p_2-k is hard in this region, corresponding to the crossed vertex in the figure. For both of these two collinear regions, the end-point $x=1$ corresponds to the region where the gluon with momenta k becomes soft or $k=0$.

With the presence of gauge link propagators, namely $D_i = n_i \cdot k$ for some is, the Landau equation can be generalized straightforwardly. If the gauge-link participates in the pinching, one receives contributions proportional to $x_i \partial_k n_i \cdot k = x_i n_i$ in the Landau equation. These can be identified as displacements along the gauge-link directions. Combining with collinear particles, the Landau equation indicates that the collinear propagators and the pinched gauge-link propagators can be realized in Minkowski space as well. The pinched gauge-link propagators correspond to displacements along the gauge-link directions which can be connected to the same end-point of the collinear particle trajectory. The total displacement along any closed contour must vanish, as in the case without the gauge link.

As an example, let us consider the diagram in Fig. 29. The gauge-link is in n direction and the external momentum p is collinear. Similar to the case without gauge-link, the Landau equation requires

$$xk - y(p-k) - (1-x-y)n = 0\,. \tag{C.16}$$

If $n^2 \neq 0$, then the non-trivial solution only supports $1-x-y=0$, which leads to the standard collinear to p and soft regions. If $n^2 = 0$ but $n \cdot p \neq 0$, then the Landau equation supports the following solution:

$$k^2 = 0\,, \tag{C.17}$$

$$xk = (1-x)n\,. \tag{C.18}$$

In this case, the gluon is collinear to the lightlike gauge-link. This type of solution corresponds exactly to the rapidity divergences.

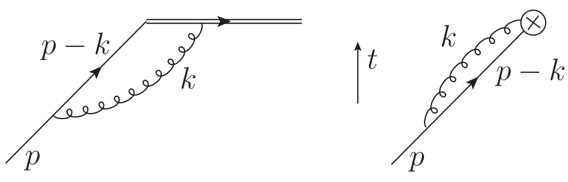

Fig. 29. Examples of an isolated hard kernel.

For quasi-TMDPDFs, there is only one collinear direction, then the corresponding displacement can only be timelike, while for the gauge links they are in z direction. They must add up to zero separately. Therefore, the Landau equation for the collinear propagators and gauge links decouples. For the collinear propagators, the Landau equation is completely identical to the case without any gauge links. Consequently, two collinear propagators are viewed as joining at the same spacetime points if they are both connected to the same gauge link. This is the reason why the hard kernel is contracted to the quark-link vertex. Furthermore, by analyzing the Landau equation for the gauge-link propagators, one can show that no nonzero solution of x_i is supported unless there is dipolar two-to-two amplitude insertion, in which the nonzero solution is nothing but the pinch-pole singularity for the staple-shaped gauge links.

Appendix D

IR safety for timelike $S_{\rm cut}$

For a generic off-lightcone soft function, there are two types of IR divergences: one is the pinch-pole singularity and the other is the ultra-soft mode (the Wilson line self-energy has been subtracted by the vacuum expectation value of Wilson loop). Both IR divergences behave as power divergences. However, for a timelike soft function (v_1 and v_2 are both timelike) with double time-ordering, we show that it is free from IR divergences. We first show the heuristic argument made in Ref. [1] and point out the loophole caused by linear divergence. We then present a proper treatment on the pinch-pole singularity and the ultra-soft mode to prove that the timelike $S_{\rm cut}$ is indeed IR safe.

Following Ref. [1], we consider a soft function contains UV and IR regulators, $\Lambda_{\rm UV}$ and $\Lambda_{\rm IR}$. Since the logarithmic IR divergences are independent of the $b_\perp$ and the limit $\Lambda_{\rm IR} \to \infty$ commutes with the $\Lambda_{\rm UV} \to \infty$ limit, we can first fix the UV regulator and take the $b_\perp \to 0$ limit, then the soft function becomes unity. Then we can drop the IR regulator, then perform the UV renormalization. Therefore, the IR divergence vanishes for the soft function. Notice that this argument does not work with the presence of linear IR divergence, since in this case, the UV and IR divergences can mix with each other in the form of $\Lambda_{\rm UV}/\Lambda_{\rm IR}$ and the order of removing the IR and UV regulators does not commute. Hence the breakdown of the argument with the presence of the pinch-pole singularity or ultra-soft mode.

Before showing the pinch-pole singularity or ultra-soft mode vanishes in timelike $S_{\rm cut}$, we analyze the structure of the web diagram of the soft function. If we take the $b_\perp \to 0$ limit before $\Lambda_{\rm UV}$ and $\Lambda_{\rm IR}$, the soft function becomes unity and the contribution of the web diagram is zero. For example, if we use DR ($d = 4 - 2\epsilon$) as UV regulator and the length of the gauge link staple L as IR regulator, the web diagram must be of the form of

$$\int \frac{\mathrm{d}^{2-2\epsilon} k_\perp}{(2\pi)^{2-2\epsilon}} \Phi(k_\perp, \mu, L, \epsilon) \left(\mathrm{e}^{i k_\perp \cdot b_\perp} - 1 \right) , \tag{D.1}$$

where $\Phi(k_\perp, \mu, L, \epsilon)$ is the summation over all real webs at a finite transverse momentum. The above equation also indicates the cancellation between real and virtual diagrams. We will show that $\Phi(k_\perp, \mu, L, \epsilon)$ is IR safe and the small-$k_\perp$ behavior of Φ is of the form of $1/k_\perp^{2+n\epsilon}$. Therefore, due to cancellation between real and virtual contributions in the small-$k_\perp$ region, the resulting integral is IR safe.

We show that there is no pinch-pole singularity in timelike $S_{\rm cut}$ before the Wilson loop subtraction. It suffices to consider the self-interaction webs for the gauge link staple, since it is straightforward to see that there is no pinching for the 2PI vertex part. For the self-interactions diagrams, there are again those intermediate gauge link pairs between the dipolar 2PI amplitudes insertions that generate the pinch, see Fig. 7. The propagator of a pair of such gauge links is

$$\frac{1}{k \cdot v + i0} \frac{1}{k \cdot v - i0} \,. \tag{D.2}$$

Based on the momentum conservation, k equals the total on-shell momentum flowing from one side of the gauge link crossing the cut to another side of the gauge link

$$k^\mu = \sum_{i \in \text{cut}} k_i^\mu \,, \tag{D.3}$$

$$k_i^\mu = \left(\sqrt{\vec{k}_i^2 + m_i^2}, \vec{k}_i \right) \,, \tag{D.4}$$

where m_is are the masses of quarks and gluons. Therefore, k is always timelike and within the forward lightcone, thus $k \cdot v > 0$ if any of the m_is is nonzero. In such case, $i0$ prescription in the gauge link propagator can be dropped and there is no pinch-pole singularity. If all $m_i = 0$, then $k \cdot v = 0$ when all the $\vec{k}_i = 0$. In such a case, the gauge link can produce standard infrared divergences which are not regulated by $i0$. This $i0$ is important only if $k \cdot v$ can approach zero from both positive and negative sides. Therefore, in this case, the $i0$ prescription can still be neglected.

We then consider the 2PI vertex diagrams. To study the IR divergence, it suffices to treat $k_\perp$ as a hard scale and do power-counting correspondingly. Let us denote the hard kernel containing the vertex as $H_{\rm V}$. Due to the absence of pinching, the infrared gauge links in the standard double-line representation can be counted as a soft particle with dimension $\frac{3}{2}$, therefore the power-counting reads

$$\lambda^{\frac{3}{2}N\left(SH_{\rm V},\frac{3}{2}\right)+N(SH_{\rm V},1)-6} \prod_i \lambda^{\frac{3}{2}N\left(SH_i,\frac{3}{2}\right)+N(SH_i,1)-4} \,. \tag{D.5}$$

The disconnected hard region can then be absorbed into soft regions. The leading region then reads

$$N\left(SH_{\rm V},\tfrac{3}{2}\right) = 4 \,, \tag{D.6}$$

with all other connection numbers equal zero. Thus, the IR divergences are caused by soft gauge links inserted into the central hard core in which the $k_\perp$ is flowing across the cut. The relevant diagrammatic structure can then be stated as follows.

We define a 4PI "connected" vertex to be a vertex web that cannot be cut into two disconnected pieces by cutting at 4 gauge links, 2 for each side. Therefore, a 4PI diagram is free from IR divergence. A generic web diagram can then be decomposed into a composition of N 4PI webs, between the 4PI webs there can be 2-to-2 link amplitudes insertions. Each such insertion is counted as a 4PI web as well. The leading region then can be labeled R_i, in which there are i hard 4PI webs inside and $N-i$ soft webs outside. The soft

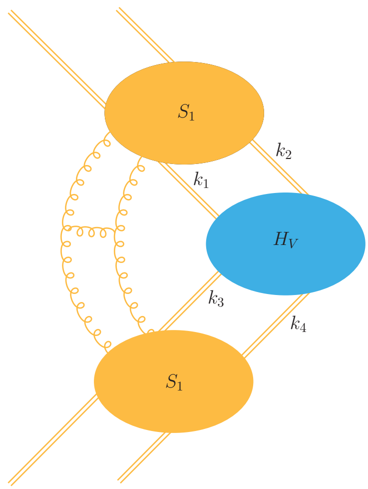

Fig. 30. A diagram with 2 4PI webs. The central one containing the vertex is hard, and the outside one is soft. To obtain the leading IR divergence, one can neglect k_1 to k_4 in $H_{\rm V}$.

divergence in the region R_i can be approximated by neglecting all the soft momenta inside the hard webs, provided there is no power-IR divergence, see Fig. 30 for example. Then the leading IR divergences in R_i are contained in soft functions evaluated at $b_\perp = 0$, but with $N-i$ 4PI webs and arbitrary color structures at the vertex. Assuming up to $N-1$ 4PI webs, all these soft functions are free from the power-IR divergence, and their vertex part can be written in the form of Eq. (D.1) with finite Φ_{c_i} in which c_i denotes the color structure at the vertex. There is a finite number of linear independent color structures. In each of the region R_i with $i > 0$, the IR divergences are contained in the combination

$$\int \frac{{\rm d}^{2-2\epsilon}k_\perp}{(2\pi)^{2-2\epsilon}}\Phi_{c_i}(k_\perp,\mu,L,\epsilon)(1-1) \tag{D.7}$$

which vanish exactly. Notice that the leading power approximation can only be performed if there are no power-IR divergences, which is true given our assumption. Therefore, in region R_i there are no IR divergences. Since there must be at least a hard region, $i \neq 0$, the real vertex diagram $\Phi(k_\perp)$ for the original soft function at finite $k_\perp$ is, therefore, IR finite. Moreover, we can put an arbitrary color factor at the vertexes without changing the argument. The IR finiteness for N 4PI webs is, therefore, established and by induction, it works to $N+1$ webs as well.

Appendix E

Alternative proof of rapidity divergence factorization

In this appendix, we provide a different approach to the rapidity factorization. We hope that the treatment here illustrates the key points in a transparent way. We choose to work in the axial gauge $n \cdot A = 0$. Similar to the arguments in [1], we choose $n = \hat{z} + \vec{n}_\perp$, where $\vec{n}_\perp$ is a non-vanishing vector in the transverse plane. We choose the boundary condition $A^\mu(n \cdot x = +\infty) = 0$, and we can choose either the single or mixed time-ordering with spacelike off-lightcone vectors for the SIDIS kinematics. In this case, the transverse gauge links in the infinity can be neglected. Notice that in this case, the hyperbolic angle reads $\theta = Y + Y' + i\pi$. The so-called pinch-pole singularities are not relevant to the rapidity divergence and can be factorized. One can also choose a finite box in n direction or include transverse gauge links to regulate them. We separate the webs for the off-lightcone soft function into two types: the self-interaction webs for the staples and the 2PI vertex webs connecting the two staples. We need to show that the vertex webs are free from rapidity divergences to all orders. Then, the rapidity divergences are isolated to the self-interaction webs. Denote the divergent part of the full webs of the soft function as $\mathrm{div}_1(Y+Y')$ and those for the self-interaction webs as $\mathrm{div}_2(Y)$. We then end up at the functional equation

$$\mathrm{div}_1\left(Y+Y'\right) = \mathrm{div}_2(Y) + \mathrm{div}_2\left(Y'\right) . \tag{E.1}$$

This functional relation can only be solved by linear functions in Y. Indeed, we can choose a large but finite Y_0 above which the divergent part is a continuous function. Then from the functional equation we have

$$\mathrm{div}_1(Y) = \mathrm{div}_2(Y - Y_0) + \mathrm{div}_2(Y_0) . \tag{E.2}$$

Therefore,

$$\mathrm{div}_2\left(YY_0+Y'-Y_0+Y_0\right)+\mathrm{div}_2(Y_0) = \mathrm{div}_2(Y-Y_0+Y_0)+\mathrm{div}_2\left(Y'-Y_0+Y_0\right) . \tag{E.3}$$

Thus, for $f(t)=\mathrm{div}_2(Y_0+t)-\mathrm{div}_2(Y_0)$, we obtain the equation

$$f\left(t+t'\right)=f(t)+f\left(t'\right)\,. \tag{E.4}$$

Then we can deduce from it that $f(\frac{m}{n})=\frac{m}{n}f(1)$ for any positive rational number $\frac{m}{n}>0$, and since the function is continuous, we must have $f(t)=tf(1)$. This shows the linearity of the divergence. Keeping only the divergent part, we must have $\mathrm{div}_1(Y)=\mathrm{div}_2(Y)=KY$ where K is a function of $b_\perp$. Furthermore, there are no natural hard scales available for the soft function, thus no Y dependency can be generated from hard regions as well. This leads to the rapidity factorization.

We now show that the vertex webs are free from rapidity divergences after summing over diagrams. For this purpose, we need to know the nature of rapidity divergence. We claim that they are collinear divergences for the lightlike gauge links. Indeed, if one directly puts the gauge links on the lightcone, then the corresponding Landau equation supports nontrivial solution of collinear divergences in the lightcone direction. They correspond to nothing but the rapidity divergences. With a rapidity cutoff being imposed, the modes generating rapidity divergences may not necessarily be exactly at the rapidity cutoff, but will remain in the large rapidity region and will be pushed into infinity as one removes the rapidity regulator. The quantitative behavior of such a process is very sensitive to the detailed form of the rapidity regulator. But a common lesson is that the rapidity divergence is the result of lacking a uniform large rapidity limit and can be obtained by analyzing the leading regions which supports large rapidity modes.

The generic structure of the region is determined by the solution of the Landau equation and is independent of the regulator. However, to determine which regions are leading, we need power-counting information, which may depend on the regulator. For the off-lightcone soft function, the large rapidity modes are simply boosted from the rest frames of the gauge links, therefore, the power scounting for the collinear modes reads $(\mathrm{e}^{\pm Y},\mathrm{e}^{\mp Y},1,1)k_\perp$. The soft region as the solution to Landau equation simply corresponds to a point. But based on the IR safety of the soft functions, the power counting for the soft modes reads $(1,1,1,1)k_\perp$. The soft and collinear modes are separated in the rapidity space instead of in the $k_\perp$ space. The rapidity divergence is induced by those modes with rapidity much larger than 1 but smaller than Y, namely, they are near the border between collinear and soft regions. Without a collinear region, however, no rapidity divergences can be generated. Based on the power-counting information, the leading region for the soft function is shown in Fig. 31. There are two collinear regions and a soft region. For real diagrams, the $k_\perp$ is of the order of $1/b_\perp$ and for virtual diagrams the $k_\perp$ can be up to the UV cutoff. Due to eikonal exponentiation, the virtual and real diagrams can be treated separately. There are also two possible hard regions around each of the gauge link cusps.

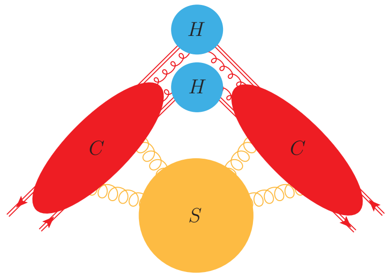

Fig. 31. The generic leading region for the off-lightcone soft factor.

In the axial gauge, the structure of the leading region can be further simplified. Since the power-leading components $A^{\pm}$ of collinear gluons are killed by the axial-gauge condition when they are inserted into "hard-parts", the two collinear regions cannot talk to each other directly. Thus, the hard part H is absent in the leading region, and the two collinear regions communicate with each other through soft-gluon exchanges. This is shown in Fig. 32.

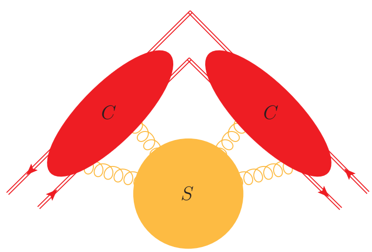

Fig. 32. The leading region in the axial gauge, the hard kernel H is absent.

To disentangle the two collinear regions, we need to use the standard soft-to-collinear eikonal approximation to factorize the leading contribution of soft gluons. This can be justified in the following way. First, the Glauber region is not a problem since $n_\perp \neq 0$. Second, the $k_\perp$s for collinear propagators are required to be at least of the same order as those for the soft propagators in order to be power-leading. Thus, both in the real and virtual diagrams, we only need to take into account the possibility that a soft gluon was inserted into a collinear gluon with a comparable or larger $k_\perp$. In this situation, we are safe to use the eikonal approximation. The result of applying the Ward identity is shown in Fig. 33.

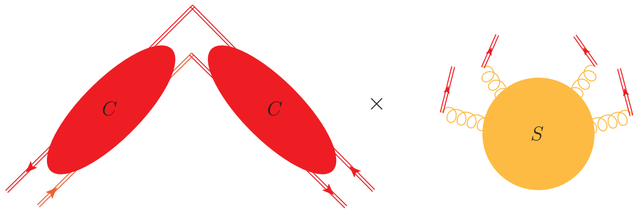

Fig. 33. The leading region in axial gauge after soft factorization.

When restricting to web diagrams, the soft factorization implies that the collinear contributions cancel between different 2PI vertex web diagrams to any order in α_s. To show this, we adopt the replica trick introduced before. We first notice that the web diagrams are linear in the replica number n. In order for the contributions in Fig. 33 to be linear in n, either C or S must be trivial. If S is trivial, then one is not dealing with vertex webs. Thus, C must be trivial, which indicates that all the power-leading collinear contributions in 2PI vertex webs vanish after summing over diagrams. Therefore, no rapidity divergence can be generated. Due to the absence of a hard region, no Y dependence can be generated from the hard region as well. One should notice that for the virtual diagram, the $k_\perp$ can be comparable to the UV cutoff, but according to our classification, it is still labeled soft.

A more quantitative argument works as follows. One chooses a large Y_0, large N. To a given order n_0 in perturbation theory, there are at most n gluon propagators. We choose $N \gg n$ with $nNY_0 \sim Y + Y'$. Now let us perform a renormalization group analysis in rapidity spaces and "integrate out" the large rapidity modes step-by-step. To enforce a clear separation between different slices in rapidity space, we first split the rapidity spaces between $-NnY_0$ and NnY_0 into N parts

$$R_k = \{Y : (k-1)nY_0 < Y < knY_0\} \,. \tag{E.5}$$

For any Feynman diagram up to the order of n_0, we partition the phase spaces for virtual gluons according to their rapidities. We define a group to be a connected group of gluons with a maximal number n and with consecutive rapidity differences no larger than Y_0. We call the group is at rapidity slice k if the average rapidity of the group is within R_k. Then, between 2 groups there is a minimal rapidity gap Y_0. Since there is only n or less gluons in the diagram, there can be at most n groups. If all the rapidity reparations are less than Y_0, then all the gluons will be within a single group. We now "integrate out" all the R_N groups, left only with contributions from R_{N-1} and lower-groups in the vertex webs diagrams. In this step, we need to control the IR behavior for the R_N group, namely we need to show that for gluons with that rapidity scales no IR divergence will be generated, and the typical "power counting" for that group is indeed consistent with $k^+k^- \sim k_\perp^2 \sim 1/b_\perp^2$. This can be non-trivial, of course. Assuming this can be done, let us consider the consequence on the R_{N-1} and lower groups after the "integrating out". For this purpose, we need to sum over all the possible connections between the R_N group and the R_{N-1} groups. We notice that since there is at least a Y_0 rapidity separation between gluons lines belonging to different groups, the rapidity of $k_{N-1}+k_N$, where k_N and k_{N-1} are in N and $N-1$ group can be estimated as below, assuming the "SCET II" type power counting

$$NnY_0 + \ln\frac{1\pm \mathrm{e}^{-Y_0}}{1\mp \mathrm{e}^{-Y_0}}\,. \tag{E.6}$$

For large enough Y_0, the second term is suppressed, and the resulting gluon with momentum $k_{N-1}+k_N$ still leaves a gap between R_{N-1} and the lower groups. Therefore, the integrating out process can be approximated in the following way: we first fix a R_N group and consider all the possible connections between R_{N-1} and the lower groups. Then, the "insertion" of R_{N-1} and lower group can be approximated using the standard eikonal approximation, with the resulting error term of the order of $\mathcal{O}\left(\mathrm{e}^{-2Y_0}\right)$ due to the rapidity gap. Therefore, the integrands factorize due to the Ward identity, which is valid at integrand level after shifting loop momentum, which is argued to be possible due to the large rapidity gap. Then, for the vertex web diagrams, if there are non-trivial R_{N-1} to R_N connections, the contribution vanishes due to the replica argument as before, thus we end up at the unmodified contributions with all the gluons within R_{N-1} or lower

$$V_N = V_{N,\mathrm{pure}} + V_{N-1} + \mathcal{O}\left(\mathrm{e}^{-Y_0}\right)\,. \tag{E.7}$$

Here, the $V_{N,\mathrm{pure}}$ is the contribution from purely R_N group, which is of the order of $\mathcal{O}\,\mathrm{e}^{-NY_0}$ due to the axial gauge condition. Thus, we end up with the following equation:

$$V_N = \mathcal{O}\,\mathrm{e}^{-NY_0} + V_{N-1} + \mathcal{O}\,\mathrm{e}^{-Y_0}\,. \tag{E.8}$$

There is a finite number of insertions at any given order, therefore, the coefficient in front of e^{-Y_0} is only a function of n. We then proceed to the lower order. For each time where we need to consider insertion of the lower group into the higher group, the usage of Ward identity results in an error of the order of $\mathcal{O}\,\mathrm{e}^{-Y_0}$. Thus, by summing over the contributions, we have

$$|V(NnY_0) - V(nY_0)| \sim (N-1)\left(\mathrm{e}^{-Y_0}\right)\,, \tag{E.9}$$

when $N \gg 1$. Let us denote $Y' = nY_0$ and $Y = NnY_0$. We then have

$$\left|V(Y) - V\left(Y'\right)\right| \sim \left(Y - Y'\right)\,\mathrm{e}^{-Y'/n}\,. \tag{E.10}$$

We now show that the large-Y limit of $V(Y)$ exists. We first show this allows a sequence

$$\left|V\left(\mathrm{e}^{k^2}\right)-V\left(\mathrm{e}^{(k-1)^2}\right)\right|\sim\left(\mathrm{e}^{k^2}-\mathrm{e}^{(k-1)^2}\right)\mathrm{e}^{-\mathrm{e}^{(k-1)^2}/n}\,. \tag{E.11}$$

Thus,

$$\begin{aligned}\left|\lim_{k\to\infty}V\left(\mathrm{e}^{k^2}\right)\right| &= \left|V(k_0)+\sum_{k=k_0+1}\left(V\left(\mathrm{e}^{(k+1)^2}\right)-V\left(\mathrm{e}^{k^2}\right)\right)\right| \\ &\leq |V(k_0)|+\sum_{k=k_0+1}\left(\mathrm{e}^{k^2}-\mathrm{e}^{(k-1)^2}\right)\mathrm{e}^{-\mathrm{e}^{(k-1)^2}/n}<\infty\,. \end{aligned}\tag{E.12}$$

Therefore, along tower-exponential sequences such as $Y=\mathrm{e}^{k^2}$, the large-Y limit exists. Let us denote the limit as a. Then, we have

$$\begin{aligned}|V(Y)-a| &\leq \left|V(Y)-V\left(\mathrm{e}^{\left[\sqrt{\ln Y}-1\right]^2}\right)\right|+\left|V\left(\mathrm{e}^{\left[\sqrt{\ln Y}-1\right]^2}\right)-a\right| \\ &\leq \left(Y-\mathrm{e}^{\left[\sqrt{\ln Y}-1\right]^2}\right)\mathrm{e}^{-\mathrm{e}^{\left[\sqrt{\ln Y}-1\right]^2/n}}+\left|V\left(\mathrm{e}^{\left[\sqrt{\ln Y}-1\right]^2}\right)-a\right|\,, \end{aligned}\tag{E.13}$$

where $[x]$ denotes the integer part of x. Thus, if we choose large enough Y, both terms at the right-hand side of the last line can be made arbitrarily small, thus $V(Y)$ converge to a.

Therefore, the vertex webs are free from collinear divergences, and all the collinear divergences are factorized into self-interacting webs for the two gauge link staples. This leads to the functional equation given before solved by linear functions in Y. From the arguments above, the rapidity factorization is the consequence of gauge-invariance, the structure of the leading region for the soft function, and the non-Abelian exponentiation. Without any one of these, the factorization would not work.

Appendix F

Alternative proof of $S=S_{\mathrm{DY}}$

We now provide two alternative proofs for the equality between $S_{\mathrm{DY}}(Y,Y',b_\perp)$ and $S(Y,Y',b_\perp)$, which applies to the arbitrary finite gauge link lengths as well. We will show that

$$W\left(-iT_1,-iT_2,b_\perp,\mu,v,v'\right)=W\left(T_1,T_2,b_\perp,\mu,u,u'\right)\,. \tag{F.1}$$

We first state a proof based on a variation of the methods shown in the main text. In the DY-shape soft function, we keep $v_1^z=v_2^z=1$ and analytically continue in $v_1^0 = -v_2^0 = v^0$. We keep the staple length in z direction as L. This defines a function $f(z, L)$, analytic in z but not necessarily in L. It relates to the $f(z)$ defined in the main text through $f(z) = \lim_{L\to\infty} f(z, L)$.

In the SIDIS-shape soft function, we consider the consecutive increments in longitudinal directions

$$\Delta_{ff} = v^0 l\,(s - s')\,\hat{t} + (s - s')\,l\hat{z}\,, \tag{F.2}$$
$$\Delta_{fi} = v^0 l\,(s - s')\,\hat{t} + (s + s')\,l\hat{z}\,, \tag{F.3}$$
$$\Delta_{ii} = v^0 l\,(s - s')\,\hat{t} - (s - s')\,l\hat{z}\,, \tag{F.4}$$

with the s, s' parameterizing the gauge links in initial and final states. $s < 0$ denotes the link is in the initial state and $s > 0$ in the final state. l is the common "length" in the z direction. Notice that for all the three cases, we have $s - s' \geq |s \mp s'|$. Therefore, we can analytically continue simultaneously in $zl = v^0 l$ and l, provided that $|\Im(zl)| > |\Im l|$ to guarantee the exponential decay. Let un denote the resulting functions as $g(zl, l)$. It relates to the $g(z)$ through $g(z) = \lim_{l\to\infty} g(zl, l)$. Notice that this function is analytic in the second variable including $\Im l = 0$, as far as $\Im(zl) > \Im l$, since there is always an exponential decay provided by the first variable.

We now inspect $f(-iv_0, L)$ and $g(-iL, -v_0 L)$. One can see that they are two identical Euclidean Wilson loops related to each other by a rotation, therefore, they are equal for arbitrary $v_0 > 0$. Let us consider the two analytic functions in z at fixed L in the region $|\Re z| < 1$, $f(z, L)$ and $g(-iL, -izL)$. They are equal at $z = -iv_0$, therefore, equal everywhere in the domain of analyticity due to uniqueness of analytic continuation. Let us choose $\beta < 1$, then the equality indicates

$$f(\beta - i\epsilon, L) = g(-iL, -i(\beta - i\epsilon)L)\,. \tag{F.5}$$

Taking $\epsilon \to 0$ shows the desired equality.

The second proof is based on the properties of Wightman functions. Let us denote the Wilson loop for the S as W, and for $S_{\rm DY}$ as $W_{\rm DY}$. We again assume that there is a regularization scheme in which the Lorentz invariance in the longitudinal direction is preserved, and the energy is positive definite. We choose arbitrary $N+M$ points on the contour for the W according to the time-ordering and show that the analytically continued version for the gluon Wightman function for these points contracted with direction vectors equals a corresponding contribution for the $W_{\rm DY}$. Then, integrating along the contour shows the equality. For simplicity, one considers points along links in v and v' direction, points on the transverse links can be included without changing the argument. For W, one obtains the Wightman functions $v'^{\mu_1}\dots v'^{\mu_M} v^{\nu_1}\dots v^{\nu_N}\mathcal{W}_{\mu_1,\dots\mu_M;\nu_1,\dots\mu_N}(s_i' v'(1-i\epsilon) + t_i' b_\perp, s_j v(1-i\epsilon) + t_j b_\perp)$, where $0 < s'_1 < s'_2 < \dots s'_M < T_2$ and $-T_1 < s_1 < \dots s_N < 0$. Now, the analytic continuation simply means $s_i \to -is_i$ and $s'_i \to -is'_i$. This analytic continuation is possible due to the fact that the consecutive increments $(s_i - s_{i-1})v(1-i\epsilon)$, $(s'_i - s'_{i-1})v'(1-i\epsilon)$ and $(v's'_1 - vs_N)(1-i\epsilon)$ are all in the forward lightcone, as a result, all s and s' can be analytically continued to negative imaginary number by multiplying them by an overall $-i$, due to the fact that the Fourier transform of these consecutive increments are supported in the forward lightcone. After analytic continuations, these Wightman functions are in the natural analyticity domain called the tube of the form of $R^4 - iV_+$, where V_+ denote the forward lightcone. This is nothing but a Paley–Wiener-type result which relates the support property of the Fourier transform of a distribution $\hat{f}(k)$ to the analyticity of the original distribution $f(z)$. Now we choose the same $N+M$ points from the contour of $W_{\rm DY}$, but according to the z-ordering. This is possible since $W_{\rm DY}$ is insensitive to time-ordering. Then one obtains $n'^{,\mu_1}\dots n'^{,\mu_M} n^{\nu_1}\dots n^{\nu_N}\mathcal{W}_{\mu_1,\dots\mu_M;\nu_1,\dots\mu_N}(s'_i n'_i v'(1-i\epsilon)+t'_i b_\perp, s_j n(1-i\epsilon)+t_j b_\perp)$ where all parameters s and s' for W and $W_{\rm DY}$ are in one-to-one correspondence. Then both Wightman functions are in their analytic region, and all arguments relate with each other through the complex Lorentz transform $\Lambda(t,z)\to(it,iz))$ since $\Lambda(-iv,-iv')=(n,n')$. Then one needs to use the "edge of the wedge" theorem. This theorem states that the Wightman functions in their analytic region called the "extend tube" transform under complex Lorentz transform in a covariant way. In fact, the extended tube is constructed exactly through complex-Lorentz transforms from the tubes. Given the theorem, we have

$$\begin{aligned}
&(-i)v'^{\mu_1}\dots(-i)v'^{\mu_M}(-i)v_{\nu_1}\dots(-i)v_{\nu_N}\\
&\times\mathcal{W}^{\nu_1,\dots\mu_N}_{\mu_1,\dots\mu_M}\left(-is'_iv'(1-i\epsilon)+t'_ib_\perp,-is_jv(1-i\epsilon)+t_jb_\perp\right)\\
&=n'^{\mu_1}\dots n'^{\mu_M}n_{\nu_1}\dots n_{\nu_N}\\
&\times\mathcal{W}^{\nu_1,\dots\mu_N}_{\mu_1,\dots\mu_M}\left(s'_in'_iv'(1-i\epsilon)+t'_ib_\perp,s_jn(1-i\epsilon)+t_jb_\perp\right)\,,
\end{aligned}\tag{F.6}$$

and integrating s_i and s'_i from $-L_1$ to 0 or from 0 to L_2 leads to the equality. Note that the theorems mentioned above only rely on the tempered nature of the Wightman functions, causality (for the "edge of the wedge" theorem), and support property, but do not require any positivity, thus should also be valid in a theory with ghost modes. This defines the imaginary time version for W and finishes the proof of the equality.

We state another proof that avoids the usage of properties of Wightman functions.

Appendix G

Gauge invariance of double-time ordering

Naively looking, the gauge invariance of the double time-ordered soft functions follows immediately from the operator definition. However, as one knows, in the quantum field theory, the real-time correlation functions are boundary values of analytic functions with imaginary time components. The correct $\pm$ choices of the imaginary parts are normally associated with the spacetime picture of the given correlation function. For the single time-ordered soft function, there is a natural interpretation as heavy-quark pairs propagating forwardly in time, thus the analyticity, consequently, the $\pm$ choices are the standard ones and there is no issue regarding the gauge invariance. But for the double time-ordered soft function, the time orderings at the two sides of the "cut" are opposite, thus the $\pm$ choices should also differ. This can lead to problems regarding the gauge invariance. For example, let us consider the "quasi-TMD"-type soft function, and let the timelike gauge links start at $t = -t_0 < 0$. Then, the $-t_0$ should be viewed as $-t^0(1 - i0)$ on the left-hand side of the cut, but at the right hand side of the cut, we should choose $-t_0(1 + i0)$. This leads to a $2it_0 0$ difference, which can be dangerous.

Appendix H

Analyticity and universality in δ regularization schemes

In this section, we study the analyticity in δ-regulator soft functions.

Single time-ordering

The case of single time-ordering is similar to that of the off-lightcone scheme. We first define the generalized soft function with δ,δ' that can be both imaginary or real

$$S\left(b_\perp, \mu, \delta, \delta'\right) = \langle 0|\mathcal{T} W_n\left(\vec{b}_\perp, \delta'\right) W_n^\dagger\left(0, -\delta'^\dagger\right) W_p(0, \delta) W_p^\dagger\left(\vec{b}_\perp, -\delta^\dagger\right)|0\rangle \,. \tag{H.1}$$

Here, the gauge link is defined to be

$$W_p(\xi, \delta) = \mathcal{P}\mathrm{exp}\left[-ig \int\limits_{-\mathrm{sign}(\Im\delta)\infty} \mathrm{d}s e^{-i\delta s} A(ps + \xi)\right] \,. \tag{H.2}$$

Notice that the gauge link direction is fixed by the imaginary part of the δ. If $\Im\delta > 0$ the link is past-pointing, otherwise is future-pointing. If $\Im\delta = 0$

then we choose the $\pm i0$ to distinguish them. We first consider the case $\Im\delta, \Im\delta' > 0$, which corresponds to the "DY-shape". In this case, we can actually choose to let the gauge links be off-lightcone as well and define an analytic function in both the off-lightcone vector and the δ regulators. For this purpose we simply change n, p to be the corresponding off-lightcone vectors. Let $p = (v^0, 1, 0, 0)$ and $n = (v^0, -1, 0, 0)$, then the consecutive increments read

$$\mathrm{e}^{-i\delta s - i\delta' s'} \mathrm{e}^{-iv^0 E(s-s')} \, . \tag{H.3}$$

Let $z = \Re v^0 + i\Im v^0$, then we have an analytic function $f(\delta, \delta', z)$ in the domain $\Im z < 0$ and $\Im\delta \geq 0$. In particular, the S^- corresponds to $\delta = \delta' = i\delta$ and $z = 1 - i0$.

Similarly, let us consider the case where $\Im\delta > 0$ but $\Im\delta' < 0$. This case corresponds to the shape of S^+, and one obtains an analytic function $g(\delta, \delta', z)$ in the domain $\Im\delta > 0, \Im\delta' < 0$. In particular, the S^+ corresponds to $\delta = i\delta, \delta' = -i\delta'$, and $z = 1 - i0$.

We now consider $F(\delta, \delta', z) = \bar{f}(i\bar{\delta}, i\bar{\delta}', \frac{1}{\bar{z}})$ and $G(\delta, \delta', z) = g(i\delta, -i\delta', z)$ with $z = -iv_0$. Then, by inspecting the shape of the resulting Euclidean Wilson loops and using rotational invariance, one obtains the relation $F(\delta, \delta', z) = G(iz\delta, iz\delta', z)$ for $\delta > 0$, $\delta' > 0$ and $z = -iv_0$, thus by the uniqueness of analytic continuation to the whole domain of analyticity. By taking $z = 1 - i0$, it indicates the following relation for $\Re\delta, \Re\delta' > 0, \Im\delta \leq 0, \Im\delta' \leq 0$:

$$\bar{f}\left(i\bar{\delta}, i\bar{\delta}', 1 - i0\right) = g(-\delta(1 - i0), \delta'(1 - i0), 1 - i0) \, . \tag{H.4}$$

By taking $\delta, \delta' > 0$, this relation relates the $S^{\pm}(b_\perp, \mu, \delta, \delta)$ through

$$S^+(b_\perp, \mu, \delta, \delta) = S^{-\dagger}\left(b_\perp, \mu, \frac{i\delta}{1 + i0}, \frac{i\delta}{1 + i0}\right) \, . \tag{H.5}$$

Thus, at small δ, the S^+ can be obtained from S^- through the substitution

$$\ln\frac{\mu^2}{2\delta^+\delta^-} K(b_\perp, \mu) \to \left(\ln\frac{\mu^2}{2\delta^+\delta^-} + i\pi\right) K(b_\perp, \mu) \, . \tag{H.6}$$

The above relation also indicates that all the single-time-ordered soft functions with δ-type regulator can be represented by a single analytic function in δ.

Double time-ordering

We first define the following generalized soft functions where the δs can differ at the two sides of the cut:

$$S\left(b_\perp, \mu, \delta, \bar{\delta}, \delta', \bar{\delta}'\right) = \langle 0|\bar{\mathcal{T}} W_p^\dagger\left(\vec{b}_\perp, \bar{\delta}^\dagger\right) W_n\left(\vec{b}_\perp, \bar{\delta}'\right) \mathcal{T} W_n^\dagger\left(0, \delta'^\dagger\right) W_p(0, \delta)|0\rangle \, , \tag{H.7}$$

and the gauge links are defined in Eq. (H.2). We always choose $\Im\delta\Im\bar{\delta} < 0$ and $\Im\delta'\Im\bar{\delta}' < 0$ to make sure the gauge links in the same lightcone direction are pointing to the same direction. We now show that $F(\delta,\bar{\delta};\delta',\bar{\delta}') = S(b_\perp,\mu,\delta,\bar{\delta},\delta',\bar{\delta}')$ defines an analytic function in all the four variables. We first consider the case where $\Im\delta < 0$ and $\Im\delta' < 0$. By inspecting the shape of the gauge link, this corresponds to the DY shape. We can use a lightcone perturbation theory in p direction. The gauge link staple in the n direction then becomes an equal-lightcone-time observable. The energy denominator has, in general, the following form:

$$\prod_i \frac{D_i}{i\delta - k_i^-} N\left(\delta',\bar{\delta}'\right) \prod_j \frac{D_j}{j\bar{\delta} - k_i^-}\,, \tag{H.8}$$

where the $\prod_i$ are the energy denominators in the "initial state" from $-\infty \to 0$ and the $\prod_j$ are in the "final state" from $0 \to -\infty$. k_i^- is the total lightcone energy in the i^{th} state, and similarly for k_j^-. The D_i, D_j are numerators and the $N(\delta',\bar{\delta}')$ collects the contributions from the equal lightcone time gauge link staple. The first observation is, since all the intermediate states pose a positive lightcone energy, $k_i^- > 0$ and $k_j^- > 0$, the Feynman integral defines an analytic function in δ and $\bar{\delta}$ in the complex plane with the positive real axis being removed. Indeed, the real axis is where the energy denominators can be zero, and after integration we expect a branch cut to be developed there. It is again the positivity of energy that leads to analyticity. We further notice that in the case with $\Im\delta < 0$ and $\Im\delta' < 0$, the DY-shape soft function is independent of time ordering, therefore, invariant under simultaneous change of $\delta \to \delta'$ and $\bar{\delta} \to \bar{\delta}'$. Thus, we obtain the same analyticity in δ' and $\bar{\delta}'$ as well and the soft function in this region satisfies the relation

$$F\left(\delta,\bar{\delta};\delta',\bar{\delta}'\right) = F\left(\delta',\bar{\delta}';\delta,\bar{\delta}\right)\,. \tag{H.9}$$

We now try to move outside this region.

We first analytically continue in δ and $\bar{\delta}$ to the region where $\Im\delta > 0$ and $\Im\bar{\delta} < 0$. Notice that for any $\delta,\bar{\delta}$, we actually have an analytic function in $\delta',\bar{\delta}'$ in the region $\Im\delta' < 0, \Im\bar{\delta}' > 0$. Thus, we obtain a separately analytic function with $\Im\delta' < 0$ but with $\Im\delta$ not constrainted. Then based on the Hartog's theorem on separately holomorphic functions, we obtain an analytic function in all the four variables. To use this theorem we need to slightly relax the $\Im\delta\Im\bar{\delta} < 0$ condition for $\delta,\bar{\delta}$ to form an open connected domain, but that is always possible as far as we chose their real parts to be negative to make sure we are not going to cross the cut.

Similarly, we can fix a δ and $\bar{\delta}$, and analytically continue in $\delta',\bar{\delta}'$. This leads to an analytic function in the region where $\Im\delta < 0$ but $\Im\delta'$ unconstrainted. We therefore obtain an analytic function $F(\delta',\bar{\delta}';\delta,\bar{\delta})$ in the region where one of the $\Im\delta$, $\Im\delta'$ is negative and we have the relation $F(\delta,\bar\delta;\delta',\bar\delta') = F(\delta',\bar\delta';\delta,\bar\delta)$ throughout the region.

We now consider the special example where $\delta = \eta - i0, \bar\delta = \eta + i0$ with $\eta < 0$ and consider arbitrary $\delta' = \bar\delta'^\dagger$. Then we notice that for $\eta < 0$, the energy denominators involving δ, $\bar\delta$ are all negative and independent of $i0$ choice. Since all the color factors and polarization sums are real, all the imaginary parts are then provided by the $i0$ prescriptions for the gauge link staple in the conjugating lightcone direction. By taking complex conjugate, we find that the gauge link staple in $-$ direction change from past to future pointing. Since the soft function is real, we find that the two orientations are equivalent. In conclusion, there is a regularization scheme, corresponding to the choice $\delta = \bar\delta^\dagger = \eta - i0$, $\delta' = \bar\delta'^\dagger = \eta' \mp i0$, analytically connected to the standard δ regularization scheme, in which the DY and SIDIS soft functions are equal. We can also choose $\delta' = \bar\delta'^\dagger = \mp i\delta$. In this case, the $\mp$ does not matter either.

We now perform a factorization argument to the SIDIS soft function in the standard delta regularization. We can regularize all the auxiliary lightcone gauge links using the $\eta - i0$ version of the delta regulator and in the initial state. The choice is possible since for the standard *delta* regularization scheme, we have only initial state poles for k^- and final state poles for k^+. Thus, we can choose to deform in the k^- direction, instead of in k^+ and put all the gauge links in the initial state. We then find the factorization formula

$$\begin{aligned} &SS_{\rm SIDIS}\left(b_\perp,\mu,\delta,\delta'\right) = \left(-i\delta, i\delta; i\delta', -i\delta'\right) \\ &= \frac{S\left(-i\delta, i\delta; \eta' - i0, \eta' + i0\right) S\left(\eta - i0, \eta + i0; i\delta', -i\delta'\right)}{S\left(\eta - i0, \eta + i0; \eta' - i0, \eta' + i0\right)}\,, \end{aligned} \tag{H.10}$$

where we have omitted the variables on the other side of the cut. We can do the same type of factorization for the DY case

$$\begin{aligned} &S_{\rm DY}\left(b_\perp,\mu,\delta,\delta'\right) = S\left(-i\delta, i\delta; -i\delta', i\delta'\right) \\ &= \frac{S\left(-i\delta, i\delta; \eta' - i0, \eta' + i0\right) S\left(\eta - i0, \eta + i0; -i\delta', i\delta'\right)}{S\left(\eta - i0, \eta + i0; \eta' - i0, \eta' + i0\right)}\,. \end{aligned} \tag{H.11}$$

However, since we have shown that $S(\eta - i0, \eta + i0; i\delta', -i\delta') = S(\eta - i0, \eta + i0; -i\delta', i\delta')$, we must have $S_{\rm SIDIS}(b_\perp,\mu,\delta,\delta') = S_{\rm DY}(b_\perp,\mu,\delta,\delta')$. This builds the universality of the standard soft function in delta regularization.

For the off-lightcone soft function in double time-ordering, a similar analyticity pattern in hyperbolic angle can be found. The hyperbolic angles at two sides of the cut have to be treated differently in order to obtain analyticity. By factorizing the spacelike SIDIS soft function into the on-lightcone soft function with the generalized δ regulator, one can show that they are equal to the DY soft function in the lightcone limit.

REFERENCES

[1] J.C. Collins, D.E. Soper, «Back-to-tack jets in QCD», *Nucl. Phys. B* **193**, 381 (1981); *Erratum ibid.* **213**, 545 (1983).

[2] J.C. Collins, D.E. Soper, «Back-to-back jets: Fourier transform from b to K_{T}», *Nucl. Phys. B* **197**, 446 (1982).

[3] J.C. Collins, D.E. Soper, G.F. Sterman, «Transverse momentum distribution in Drell–Yan pair and W and Z boson production», *Nucl. Phys. B* **250**, 199 (1985).

[4] G.T. Bodwin, «Factorization of the Drell–Yan cross section in perturbation theory», *Phys. Rev. D* **31**, 2616 (1985); *Erratum ibid.* **34**, 3932 (1986).

[5] J.C. Collins, D.E. Soper, G.F. Sterman, «Soft gluons and factorization», *Nucl. Phys. B* **308**, 833 (1988).

[6] X.-d. Ji, J.-P. Ma, F. Yuan, «QCD factorization for semi-inclusive deep-inelastic scattering at low transverse momentum», *Phys. Rev. D* **71**, 034005 (2005).

[7] X.-d. Ji, J.-P. Ma, F. Yuan, «QCD factorization for spin-dependent cross sections in DIS and Drell–Yan processes at low transverse momentum», *Phys. Lett. B* **597**, 299 (2004).

[8] M.G. Echevarría, A. Idilbi, I. Scimemi, «Soft and collinear factorization and transverse momentum dependent parton distribution functions», *Phys. Lett. B* **726**, 795 (2013).

[9] A.V. Manohar, I.W. Stewart, «The zero-bin and mode factorization in quantum field theory», *Phys. Rev. D* **76**, 074002 (2007).

[10] Y. Li, D. Neill, H.X. Zhu, «An exponential regulator for rapidity divergences», *Nucl. Phys. B* **960**, 115193 (2020).

[11] J. Collins, «Foundations of Perturbative QCD. Cambridge Monographs on Particle Physics, Nuclear Physics and Cosmology Vol. 32», *Cambridge University Press*, 2011.

[12] J.C. Collins, T.C. Rogers, «Equality of two definitions for transverse momentum dependent parton distribution functions», *Phys. Rev. D* **87**, 034018 (2013).

[13] J. Collins, T.C. Rogers, «Connecting different TMD factorization formalisms in QCD», *Phys. Rev. D* **96**, 054011 (2017).

[14] T. Gehrmann, T. Luebbert, L.L. Yang, «Calculation of the transverse parton distribution functions at next-to-next-to-leading order», *J. High Energy Phys.* **1406**, 155 (2014).

[15] M.G. Echevarria, I. Scimemi, A. Vladimirov, «Universal transverse momentum dependent soft function at NNLO», *Phys. Rev. D* **93**, 054004 (2016).

[16] M.G. Echevarria, I. Scimemi, A. Vladimirov, «Unpolarized transverse momentum dependent parton distribution and fragmentation functions at next-to-next-to-leading order», *J. High Energy Phys.* **1609**, 004 (2016).

[17] D. Gutierrez-Reyes, I. Scimemi, A. Vladimirov, «Transverse momentum dependent transversely polarized distributions at next-to-next-to-leading-order», *J. High Energy Phys.* **1807**, 172 (2018).

[18] Y. Li, H.X. Zhu, «Bootstrapping Rapidity Anomalous Dimensions for Transverse-Momentum Resummation», *Phys. Rev. Lett.* **118**, 022004 (2017).

[19] A. Vladimirov, «Structure of rapidity divergences in multi-parton scattering soft factors», *J. High Energy Phys.* **1804**, 045 (2018).

[20] D. Boer, P.J. Mulders, «Time-reversal odd distribution functions in leptoproduction», *Phys. Rev. D* **57**, 5780 (1998).

[21] F. Landry, R. Brock, G. Ladinsky, C.P. Yuan, «New fits for the non-perturbative parameters in the CSS resummation formalism», *Phys. Rev. D* **63**, 013004 (2001).

[22] F. Landry, R. Brock, P.M. Nadolsky, C.P. Yuan, «Fermilab Tevatron run-1 Z boson data and Collins–Soper–Sterman resummation formalism», *Phys. Rev. D* **67**, 073016 (2003).

[23] A.V. Konychev, P.M. Nadolsky, «Universality of the Collins–Soper–Sterman nonperturbative function in gauge boson production», *Phys. Lett. B* **633**, 710 (2006).

[24] P. Sun, J. Isaacson, C.P. Yuan, F. Yuan, «Nonperturbative functions for SIDIS and Drell–Yan processes», *Int. J. Mod. Phys. A* **33**, 1841006 (2018).

[25] M.G. Echevarria, A. Idilbi, Z.-B. Kang, I. Vitev, «QCD evolution of the Sivers asymmetry», *Phys. Rev. D* **89**, 074013 (2014).

[26] Z.-B. Kang, A. Prokudin, P. Sun, F. Yuan, «Extraction of quark transversity distribution and Collins fragmentation functions with QCD evolution», *Phys. Rev. D* **93**, 014009 (2016).

[27] A. Bacchetta *et al.*, «Extraction of partonic transverse momentum distributions from semi-inclusive deep-inelastic scattering, Drell–Yan and Z-boson production», *J. High Energy Phys.* **1706**, 081 (2017); *Erratum ibid.* **1906**, 051 (2019).

[28] I. Scimemi, A. Vladimirov, «Analysis of vector boson production within TMD factorization», *Eur. Phys. J. C* **78**, 89 (2018).

[29] V. Bertone, I. Scimemi, A. Vladimirov, «Extraction of unpolarized quark transverse momentum dependent parton distributions from Drell–Yan/Z-boson production», *J. High Energy Phys.* **1906**, 028 (2019).

[30] I. Scimemi, A. Vladimirov, «Non-perturbative structure of semi-inclusive deep-inelastic and Drell–Yan scattering at small transverse momentum», *J. High Energ. Phys.* **2020**, 137 (2020).

[31] X. Ji, «Parton Physics on a Euclidean Lattice», *Phys. Rev. Lett.* **110**, 262002 (2013).

[32] X. Ji, «Parton physics from large-momentum effective field theory», *Sci. China Phys. Mech. Astron.* **57**, 1407 (2014).

[33] X. Ji *et al.*, «Large-momentum effective theory», *Rev. Mod. Phys.* **93**, 035005 (2021).

[34] X. Ji, P. Sun, X. Xiong, F. Yuan, «Soft factor subtraction and transverse momentum dependent parton distributions on the lattice», *Phys. Rev. D* **91**, 074009 (2015).

[35] X. Ji, L.-C. Jin, F. Yuan, J.-H. Zhang, Y. Zhao, «Transverse momentum dependent parton quasidistributions», *Phys. Rev. D* **99**, 114006 (2019).

[36] M.A. Ebert, I.W. Stewart, Y. Zhao, «Determining the nonperturbative Collins–Soper kernel from lattice QCD», *Phys. Rev. D* **99**, 034505 (2019).

[37] M.A. Ebert, I.W. Stewart, Y. Zhao, «Towards quasi-transverse momentum dependent PDFs computable on the lattice», *J. High Energy Phys.* **1909**, 037 (2019).

[38] M.A. Ebert, I.W. Stewart, Y. Zhao, «Renormalization and matching for the Collins–Soper kernel from lattice QCD», *J. High Energy Phys.* **2022**, 99 (2020).

[39] P. Shanahan, M. Wagman, Y. Zhao, «Collins–Soper kernel for TMD evolution from lattice QCD», *Phys. Rev. D* **102**, 014511 (2020).

[40] X. Ji, Y. Liu, Y.-S. Liu, «TMD soft function from large-momentum effective theory», *Nucl. Phys. B* **955**, 115054 (2020).

[41] X. Ji, Y. Liu, Y.-S. Liu, «Transverse-momentum-dependent parton distribution functions from large-momentum effective theory», *Phys. Lett. B* **811**, 135946 (2020).

[42] X. Ji, Y. Liu, «Computing Light-Front Wave Functions Without Light-Front Quantization: A Large-Momentum Effective Theory Approach», `arXiv:2106.05310 [hep-ph]`.

[43] M.G. Echevarria, I. Scimemi, A. Vladimirov, «Transverse momentum dependent fragmentation function at next-to–next-to–leading order», *Phys. Rev. D* **93**, 011502(R) (2016); *Erratum ibid.* **94**, 099904 (2016).

[44] J.-Y. Chiu, A. Jain, D. Neill, I.Z. Rothstein, «A formalism for the systematic treatment of rapidity logarithms in Quantum Field Theory», *J. High Energy Phys.* **1205**, 084 (2012).

[45] T. Becher, M. Neubert, «Drell–Yan production at small q_{T}, transverse parton distributions and the collinear anomaly», *Eur. Phys. J. C* **71**, 1665 (2011).

[46] J.C. Collins, A. Metz, «Universality of Soft and Collinear Factors in Hard-Scattering Factorization», *Phys. Rev. Lett.* **93**, 252001 (2004).

[47] J. Collins, «New Definition of TMD Parton Densities», *Int. J. Mod. Phys.: Conf. Ser.* **4**, 85 (2011).

[48] M.-X. Luo *et al.*, «Transverse parton distribution and fragmentation functions at NNLO: the quark case», *J. High Energy Phys.* **1910**, 083 (2019).

[49] A. von Manteuffel, E. Panzer, R.M. Schabinger, «Cusp and Collinear Anomalous Dimensions in Four-Loop QCD from Form Factors», *Phys. Rev. Lett.* **124**, 162001 (2020).

[50] S. Weinberg, «High-Energy Behavior in Quantum Field Theory», *Phys. Rev.* **118**, 838 (1960).

[51] A. Idilbi, X.-d. Ji, F. Yuan, «Resummation of threshold logarithms in effective field theory for DIS, Drell–Yan and Higgs production», *Nucl. Phys. B* **753**, 42 (2006).

[52] S. Moch, J.A.M. Vermaseren, A. Vogt, «The quark form factor at higher orders», *J. High Energy Phys.* **0508**, 049 (2005).

[53] J. Collins, «Rapidity divergences and valid definitions of parton densities», *PoS* **LC2008**, 028 (2008).

[54] J. Frenkel, J.C. Taylor, «Non-abelian eikonal exponentiation», *Nucl. Phys. B* **246**, 231 (1984).

[55] M.B. Voloshin, M.A. Shifman, «On the annihilation constants of mesons consisting of a heavy and a light quark, and $B^0 \leftrightarrow \bar{B}^{-0}$ oscillations», *Sov. J. Nucl. Phys.* **45**, 292 (1987), [*Yad. Fiz.* **45**, 463 (1987)].

[56] H.D. Politzer, M.B. Wise, «Leading logarithms of heavy quark masses in processes with light and heavy quarks», *Phys. Lett. B* **206**, 681 (1988).

[57] X.-D. Ji, M.J. Musolf, «Sub-leading logarithmic mass-dependence in heavy-meson form-factors», *Phys. Lett. B* **257**, 409 (1991).

[58] D.J. Broadhurst, A.G. Grozin, «Two-loop renormalization of the effective field theory of a static quark», *Phys. Lett. B* **267**, 105 (1991).

[59] K.G. Chetyrkin, A.G. Grozin, «Three-loop anomalous dimension of the heavy–light quark current in HQET», *Nucl. Phys. B* **666**, 289 (2003).

[60] J.G.M. Gatheral, «Exponentiation of eikonal cross-sections in nonabelian gauge theories», *Phys. Lett. B* **133**, 90 (1983).

[61] T. Appelquist, M. Dine, I.J. Muzinich, «Static limit of quantum chromodynamics», *Phys. Rev. D* **17**, 2074 (1978).

[62] N. Brambilla, A. Pineda, J. Soto, A. Vairo, «Infrared behavior of the static potential in perturbative QCD», *Phys. Rev. D* **60**, 091502 (1999).

[63] S. Weinberg, «The Quantum theory of fields. Vol. 1: Foundations», *Cambridge University Press*, 2005.

[64] A.A. Vladimirov, A. Schäfer, «Transverse-momentum-dependent factorization for lattice observables», *Phys. Rev. D* **101**, 074517 (2020).

[65] A. Grozin, J.M. Henn, G.P. Korchemsky, P. Marquard, «The three-loop cusp anomalous dimension in QCD and its supersymmetric extensions», *J. High Energy Phys.* **1601**, 140 (2016).

[66] R.F. Streater, A.S. Wightman, «PCT, Spin and Statistics, and All That», *Princeton University Press*, 1989.

[67] U. D'Alesio, M.G. Echevarria, S. Melis, I. Scimemi, «Non-perturbative QCD effects in q_{T} spectra of Drell–Yan and Z-boson production», *J. High Energy Phys.* **1411**, 098 (2014).

[68] H.-N. Li, G.F. Sterman, «The perturbative pion form factor with Sudakov suppression», *Nucl. Phys. B* **381**, 129 (1992).

[69] L.D. McLerran, R. Venugopalan, «Gluon distribution functions for very large nuclei at small transverse momentum», *Phys. Rev. D* **49**, 3352 (1994).

[70] E.A. Kuraev, L.N. Lipatov, V.S. Fadin, «The Pomeranchuk Singularity in Nonabelian Gauge Theories», *Sov. Phys. JETP* **45**, 199 (1977); [*Zh. Eksp. Teor. Fiz.* **72**, 377 (1977)].

[71] I.I. Balitsky, L.N. Lipatov, «The Pomeranchuk Singularity in Quantum Chromodynamics», *Sov. J. Nucl. Phys.* **28**, 822 (1978); [*Yad. Fiz.* **28**, 1597 (1978),].

[72] I. Balitsky, «Operator expansion for high-energy scattering», *Nucl. Phys. B* **463**, 99 (1996).

[73] Y.V. Kovchegov, «Small-x F_2 structure function of a nucleus including multiple Pomeron exchanges», *Phys. Rev. D* **60**, 034008 (1999).

[74] Y.V. Kovchegov, E. Levin, «Quantum chromodynamics at high energy. Cambridge Monographs on Particle Physics, Nuclear Physics and Cosmology Vol. 33», *Cambridge University Press*, 2012.

[75] A.V. Belitsky, X.-d. Ji, F. Yuan, «Quark imaging in the proton via quantum phase-space distributions», *Phys. Rev. D* **69**, 074014 (2004).

[76] C. Lorcé, B. Pasquini, X. Xiong, F. Yuan, «Quark orbital angular momentum from Wigner distributions and light-cone wave functions», *Phys. Rev. D* **85**, 114006 (2012).

[77] M. Burkardt, «Impact parameter dependent parton distributions and off-forward parton distributions for $\vec{\zeta}0$», *Phys. Rev. D* **62**, 071503 (2000); *Erratum ibid.* **66**, 119903 (2002).

[78] D. Boer *et al.*, «Gluons and the quark sea at high energies: distributions, polarization, tomography», `arXiv:1108.1713 [nucl-th]`.

[79] H. Dorn, «Renormalization of Path Ordered Phase Factors and Related Hadron Operators in Gauge Field Theories», *Fortsch. Phys.* **34**, 11 (1986).

[80] X. Ji, J.-H. Zhang, Y. Zhao, «Renormalization in Large Momentum Effective Theory of Parton Physics», *Phys. Rev. Lett.* **120**, 112001 (2018).

[81] W. Rudin, «Real and Complex Analysis. 3rd edition», *McGraw-Hill Education*, 1986.

[82] U. Aglietti, M. Crisafulli, M. Masetti, «Problems with the euclidean formulation of heavy quark effective theories», *Phys. Lett. B* **294**, 281 (1992).

[83] U. Aglietti, «Consistency and lattice renormalization of the effective theory for heavy quarks», *Nucl. Phys. B* **421**, 191 (1994).

[84] V.M. Braun, K.G. Chetyrkin, B.A. Kniehl, «Renormalization of parton quasi-distributions beyond the leading order: spacelike *vs.* timelike», *J. High Energy Phys.* **2007**, 161 (2020).

[85] S. Coleman, R.E. Norton, «Singularities in the physical region», *Nuovo Cim.* **38**, 438 (1965).